

~~RESTRICTED~~

NACA RM No. A7J22

TECH LIBRARY KAFB, NM

0099288



RESEARCH MEMORANDUM

S 275

HIGH-SPEED AERODYNAMIC CHARACTERISTICS OF A MODEL

TAIL PLANE WITH MODIFIED NACA 65-010 SECTIONS

AND 0° AND 45° SWEETBACK

By

Joseph L. Anderson and Andrew Martin

Ames Aeronautical Laboratory
Moffett Field, Calif.

Declassified by Authority of LABC Security Classification
Office (Sco) Letter dated June 16, 1983
Maurice F. Barnes

~~This document contains classified information relating to the National Defense of the United States. Under the meaning of the Espionage Act, USC 793 and 794, its transmission, or the revelation of its contents to anyone other than an authorized person is prohibited by law. Information so obtained may be imparted only to persons in the military and naval services of the United States, appropriate civilian officials and employees of the Federal Government who have a legitimate interest therein, and to United States citizens of proved loyalty and discretion who of necessity must be informed thereof.~~

AFMDC
TECHNICAL INFORMATION
AFI 2011

NATIONAL ADVISORY COMMITTEE FOR AERONAUTICS

WASHINGTON

January 12, 1948

~~RESTRICTED~~

319 9912

FILE

National Aeronautics and
Space Administration
Langley Research Center
Hampton, Virginia
23665



Recon to Admin of 139A

JUN 1 6 1983

TO: Distribution
FROM: 180A/Security Classification Officer
SUBJECT: Authority to Declassify NACA/NASA Documents Dated Prior to
January 1, 1960

(informal, Correspondence)

Effective this date, all material, classified by this Center prior to January 1, 1960, is declassified. This action does not include material derivatively classified at the Center upon instructions from other Agencies.

Immediate re-marking is not required; however, until material is re-marked by lining through the classification and annotating with the following statement, it must continue to be protected as if classified:

"Declassified by authority of LaRC Security Classification Officer (SCO) letter dated June 16, 1983," and the signature of person performing the re-marking.

If re-marking a large amount of material is desirable, but unduly burdensome, custodians may follow the instructions contained in NHB 1640.4, subpart F, section 1203.604, paragraph (b).

This declassification action complements earlier actions by the National Archives and Records Service (NARS) and by the NASA Security Classification Officer (SCO). In Declassification Review Program 807008, NARS declassified the Center's "Research Authorization" files, which contain reports, Research Authorizations, correspondence, photographs, and other documentation. Earlier, in a 1971 letter, the NASA SCO declassified all NACA/NASA formal series documents with the exception of the following reports, which must remain classified:

<u>Document No.</u>	<u>First Author</u>
E-51A30	Nagey
E-53G20	Francisco
E-53G21	Johnson
E-53K18	Spooner
SL-54J21a	Westphal
E-55C16	Fox
E-56H21a	Himmel

JUN 2 3 1983

P-02

LAARC TECH LIBRARY

804 884 2375

05-05-1997 11:29

If you have any questions concerning this matter, please call Mr. William L. Simkins at extension 3281.

Jess G. Ross
Jess G. Ross
2898

Distributions:
SDL 031

cct:
NASA Scientific and Technical
Information Facility
P.O. Box 8757
BWI Airport, MD 21240

NASA--NIS-5/Security
180A/RIAD
139A/TU&AO

6-15-83
139A/WLSimkins:elf 06/15/83 (3281)

6-15-83
139A/JRS 6-15-83

31-01 HEADS OF ORGANIZATIONS
MAIL STOP 165
BLDG 1194
HESSE, JANE S.
05-05-1987 11:29

NATIONAL ADVISORY COMMITTEE FOR AERONAUTICS

RESEARCH MEMORANDUMHIGH-SPEED AERODYNAMIC CHARACTERISTICS OF A MODEL
TAIL PLANE WITH MODIFIED NACA 65-010 SECTIONS
AND 0° AND 45° SWEETBACK

By Joseph L. Anderson and Andrew Martin

SUMMARY

Wind-tunnel tests have been made to determine the aerodynamic characteristics of a model tail plane having modified NACA 65-010 sections and a tapered plan form. Results were obtained with the model tail plane unswept (flap hinge line perpendicular to air flow) and swept back (flap hinge line swept back 45° to air flow).

The data show the lift, drag, pitching-moment, and hinge-moment coefficient variation with angle of attack and flap deflection at various Mach numbers. Results are presented for Mach numbers from 0.40 to 0.875, with flap deflections from -5° to 15° at low Mach numbers and from -6° to 8° at the higher Mach numbers.

The Mach number of lift divergence for the unswept tail was found to be 0.80, while the Mach number of divergence for the swept tail was above 0.875. At a Mach number of 0.40, the unswept tail stalled at 12° angle of attack, but the swept tail did not stall at 20°.

If the unswept tail of an airplane were replaced with a swept tail (both tails similar to those tested) and the tail area were increased sufficiently to maintain equal static longitudinal stability at low speed, calculations based on the test results indicate that below a Mach number of 0.80, the swept tail would have greater drag but would require the same elevator stick force. Above 0.80 Mach number the tail drag and the elevator stick forces would both be considerably less for the airplane with the swept tail than for the airplane with the unswept tail.

INTRODUCTION

Recently, during recovery of an airplane from a high-speed dive, an unanticipated abrupt pitch-up and a large positive acceleration were encountered. (See reference 1.) In order to determine if the tail characteristics of this airplane were affected by Mach number, tests were made in the Ames 16-foot high-speed wind tunnel of a semispan model of the horizontal tail plane of the airplane. The movable surface of the model tail plane is referred to in this report as a flap, for the results are applicable to other control surfaces. The aerodynamic characteristics of this model tail plane were measured with the flap hinge line unswept and swept back 45°.

SYMBOLS

The coefficients and the symbols used in this report are defined as follows:

- C_L lift coefficient (L/qS)
- C_D drag coefficient (D/qS)
- C_m pitching-moment coefficient about one-quarter M.A.C. (M'/qS M.A.C.)
- C_{hf} flap hinge-moment coefficient ($H/q\bar{c}_f^2 b_f$)
- M Mach number (V/a)
- R Reynolds number (ρV M.A.C. / μ)
- A aspect ratio $\left(\frac{2b^2}{S}\right)$
- F stick force $\left(\frac{2 C_{hf} q b_f \bar{c}_f^2}{\text{stick length} \times \frac{d\delta_s}{d\delta_f}} \right)$, pounds

where

- L lift of semispan model, pounds
- D drag of semispan model, pounds
- M' pitching moment about the one-quarter M.A.C. of semispan model, foot-pounds

- H hinge moment about flap hinge line of semispan model,
foot-pounds
- q dynamic pressure ($\frac{1}{2}\rho V^2$), pounds per square foot
- S area of semispan model, square feet
- b semispan of model, feet
- c chord of tail plane perpendicular to the hinge line, feet
- c_f chord of flap perpendicular to the flap hinge line, feet
- c_t chord of tab perpendicular to the flap hinge line, feet
- M.A.C. mean aerodynamic chord, feet
- b_f flap span of semispan model parallel to the hinge line, feet
- b_t tab span parallel to the hinge line, feet
- $\overline{c_f}$ root-mean-square chord of flap perpendicular to the hinge
line, feet
- ρ mass density of air in the free stream, slugs per cubic
foot
- V velocity of the free air stream, feet per second
- a speed of sound in the free air stream, feet per second
- μ viscosity of air in the free stream, pound-seconds per
square foot
- and
- α angle of attack of model, degrees
- δ_f flap deflection relative to airfoil, positive when the
trailing edge is deflected downward, degrees
- δ_t tab deflection relative to flap, positive when trailing
edge is deflected downward, degrees
- δ_s control-stick deflection, degrees

$$C_{L\alpha} = \left(\frac{\partial C_L}{\partial \alpha} \right)_{\delta_f, M}$$

$$C_{L\delta} = \left(\frac{\partial C_L}{\partial \delta_f} \right)_{\alpha, M}$$

$$\alpha_\delta = \left(\frac{C_{L\delta}}{C_{L\alpha}} \right)$$

$$C_{hf\alpha} = \left(\frac{\partial C_{hf}}{\partial \alpha} \right)_{\delta_f, M}$$

$$C_{hf\delta_f} = \left(\frac{\partial C_{hf}}{\partial \delta_f} \right)_{\alpha, M}$$

ΔCD_t increment of drag coefficient

Note: The subscripts outside the parenthesis indicate the factors held constant in determining the parameters.

DESCRIPTION OF MODEL AND APPARATUS

The test model was half of the horizontal tail plane from a 1/3-scale model of a fighter airplane. The dimensions of the tail are presented in table I. This tail plane has a flat-sided flap having a chord equal to 25 percent of the tail-plane chord and a tab having a chord equal to approximately 25 percent of the flap chord. The coordinates of the airfoil section are shown in table II. The flap was restrained by a cantilever beam to which were glued resistance-type strain gages for the measurement of the flap hinge moments.

To separate the tunnel-wall boundary layer from the model and thereby eliminate the effect of this boundary layer on the test results, a reflection plate was mounted 6 inches from the tunnel wall. The tail, supported by the balance frame, had its plane of symmetry at the reflection plate. A fairing covered the model-supporting structure between the plate and the tunnel wall. A baffle was installed on the model near the reflection plate to direct the leakage flow away from the model. (See fig. 1.) Figure 2 shows the unswept tail plane mounted in the wind tunnel.

RESULTS AND DISCUSSION

The tunnel-wall effects were considered to be negligible, and the effect of leakage at the reflection plate was unknown; therefore, no corrections were applied to the data.

The Reynolds numbers for both tail planes are shown in figure 3. The increased slope of the curves above 0.80 Mach number is due to the order of running the tests; data at the higher Mach numbers were obtained first when the air stream was coolest and consequently the density highest.

The aerodynamic characteristics are presented for the unswept tail plane in figures 4 through 8 and for the swept-back tail plane in figures 9 through 13. The variation of drag coefficient with Mach number for both the unswept and swept tails is presented in figure 14. Figures 15 through 20 show the lift, flap hinge-moment, and tab hinge-moment parameters.

Analysis of Wind-Tunnel Data

Lift.—The change in slope of the lift curves for the unswept tail in figures 4(a), (b), and (c) at about 0° angle of attack for the flap deflected 10° and 15° was probably the result of a shift of the transition point on the tail surface. With the flap undeflected, the maximum lift coefficient at 0.40 Mach number was 0.74 at 12° angle of attack. Tufts showed that the tip started to stall at about 2° angle of attack and the stall progressed inboard with increase in angle of attack. The stalling of the tip at such a low angle of attack probably caused the low maximum lift coefficient. The Mach number of lift divergence at 0° angle of attack occurs at about 0.80.

The lift parameter a_8 for the unswept tail at 0° angle of attack decreased with increase in Mach number. (See fig. 17.) The decrease in a_8 from 0.40 Mach number to 0.80 was due to the increase in stabilizer effectiveness (CL_s , fig. 15) with no increase in flap effectiveness (Cl_f , fig. 16); above 0.80 the decrease in a_8 was the result of a more rapid loss in flap effectiveness than stabilizer effectiveness.

For Mach numbers of 0.40 and 0.60 there was a change in slope of the lift curves for the swept-back tail at 6° angle of attack. (See figs. 9(a) and 9(b).) Above this angle of attack the lift-curve slopes increased. This change in slope was probably the result of a shift of the transition point on the tail surface similar to that experienced for the unswept tail at 0° angle of

attack. The swept-back tail did not stall at the maximum test angle of 20° . The Mach number of lift divergence at 0° angle of attack occurs above 0.875.

The variation in the lift parameter α_3 (fig. 17) with Mach number throughout the test Mach number range was small for the swept tail in comparison to that for the unswept. The small decrease in α_3 above 0.75 Mach number was the result of the increase in swept-tail stabilizer effectiveness (CL_a) while the flap effectiveness (CL_b) did not change significantly at Mach numbers above 0.75. (See figs. 15 and 16.)

Drag.— The drag coefficients presented in figures 6 and 11 cannot be considered absolute, since the effects of the baffle plate and the end leakage are unknown; however, the relative values should be largely independent of these effects. The interference effects and the poor accuracy in obtaining the drag data probably nullified the low-drag range of these airfoils. There was a pronounced increase of the drag coefficient of the unswept tail plane above the Mach number of drag divergence due to the shock on the surface. (See fig. 14.) For the swept-back tail plane, there was no increase in drag coefficient with increase in Mach number to 0.875. Deflection of the flap increases the drag coefficient of the unswept tail plane markedly, while the drag coefficient of the swept tail increases only slightly.

Pitching moment.— Figure 7 shows that the change in slope ($\partial C_m / \partial C_L$) of the pitching-moment curves with lift coefficient was greater at 0.40 Mach number than at the higher Mach numbers. The change in the slope and the scatter of the data were probably caused by the inability of the pitching-moment balance to accurately measure the small moments on the model at this low speed.

Flap hinge moment.— Figure 8 shows that the slope of the flap hinge-moment curves for the unswept tail increased at about 8° angle of attack for Mach numbers below 0.80. This is the angle of attack at which the tail plane started to stall. The unstable variation of flap hinge-moment coefficient with angle of attack at 0.875 Mach number is the result of the flap operating in separated flow. The change in variation of Ch_{fa} and Ch_{fb} with Mach number, above 0.80, was due to the flap operating in the separated region produced by shock on the tail plane. (See figs. 18 and 19.)

As shown in figures 18 and 19, the flap hinge-moment parameters (Ch_{fa} and Ch_{fb}) for the swept tail remained about constant through the Mach number range.

Tab effectiveness.— In the determination of tab effectiveness, the tab was deflected only negatively. The variation of tab effectiveness ($\partial C_{hf} / \partial \delta_t$) with Mach number is shown in figure 20. There was a rapid loss in tab effectiveness for the unswept tail above 0.80 Mach number. Below 0.80 Mach number, a flap deflection of $+5^\circ$ or -5° changed the tab effectiveness approximately ± 0.0015 for the unswept tail. The tab effectiveness for the swept tail was about constant with increase in Mach number and changed slightly with flap deflection.

Effect of Sweepback of the Horizontal Tail Plane on the Characteristics of an Airplane

From the wind-tunnel results, a direct comparison is not possible between the characteristics of the swept tail and that of the unswept. In order to illustrate the effect of sweepback of the tail on the characteristics of an airplane, two hypothetical airplanes, one having an unswept horizontal tail, and the other having a swept-back horizontal tail, were assumed. Using the wind-tunnel data presented in this report, supplemented with other wind-tunnel data, the tail size was chosen for each airplane so that at 0.60 Mach number the static longitudinal stability ($\partial C_m / \partial C_L$) would be equal for each airplane as well as the pitching-moment coefficients at zero lift. The following table gives the major dimensions for these two airplanes which are identical except for the horizontal tails:

	<u>Unswept tail</u>	<u>Swept-back 45° tail</u>
Wing area, square feet	237.00	237.00
Wing span, feet	39.00	39.00
Horizontal-tail span, feet	15.58	13.30
Horizontal-tail area, square feet	43.56	76.59
Horizontal-tail incidence, degrees	1.5	1.5
Tail length, from 25-percent point of the wing mean aerodynamic chord to the elevator hinge line at the tail root, feet	16.47	16.47

The variation of the calculated pitching-moment coefficient with lift coefficient for both airplanes is shown in figure 21 for constant Mach numbers. Figure 22 shows the variation of the neutral point for both airplanes with the elevator free and fixed through a Mach number range of 0.60 to 0.875. For the airplane with the unswept tail, the calculated neutral point moves aft with increase in Mach number to 0.825, above which it moves forward so that its location

at a Mach number of 0.875 is practically the same as at 0.60 Mach number. (See fig. 15.) This change in neutral point with Mach number is largely the result of the change in stabilizer effectiveness, for when the stabilizer effectiveness increases the neutral point moves aft and vice versa. For the airplane with the swept-back tail the neutral point moves gradually aft with Mach number, due to the increase in stabilizer effectiveness. (See fig. 15.)

For a wing loading of 50 pounds per square foot at sea level, figure 23 shows the calculated elevator stick forces and angles needed to balance the two hypothetical airplanes in level flight. For Mach numbers from 0.60 to 0.815 the stick force for the swept tail is equal to or slightly larger than for the unswept tail. However, above 0.815 Mach number, the stick force for the swept tail is less than for the unswept tail; at 0.875 Mach number, 125 and 600 pounds, respectively, are required.

The drag increment of the horizontal tails is shown in figure 24 for various Mach numbers. The drag of the swept tail is about 3.5 times greater than for the unswept tail at 0.60 Mach number, but this is largely due to the greater area for the swept tail. At 0.875 Mach number, the drag of the swept tail is considerably lower than that for the unswept tail plane.

CONCLUSIONS

The results of the high-speed wind-tunnel tests of a semispan horizontal tail swept and unswept indicate the following:

1. The Mach number of lift divergence for the unswept tail was approximately 0.80, while that for the swept-back tail was above 0.875.

2. Above a Mach number of 0.80, and at low angles of attack, the unswept tail plane showed a decided loss in stabilizer and flap effectiveness and an increase in flap hinge-moment coefficient; whereas in comparison the swept-back tail showed little change with Mach number to 0.875.

3. For the two hypothetical airplanes assumed in this report, one having an unswept and the other having a swept-back-horizontal tail, more area would be required for the swept horizontal tail plane than for the unswept tail for equal airplane static longitudinal stability at low speed. The airplane with the swept tail would have higher stick forces and tail drag at the Mach numbers below the Mach number of lift divergence than the airplane with the unswept tail,

but above the Mach number of divergence the airplane with the swept tail would have considerably less stick force and tail drag.

Ames Aeronautical Laboratory,
National Advisory Committee for Aeronautics,
Moffett Field, Calif.

REFERENCE

1. Brown, Harvey H., Rolls, L. Stewart, and Clouzing, Lawrence A.:
An Analysis of Longitudinal Control Problems Encountered in
Flight at Transonic Speeds with a Jet-Propelled Airplane.
NACA RRM No. A7G03, July 1947.

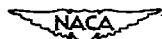
TABLE I.— MODEL DIMENSIONS

	<u>Unswept</u>	<u>Swept back</u>
Airfoil section, perpendicular to the hinge line (table I) . . .	Modified NACA 65-010	Modified NACA 65-010
Sweepback of flap hinge line (75-percent-chord line), degrees .	0	45
Sweepback of leading edge, degrees .	16	61
Sweepback of 25-percent-chord line, degrees	11.5	56.5
Tail-plane area, square feet	2.39	3.36
Span, feet	2.53	1.97
Mean aerodynamic chord, feet	1.03	1.89
Aspect ratio (based on full span) .	5.36	2.31
Flap span along flap hinge line, feet	2.36	2.36
Tail-plane root chord, feet	1.44	2.68
Equivalent tail-plane tip chord, feet	0.45	0.73
Taper ratio313	.272
Root-mean-square chord of flap, feet	.255	.255
Ratio of flap chord to tail plane chord (perpendicular to flap hinge line)25	.25
Tab span along tab hinge line, feet	.44	.44
Ratio of tab span to flap span185	.185
Ratio of tab chord to flap chord at inboard end of tab31	.31
Ratio of tab chord to flap chord at tip of tab19	.19
Trailing-edge angle	5°56"	5°56"



TABLE II.— COORDINATES IN PERCENT CHORD
FOR MODIFIED NACA 65-010 AIRFOIL

Station	Ordinate
0	0
0.5	0.767
.75	.923
1.25	1.154
2.50	1.558
5.0	2.175
7.5	2.642
10	3.040
15	3.664
20	4.142
25	4.500
30	4.760
35	4.921
40	5.000
45	4.962
50	4.800
55	4.512
60	4.114
65	3.652
70	3.115
75	2.597
80	2.087
85	1.577
90	1.066
95	.556
100	.046



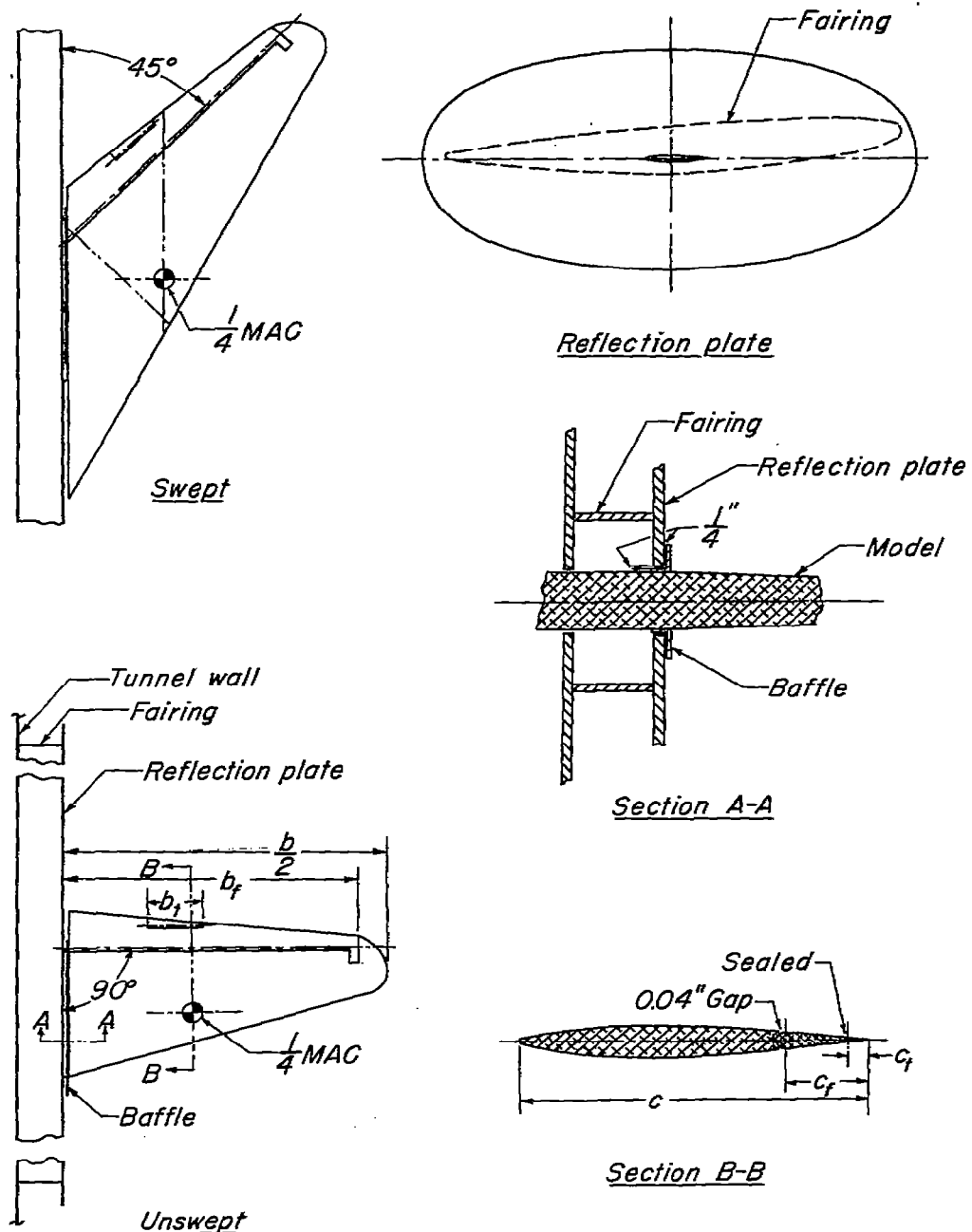
NATIONAL ADVISORY
COMMITTEE FOR AERONAUTICS

Figure 1.—Mounting arrangement.

NACA RM No. A7J22

Fig. 2

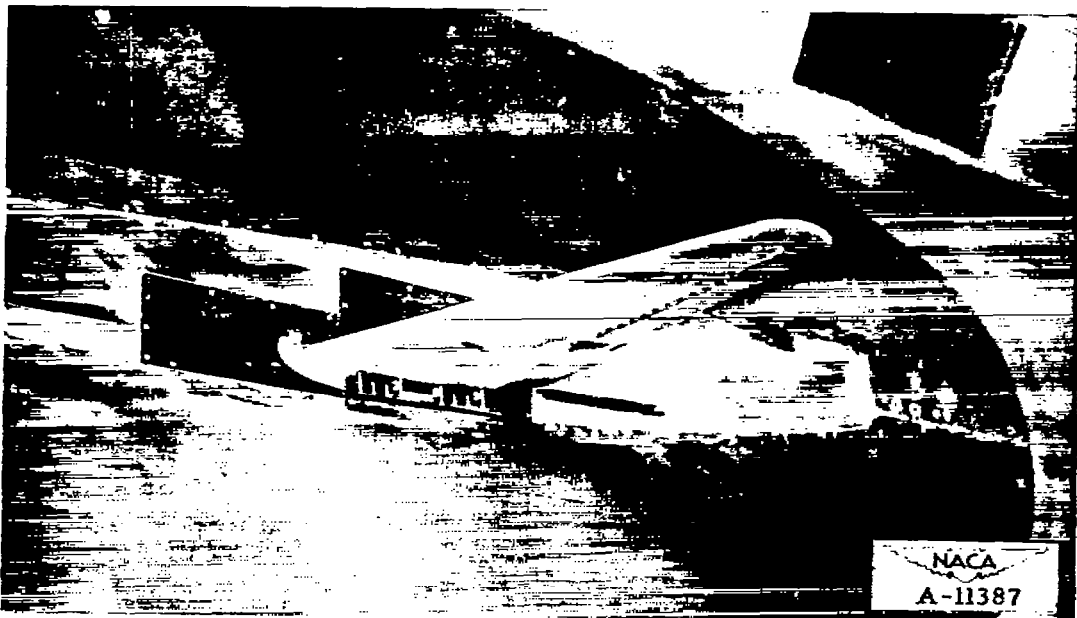


Figure 2.— Model mounted in the wind tunnel.

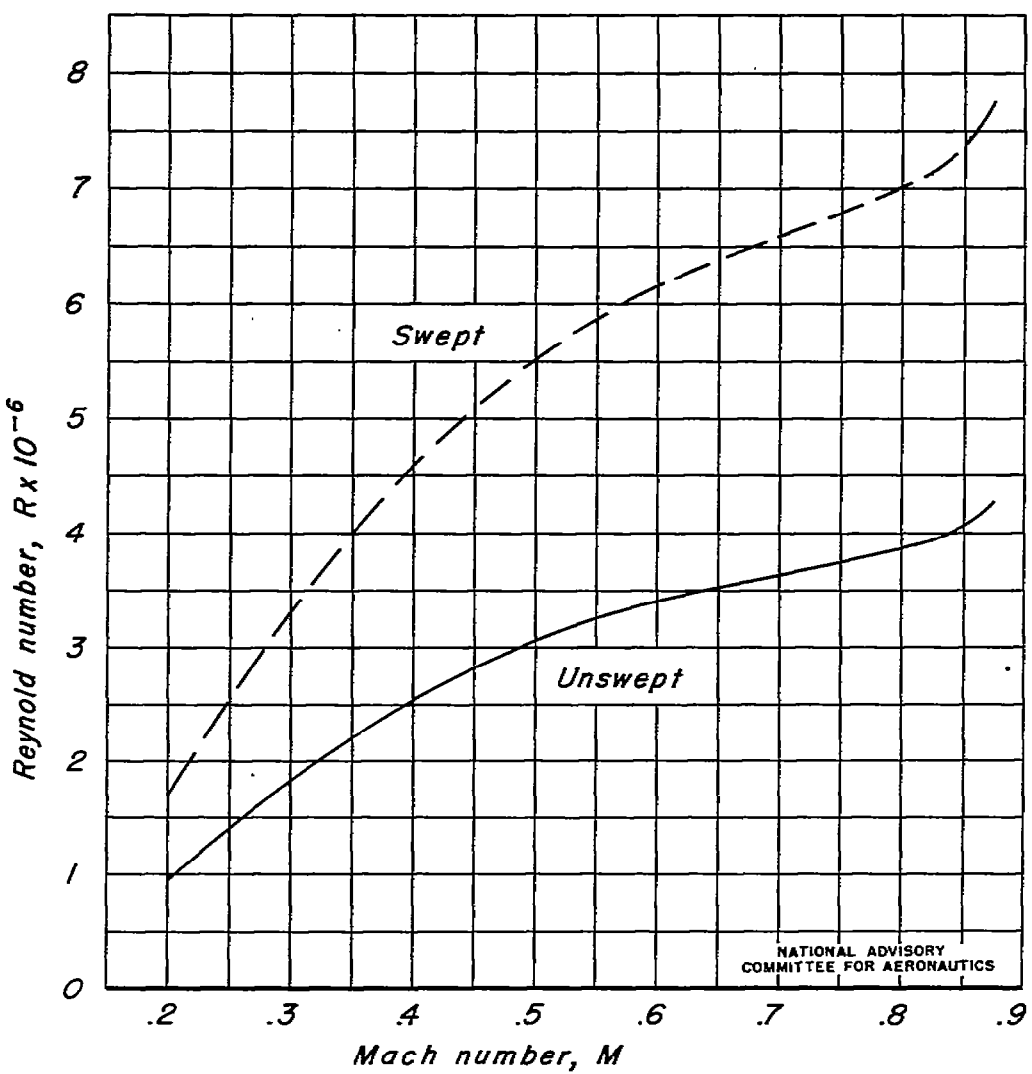


Figure 3.—Variation of Reynolds number with Mach number.

Unswept and swept back 45° .

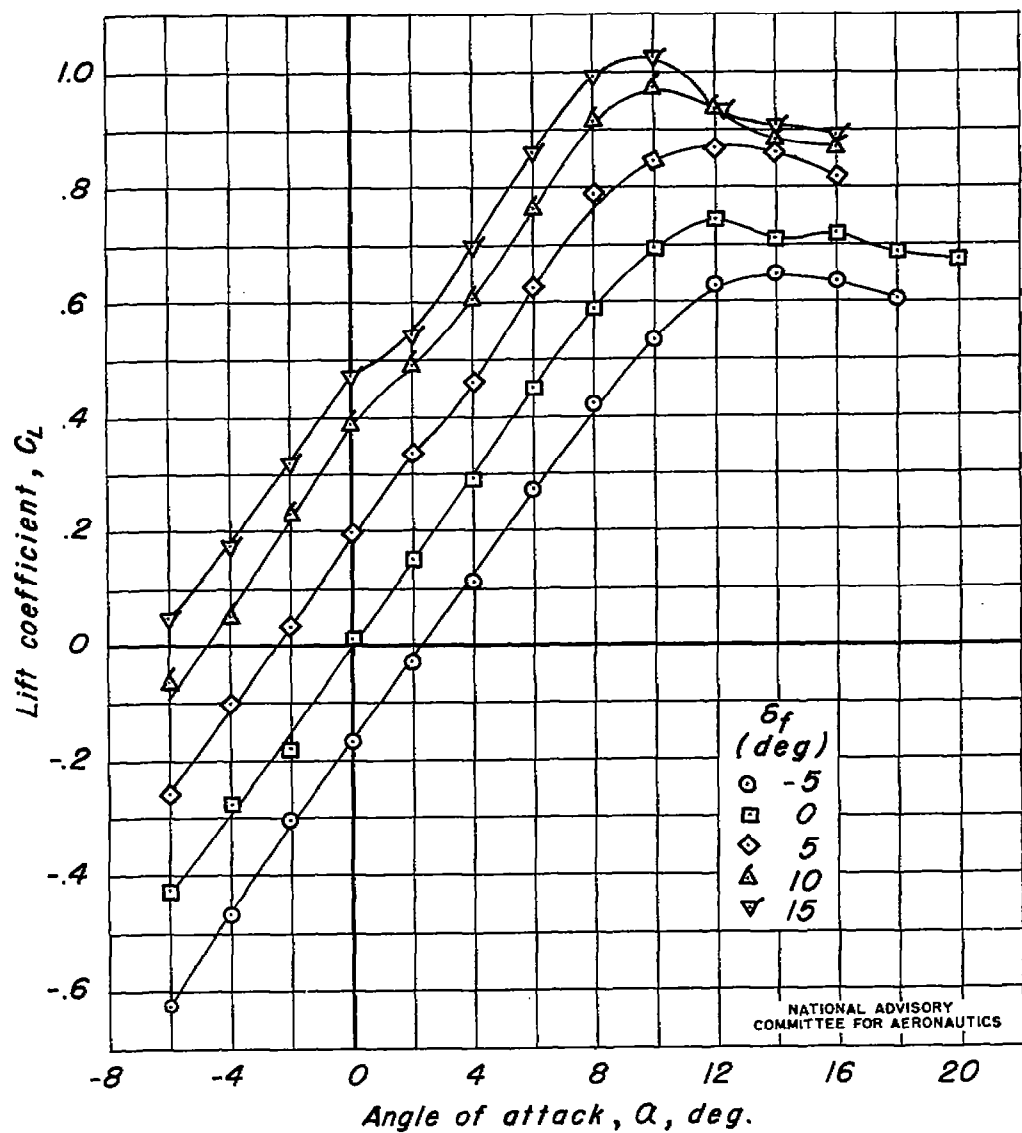
(a) $M, 0.40$

Figure 4.-Variation of lift coefficient with angle of attack.

Unswept; $\delta_t, 0^\circ$.

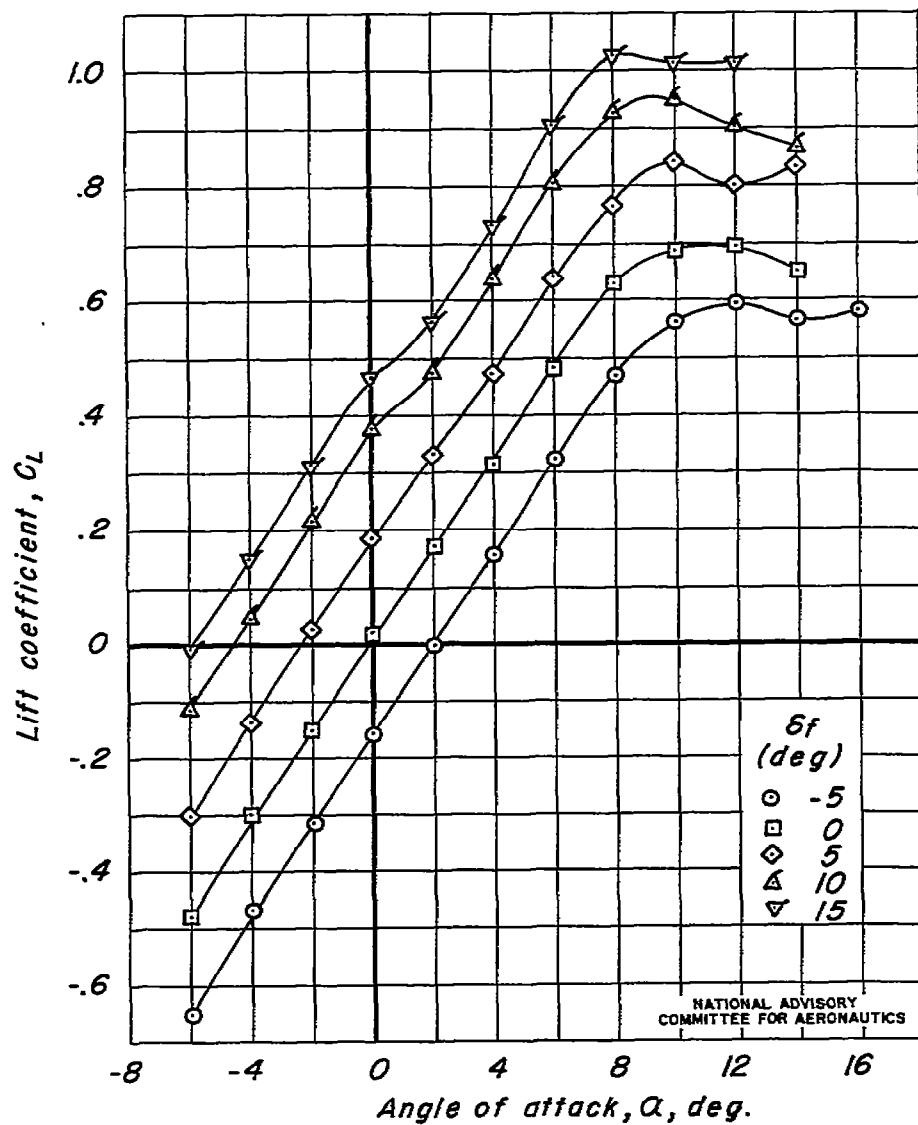
(b) $M, 0.60$

Figure 4. — Continued.

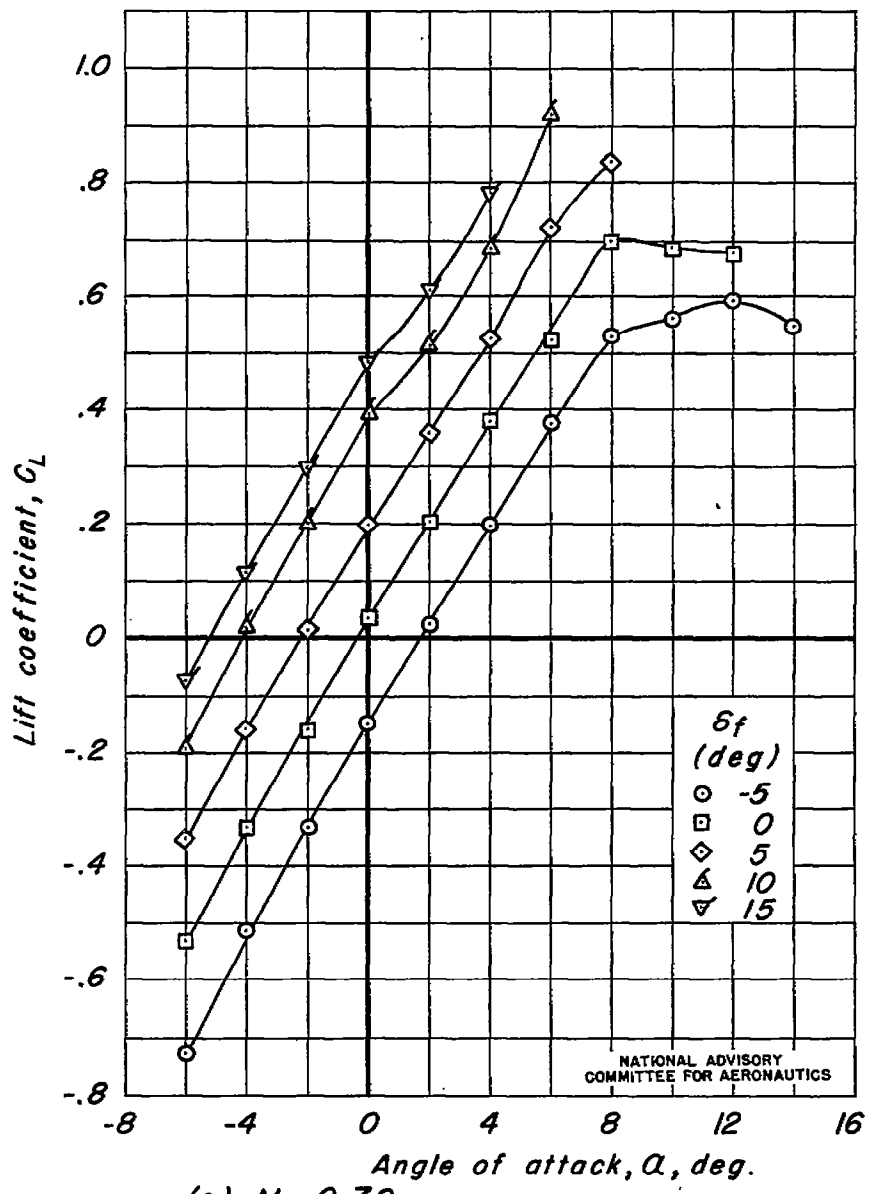
(c) $M, 0.70$

Figure 4.— Continued.

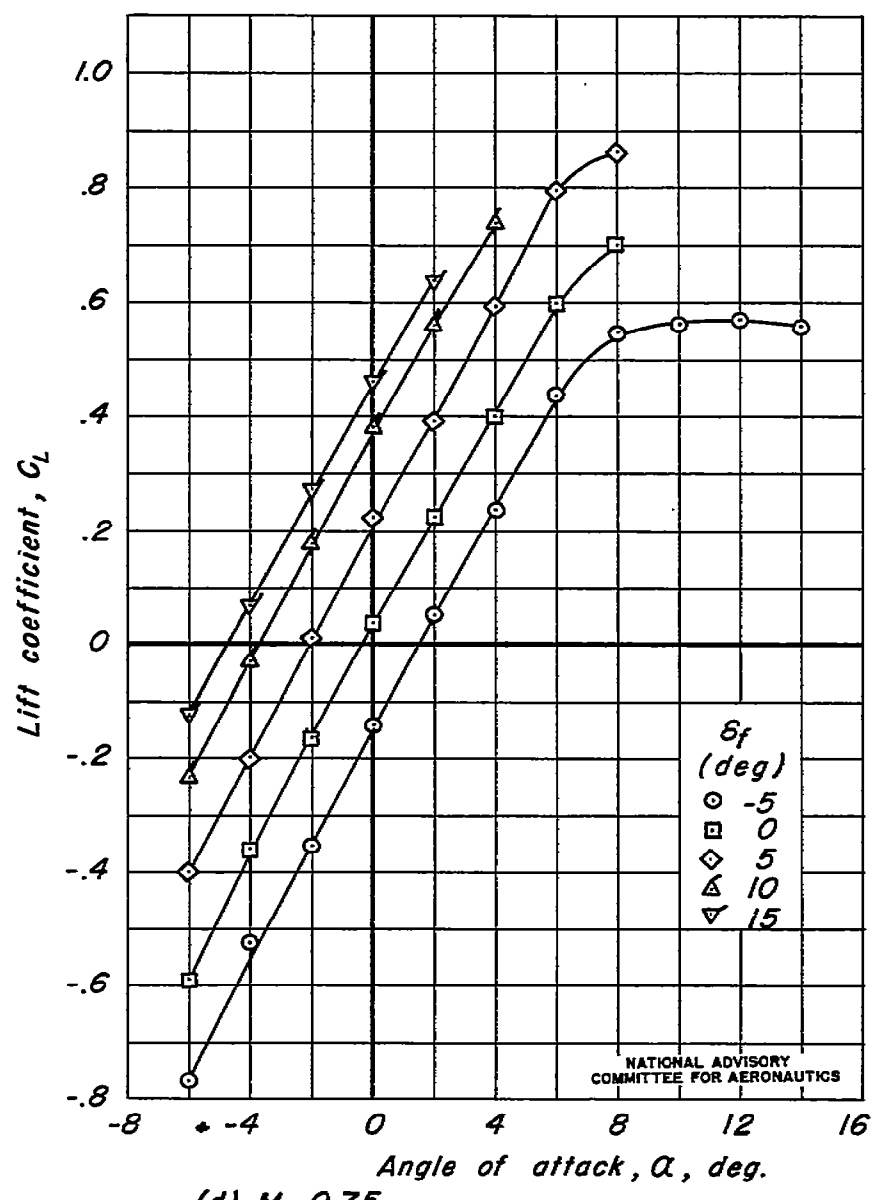
(d) $M, 0.75$

Figure 4. — Continued.

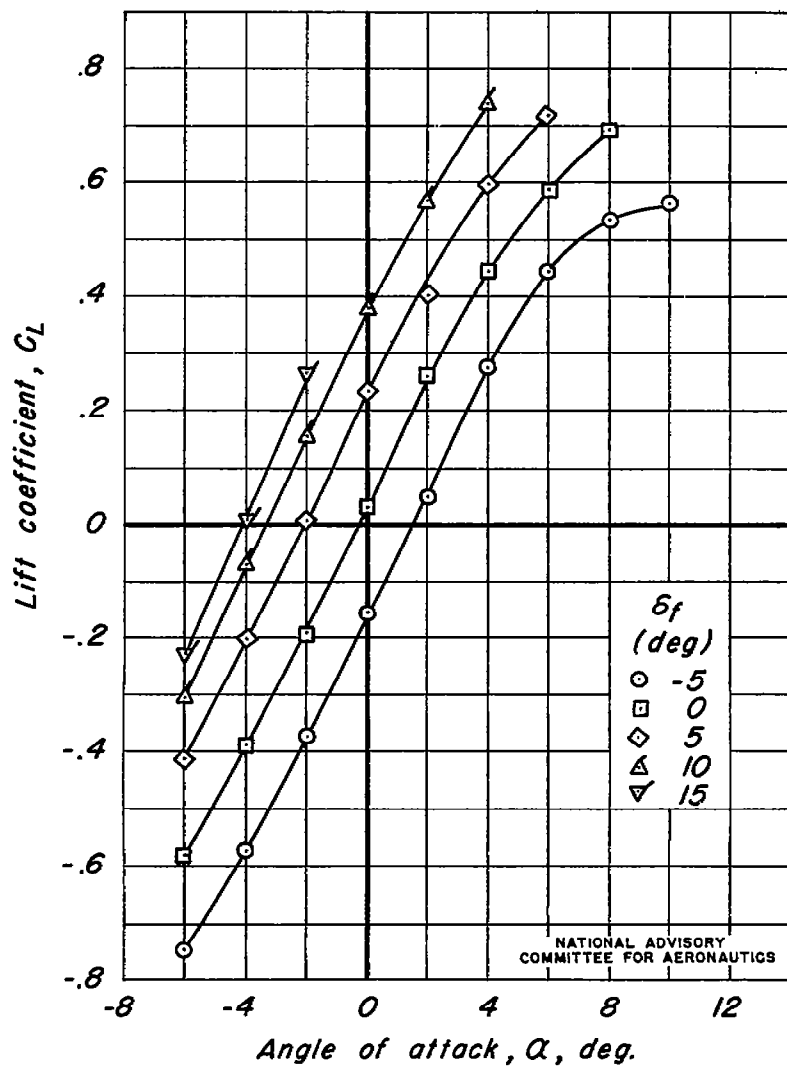
(e) $M, 0.80$

Figure 4.—Continued.

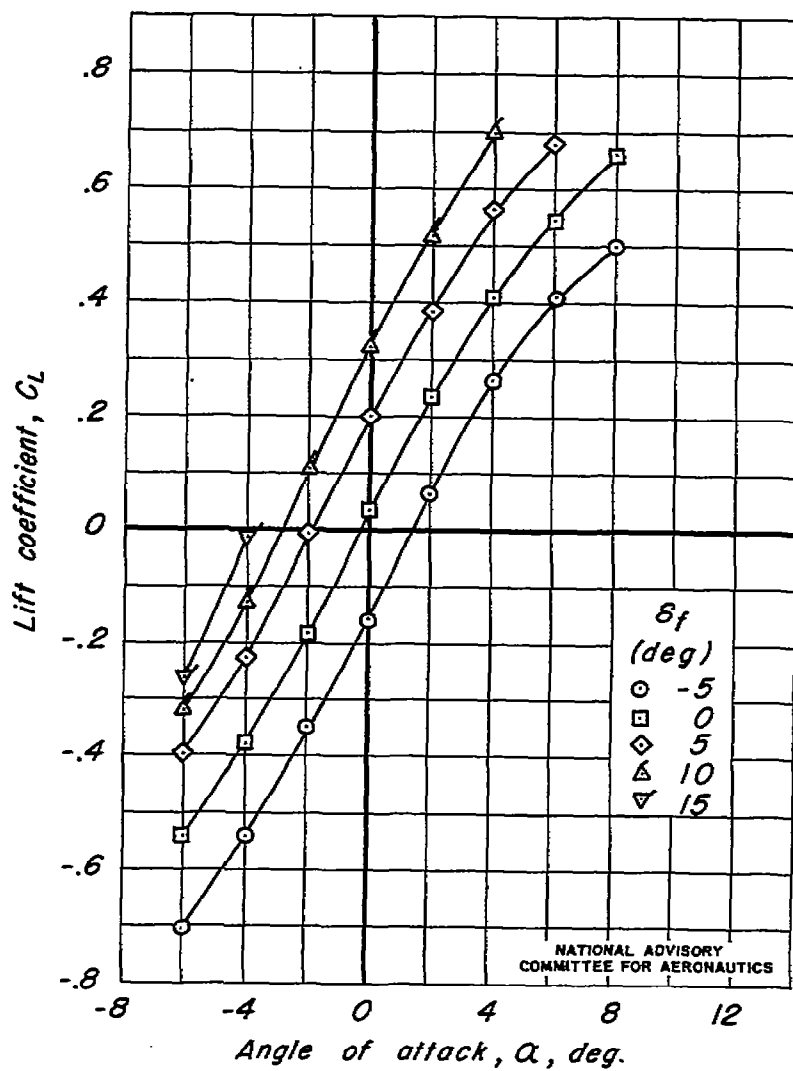
(f) $M, 0.825$

Figure 4. — Continued.

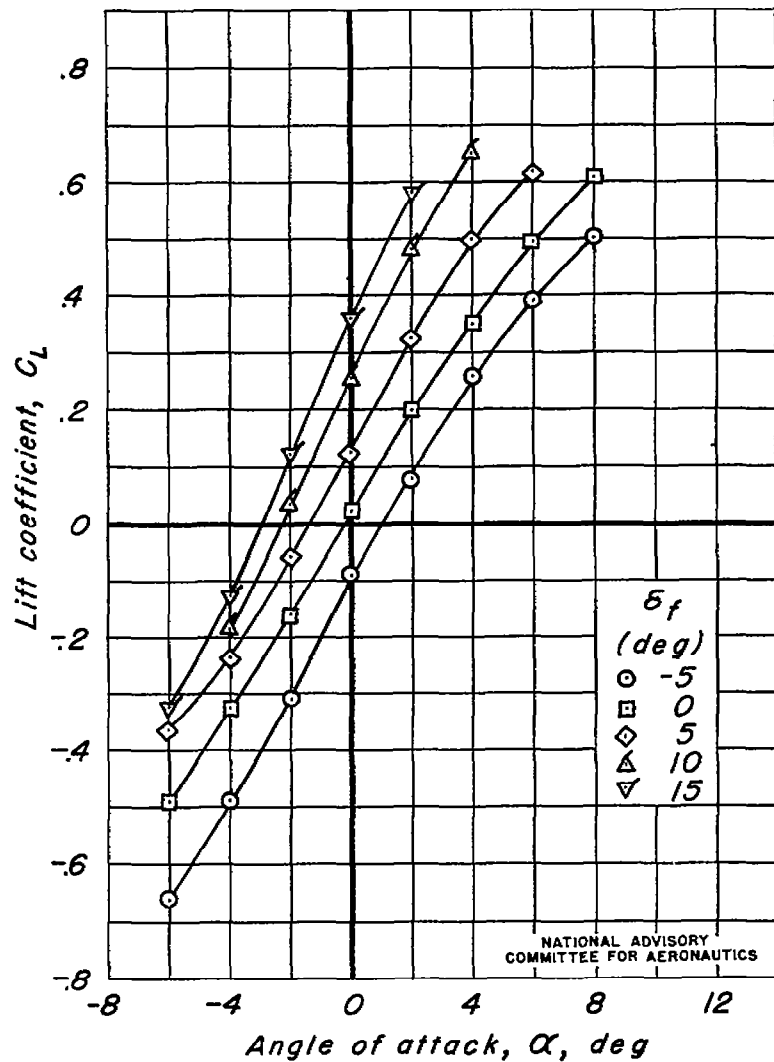
(g) $M, 0.85$

Figure 4. — Continued.

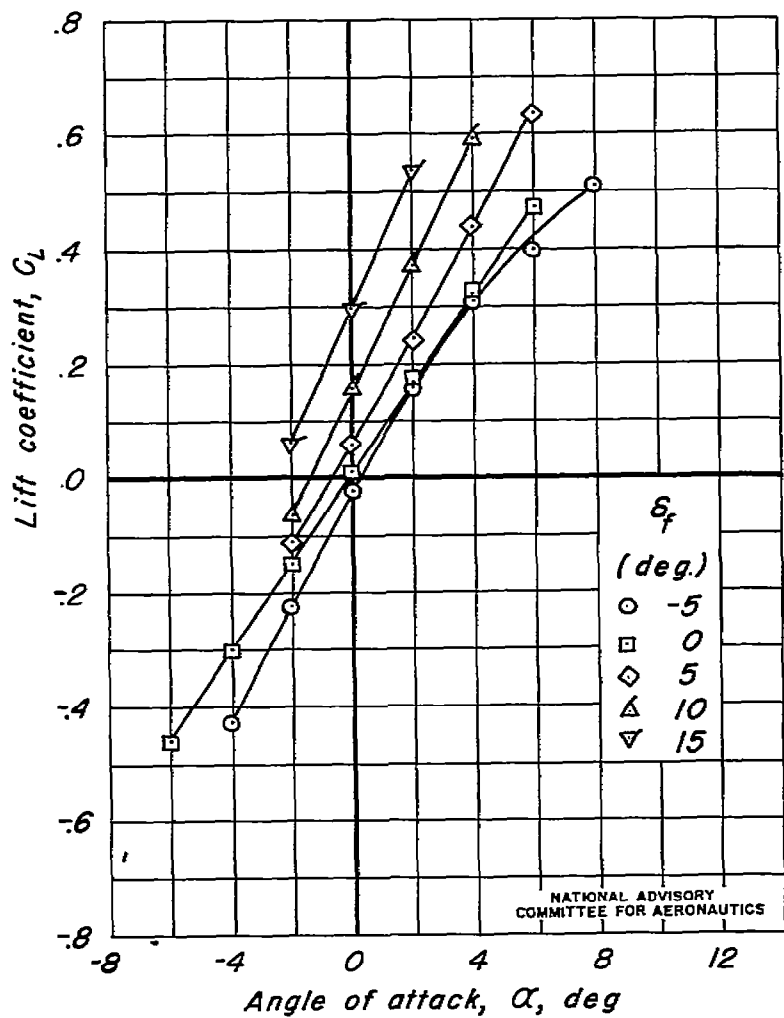
(h) $M, 0.875$

Figure 4. — Concluded.

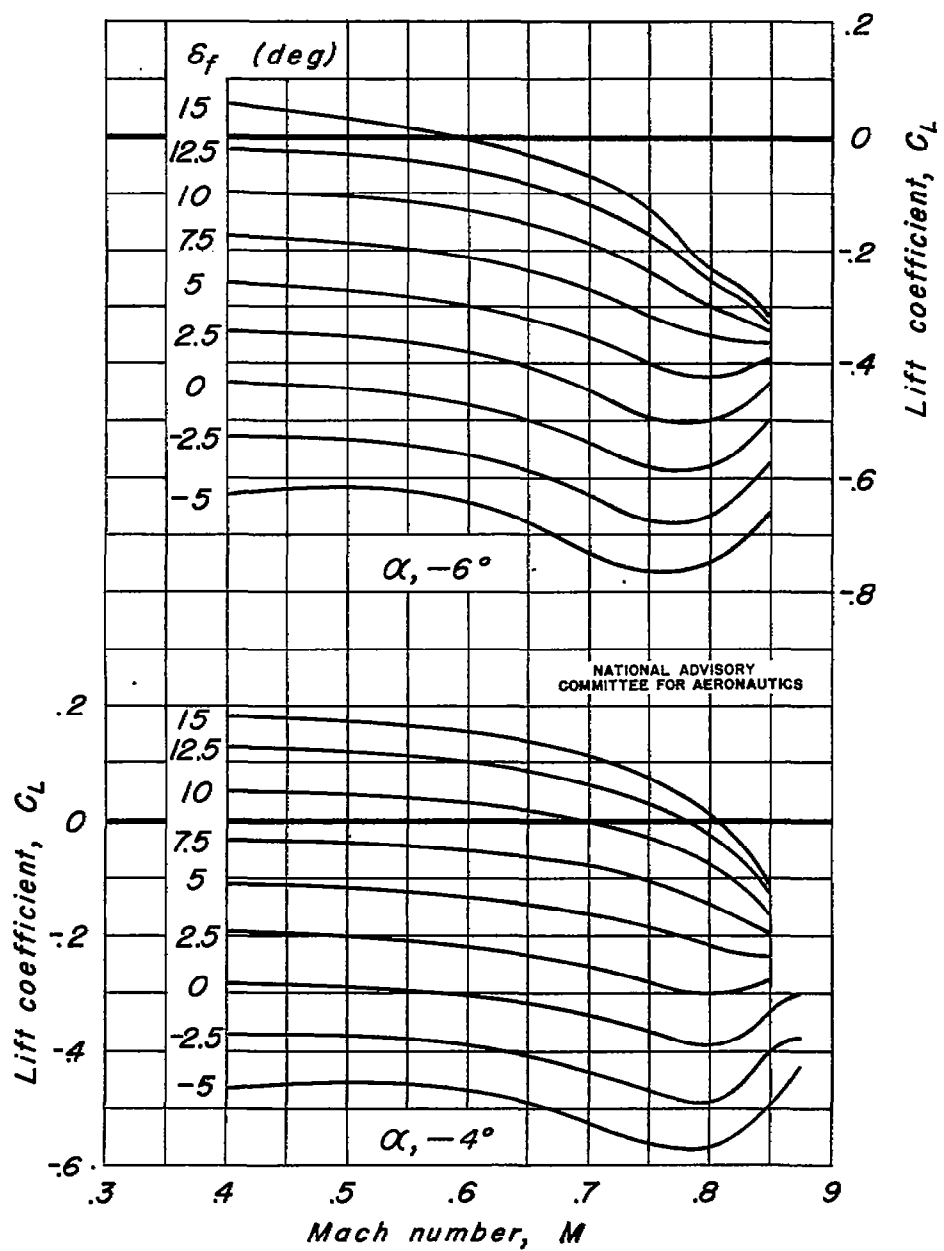
(a) $\alpha, -6^\circ; -4^\circ$.

Figure 5.—Variation of lift coefficient with Mach number.

Unswept; $\delta_f, 0^\circ$

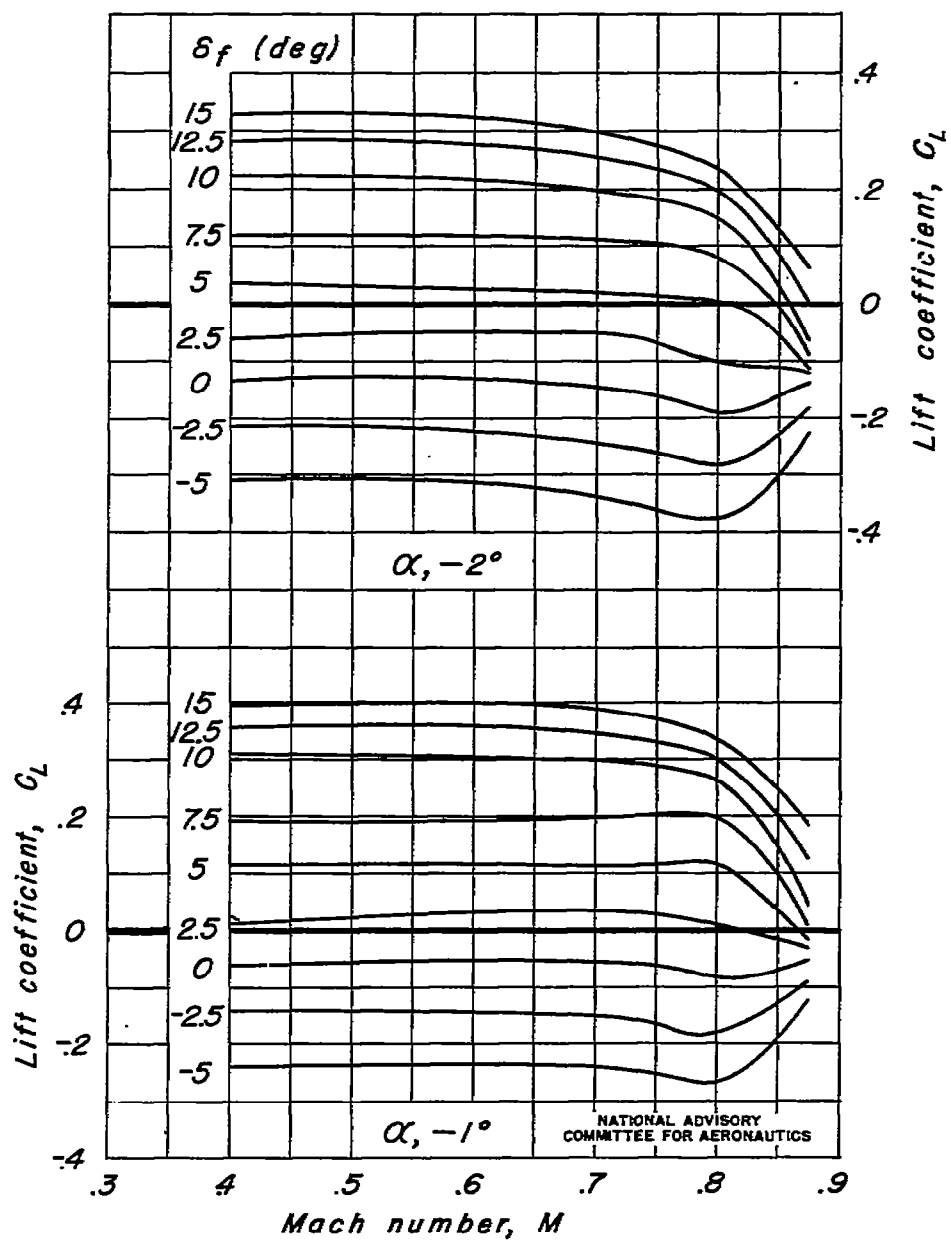
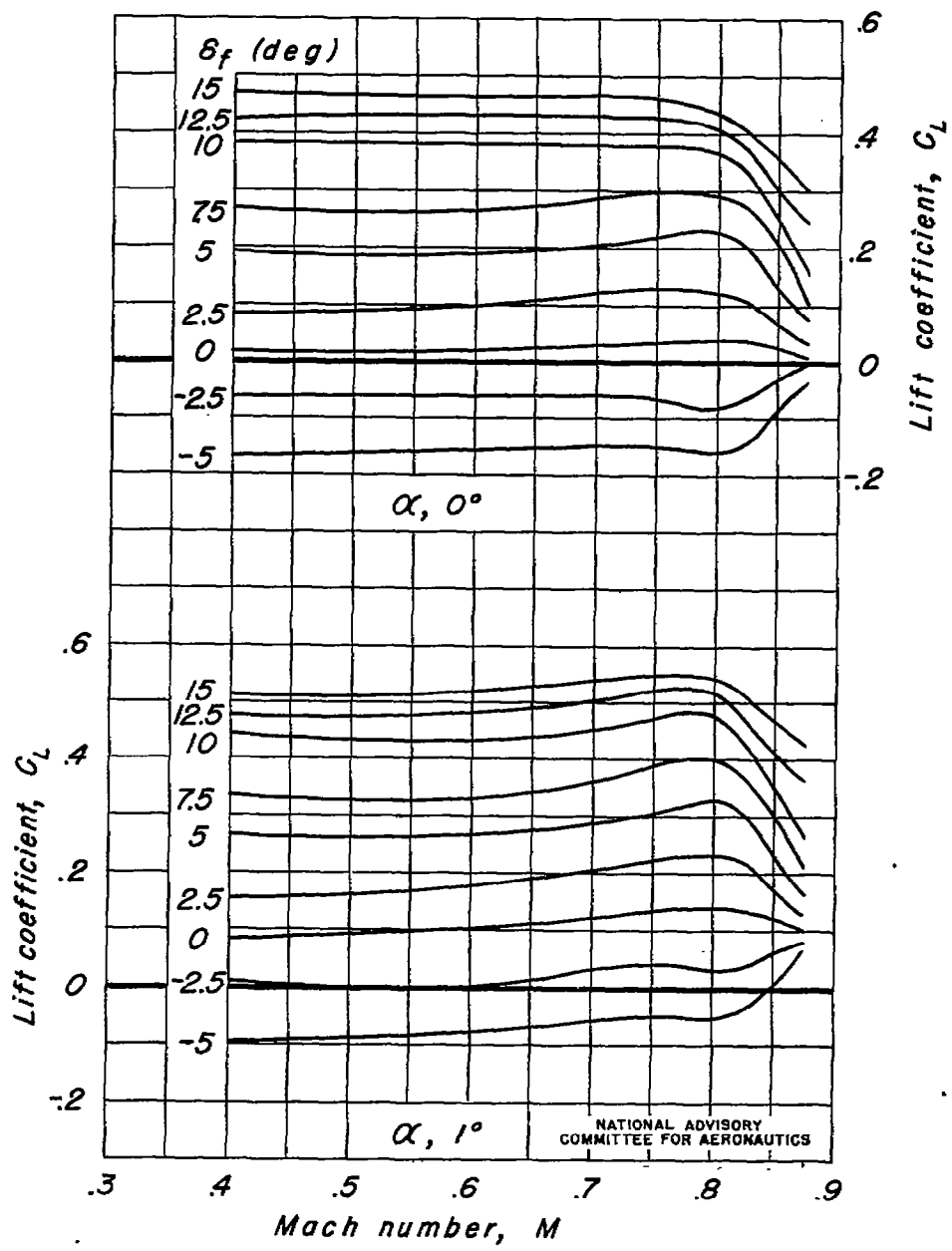
(b) $\alpha, -2^\circ; -1^\circ$.

Figure 5.—Continued.

Fig. 5 c

NACA RM No. A7J22



(a) $\alpha, 0^\circ; 1^\circ$.

Figure 5.—Continued.

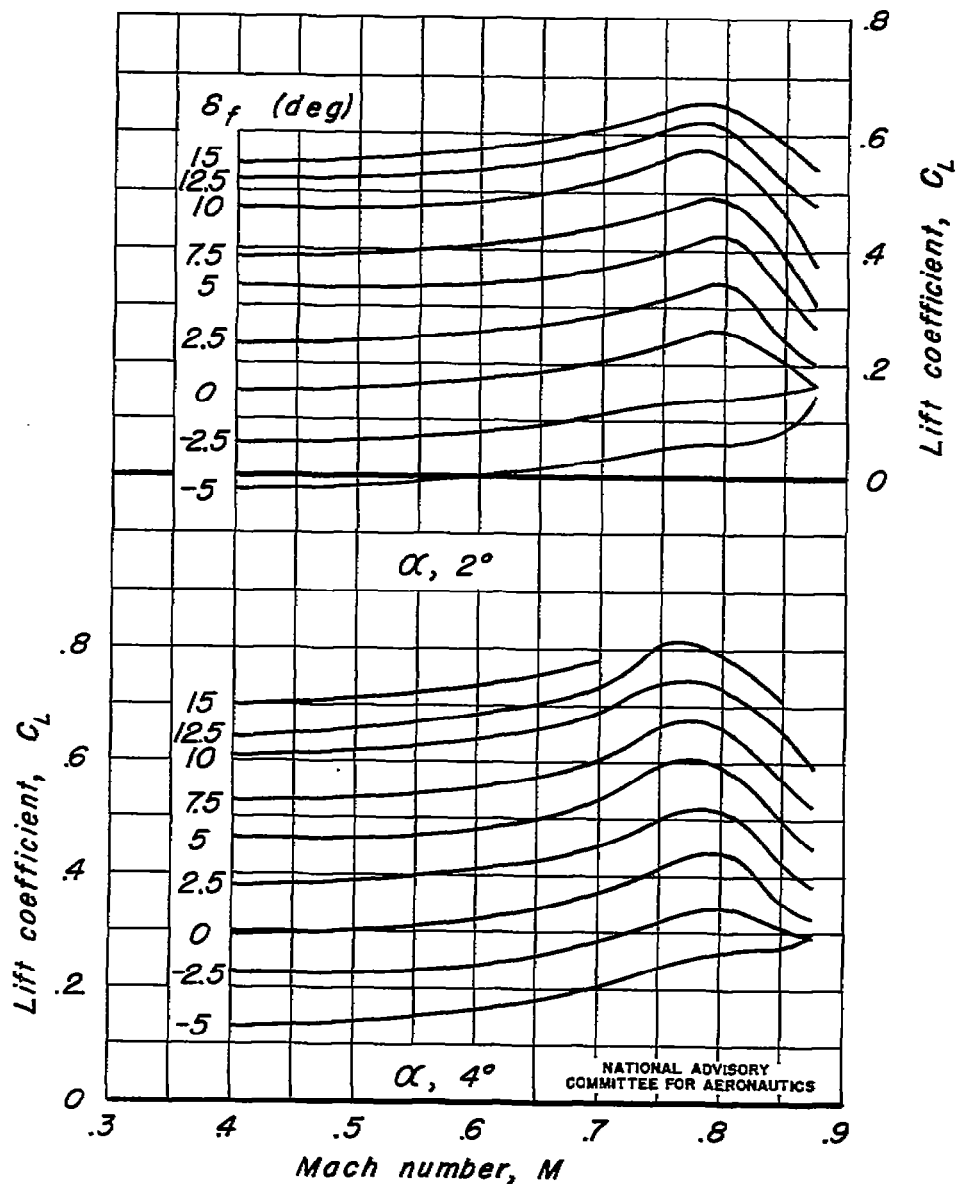
(d) $\alpha, 2^\circ, 4^\circ$

Figure 5.—Continued.

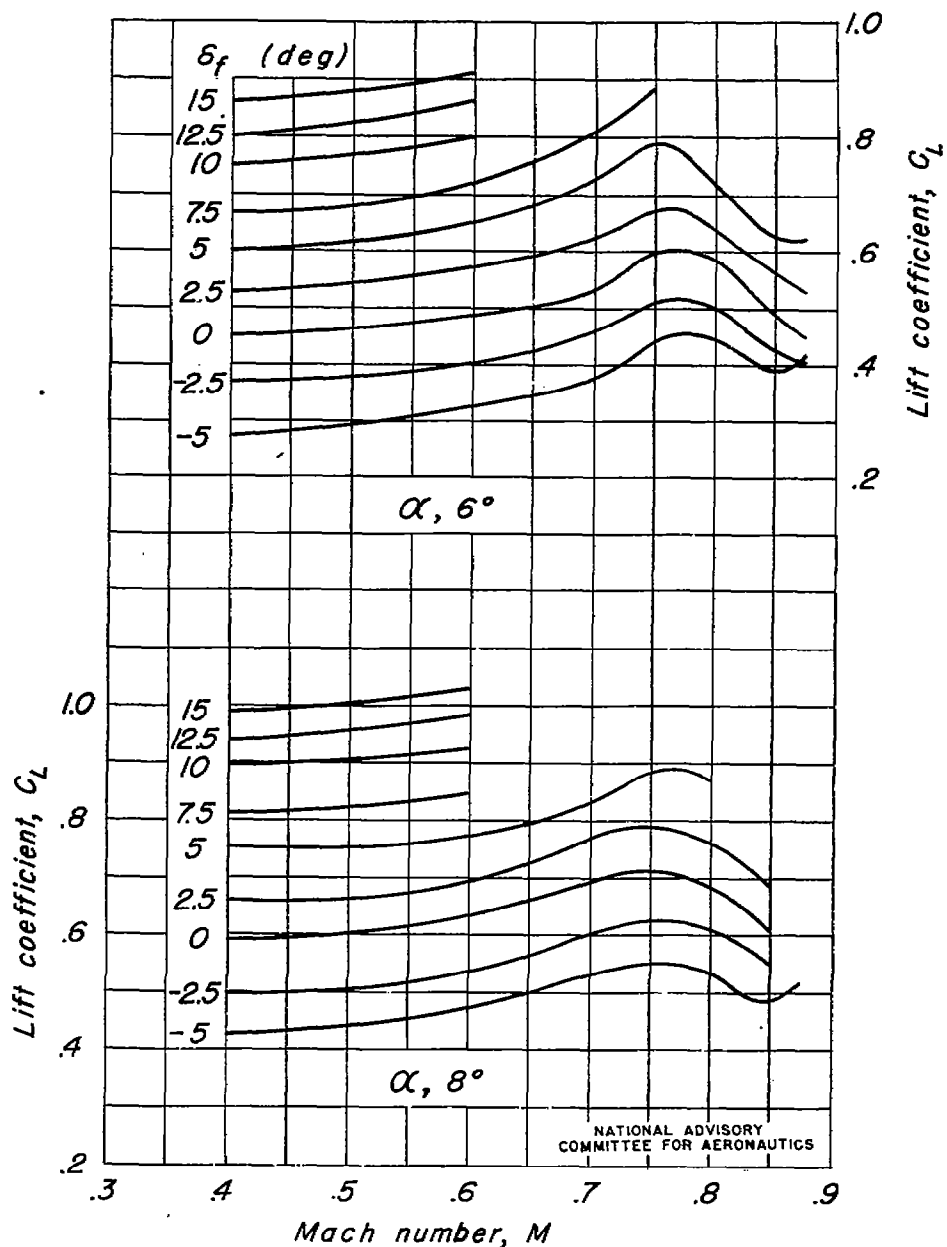
(e) $\alpha, 6^\circ; 8^\circ$

Figure 5.—Concluded.

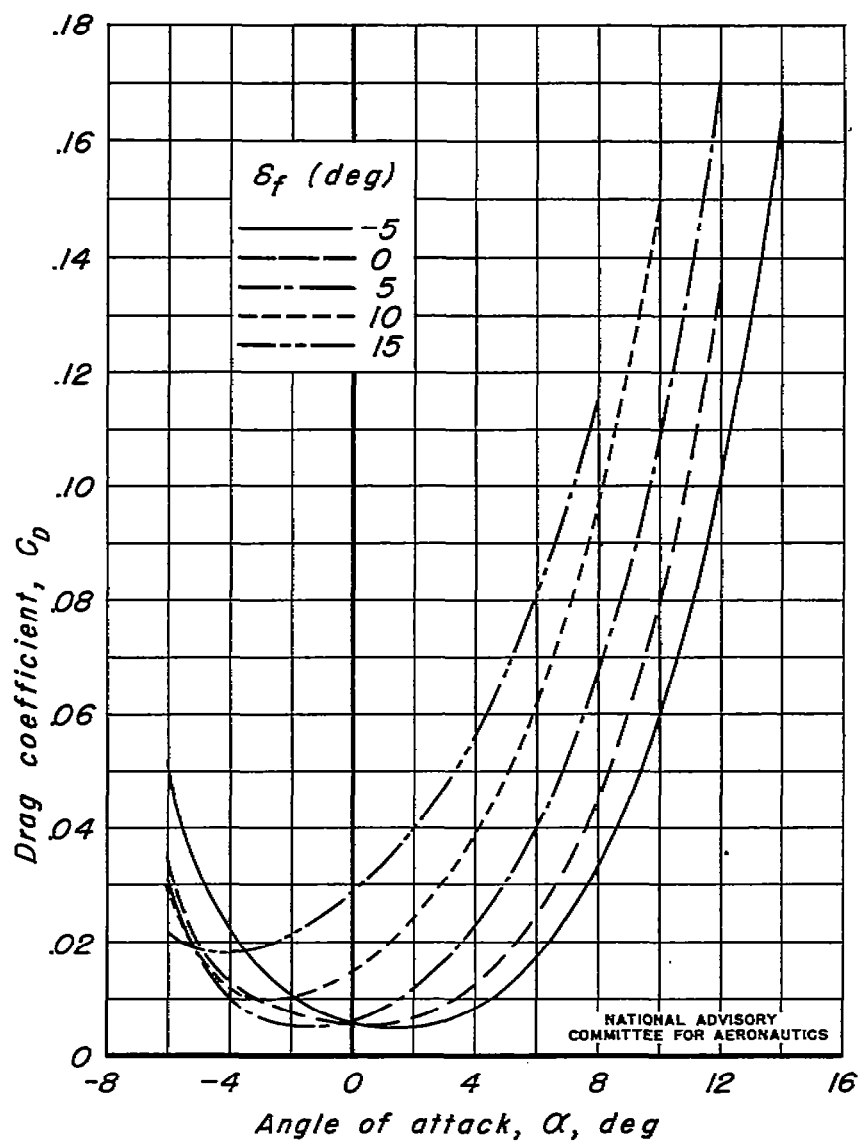
(a) $M, 0.40$

Figure 6.—Variation of drag coefficient with angle of attack. Unswept; $\delta_f, 0^\circ$.

Fig. 6 b

NACA RM No. A7J22

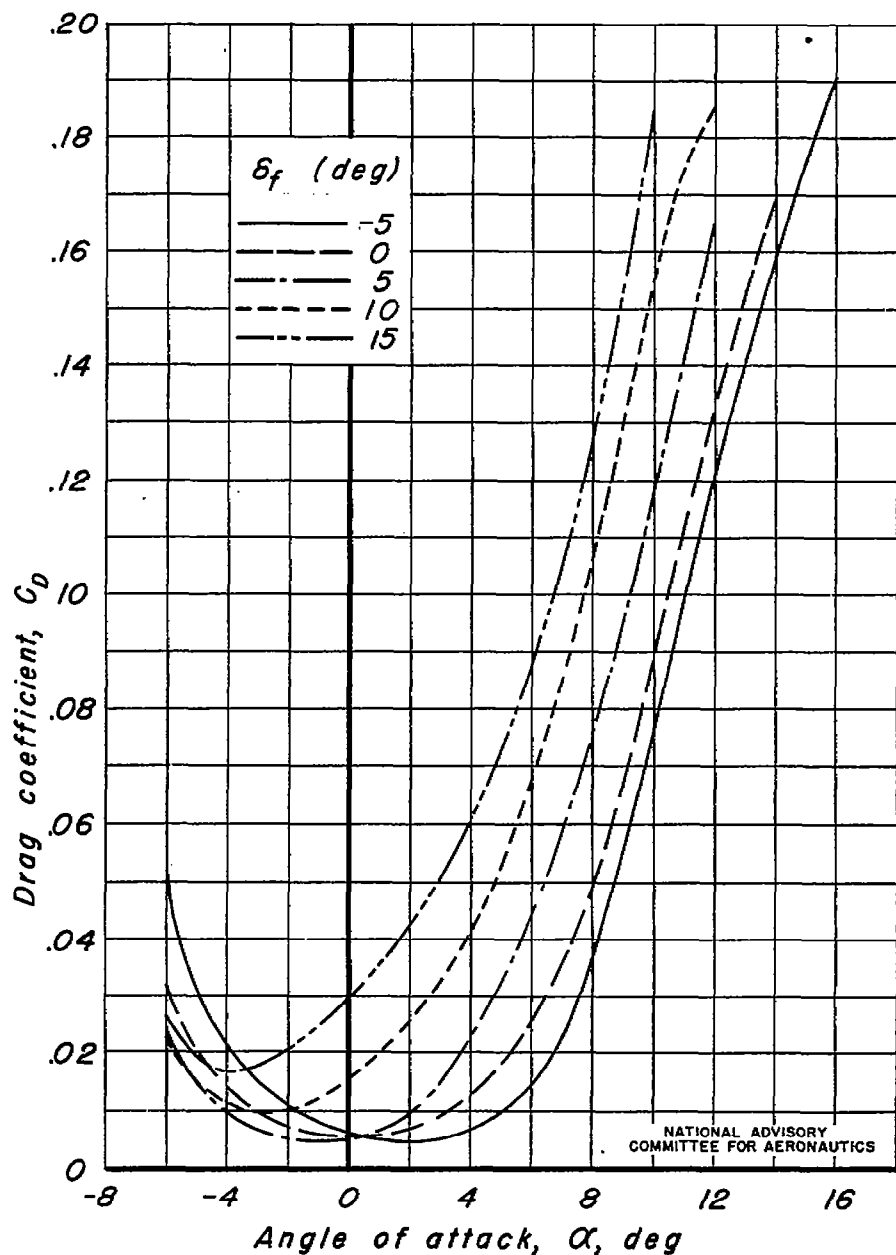
(b) $M, 0.60$

Figure 6.—Continued.

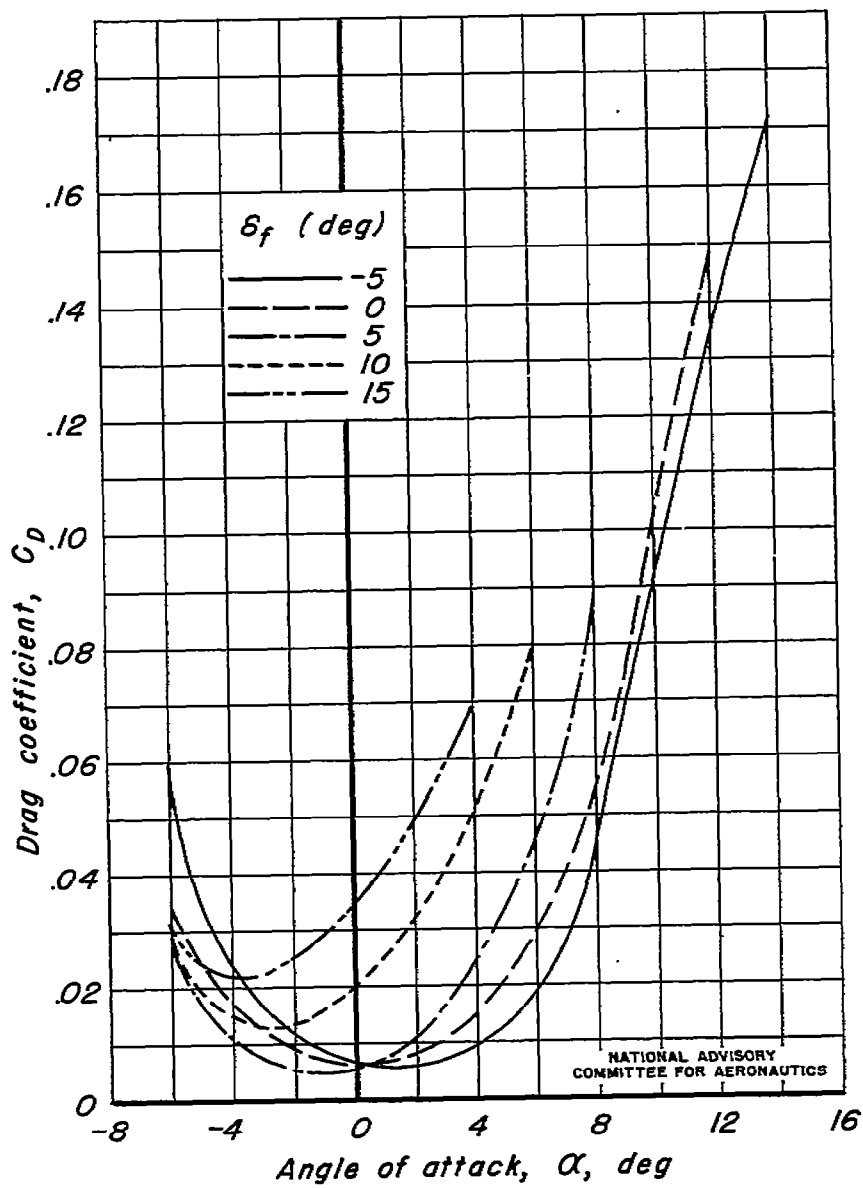
(c) $M, 0.70$

Figure 6.—Continued.

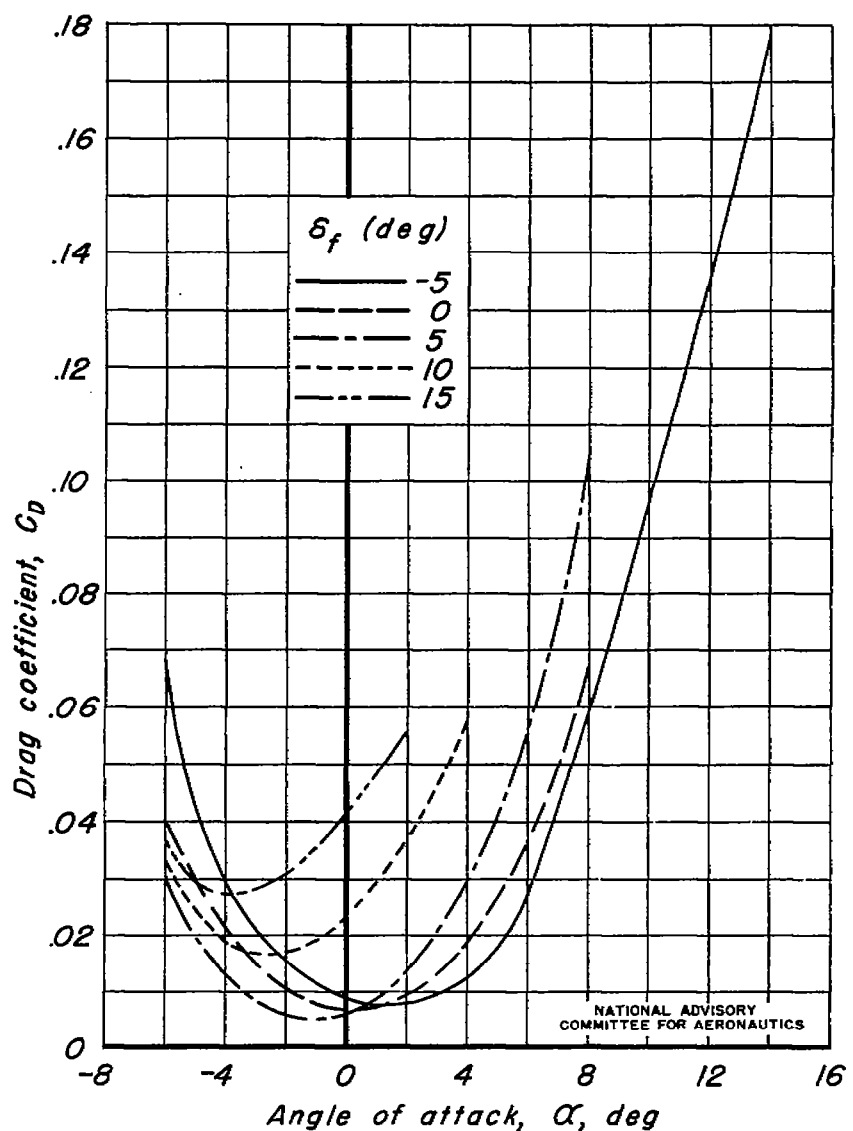
(d) $M, 0.75$

Figure 6.—Continued.

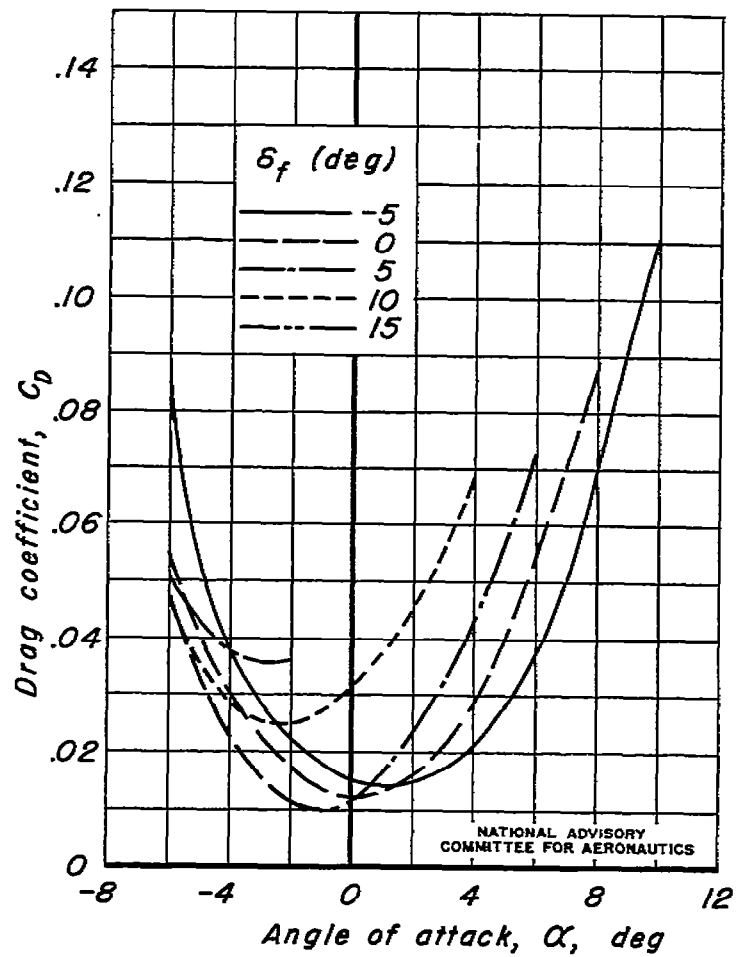
(e) $M, 0.80$

Figure 6.—Continued.

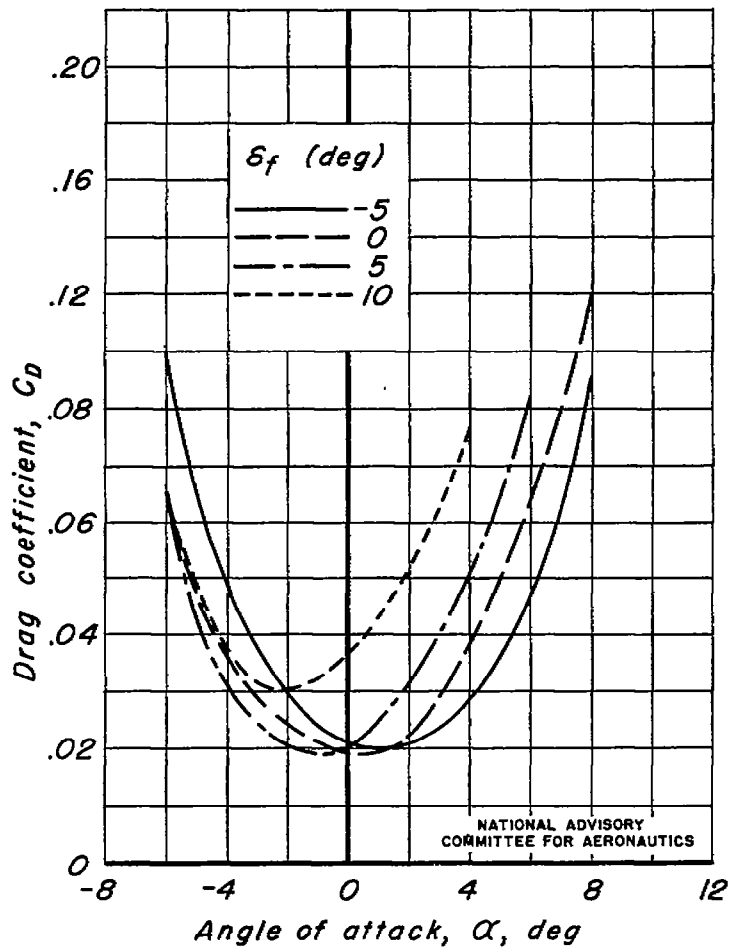
(f) $M, 0.825$

Figure 6.—Continued.

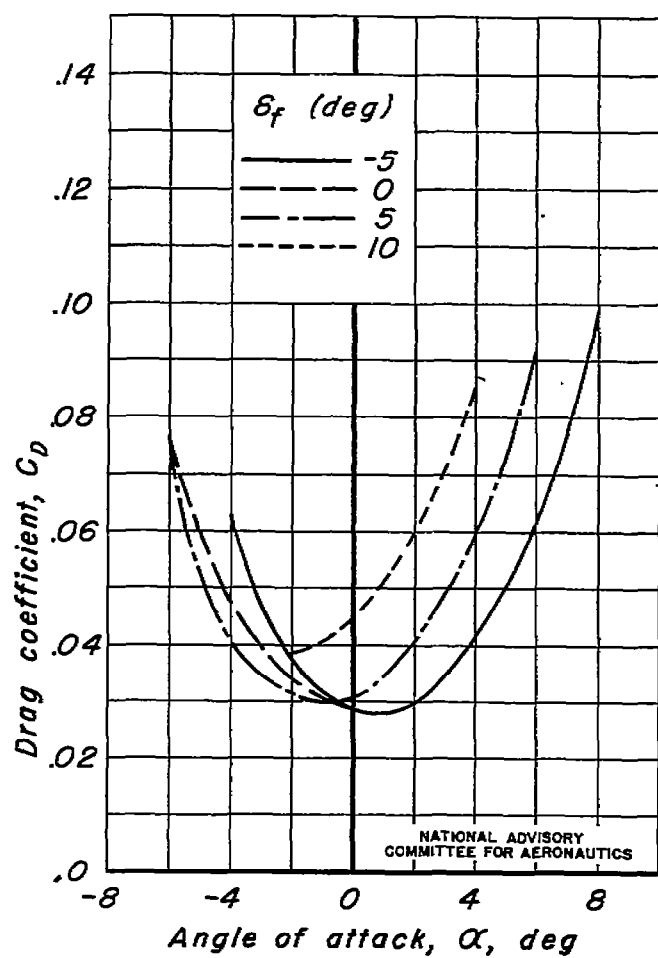
(g) $M, 0.85$

Figure 6.—Continued.

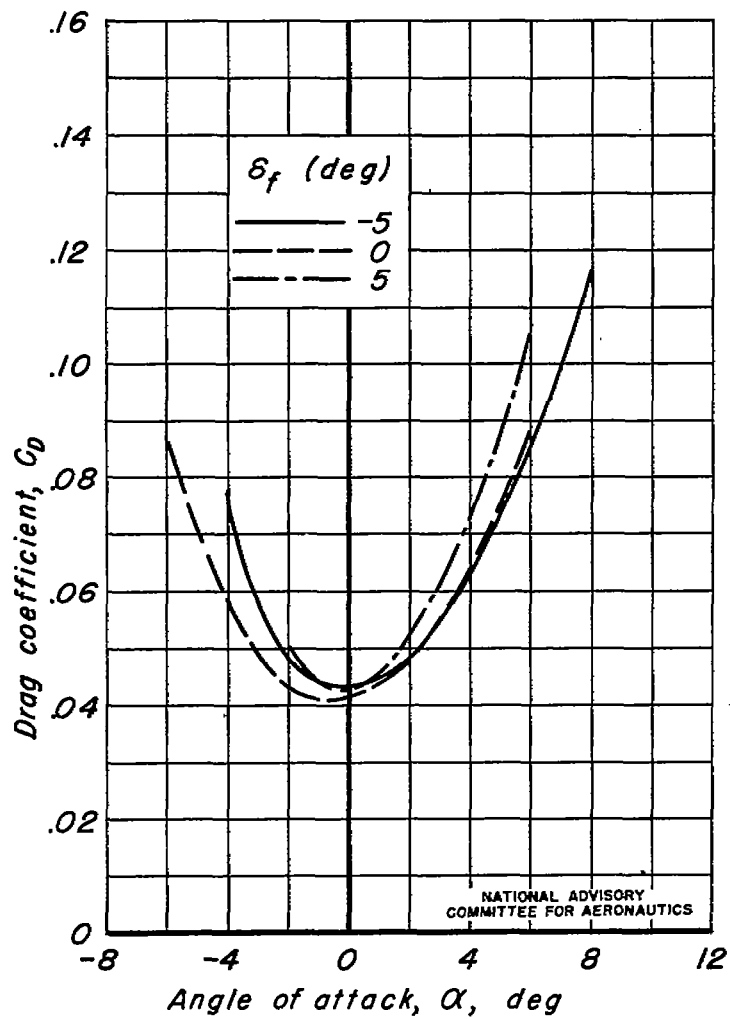
(h) $M, 0.875$

Figure 6.—Concluded.

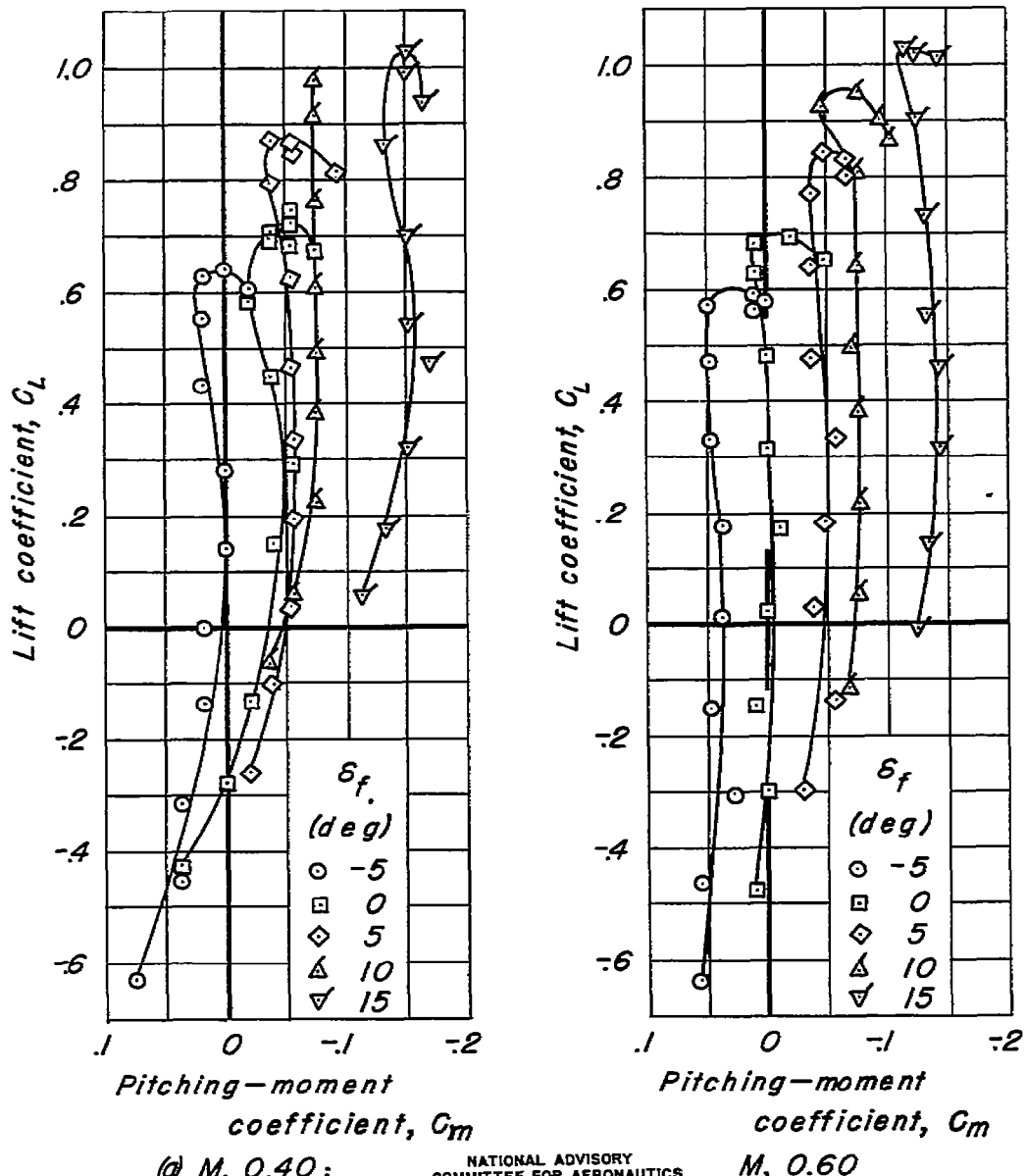


Figure 7.—Variation of pitching-moment coefficient with lift coefficient. Unswept; $\delta_t, 0^\circ$

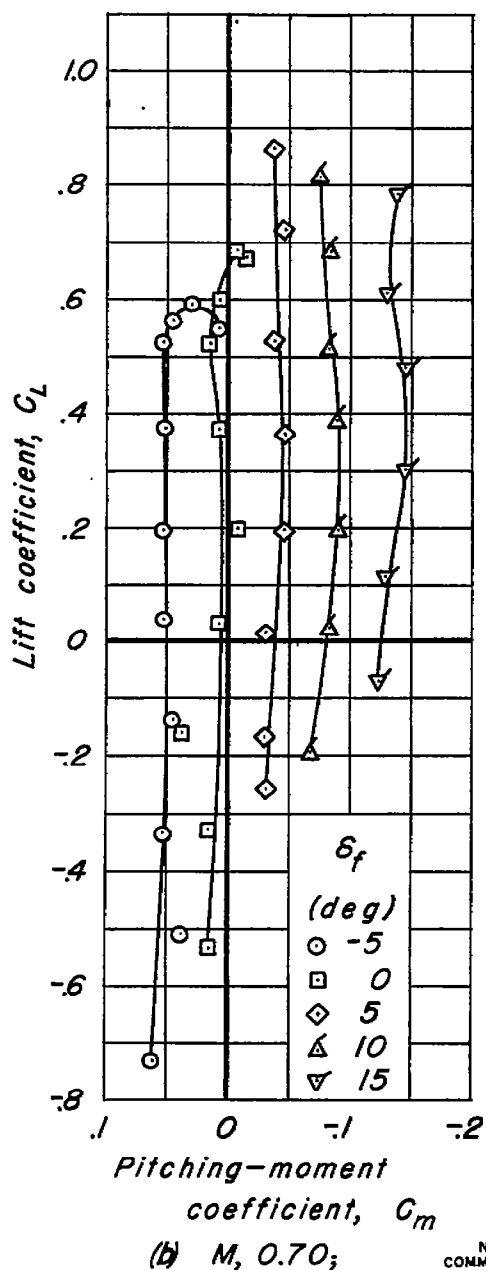
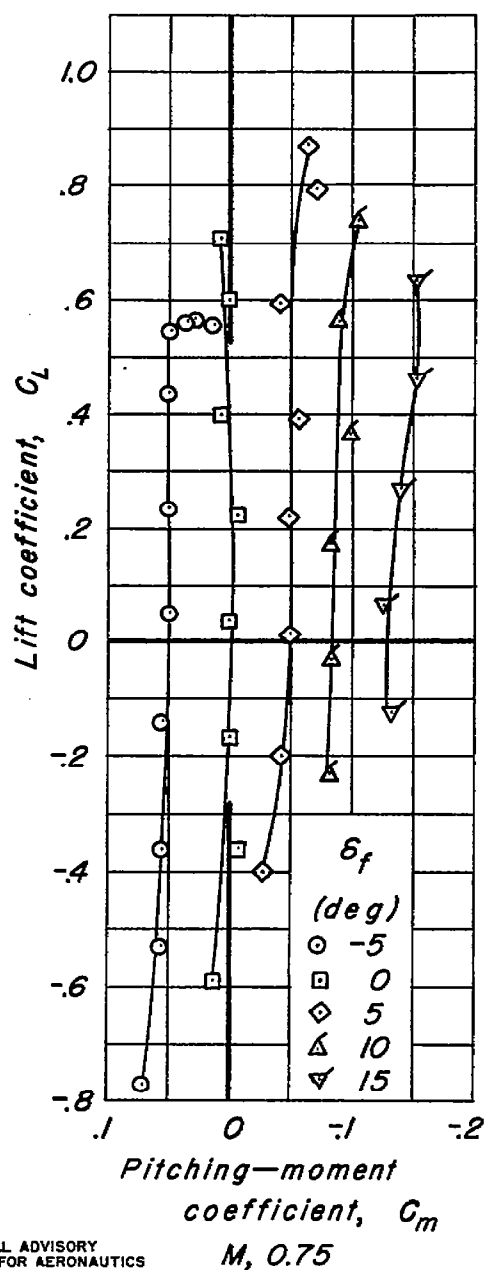
(b) $M, 0.70;$ NATIONAL ADVISORY
COMMITTEE FOR AERONAUTICS $M, 0.75$

Figure 7.—Continued.

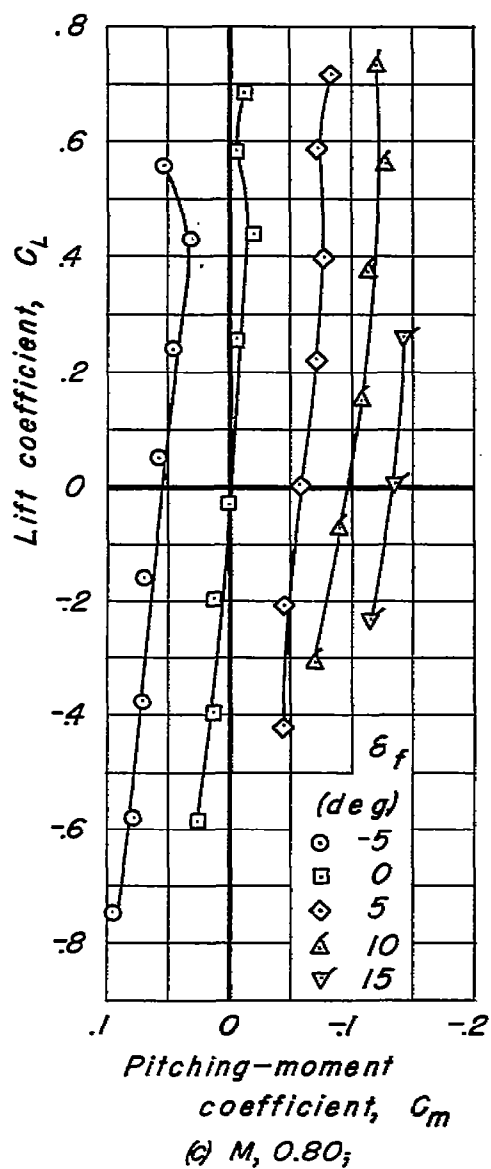
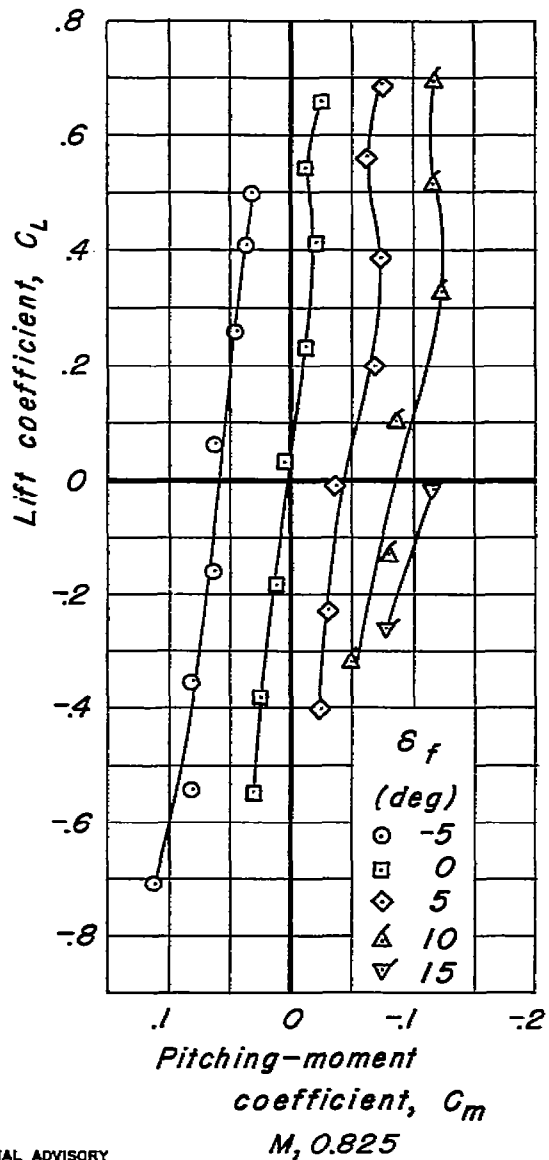
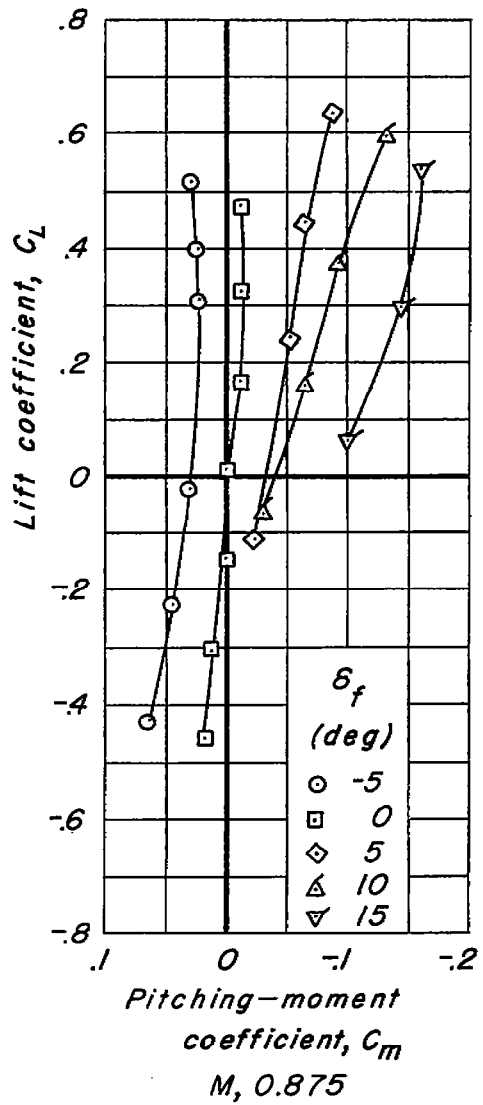
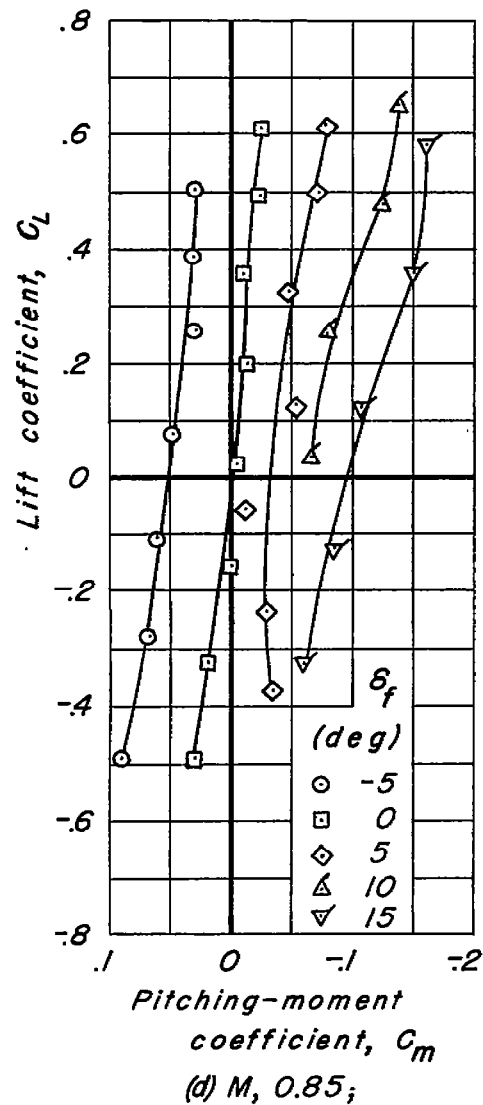
(a) $M, 0.80;$ NATIONAL ADVISORY
COMMITTEE FOR AERONAUTICS(b) $M, 0.825$

Figure 7.—Continued.



NATIONAL ADVISORY
COMMITTEE FOR AERONAUTICS

Figure 7—Concluded.

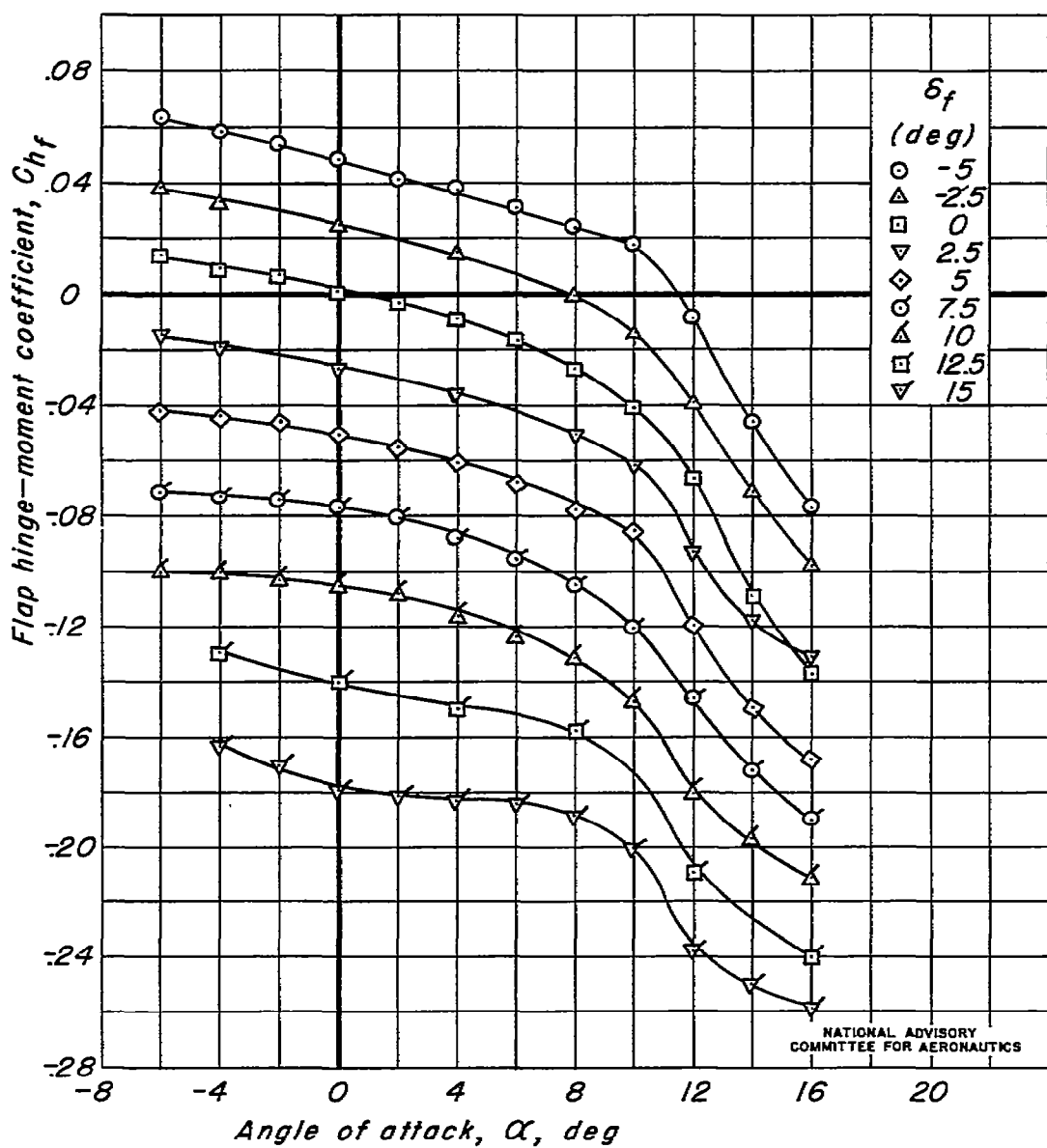
(a) $M, 0.40$

Figure 8.—Variation of flap hinge-moment coefficient with angle of attack. Unswept; $\delta_t, 0^\circ$.

Fig. 8 b

NACA RM No. A7J22

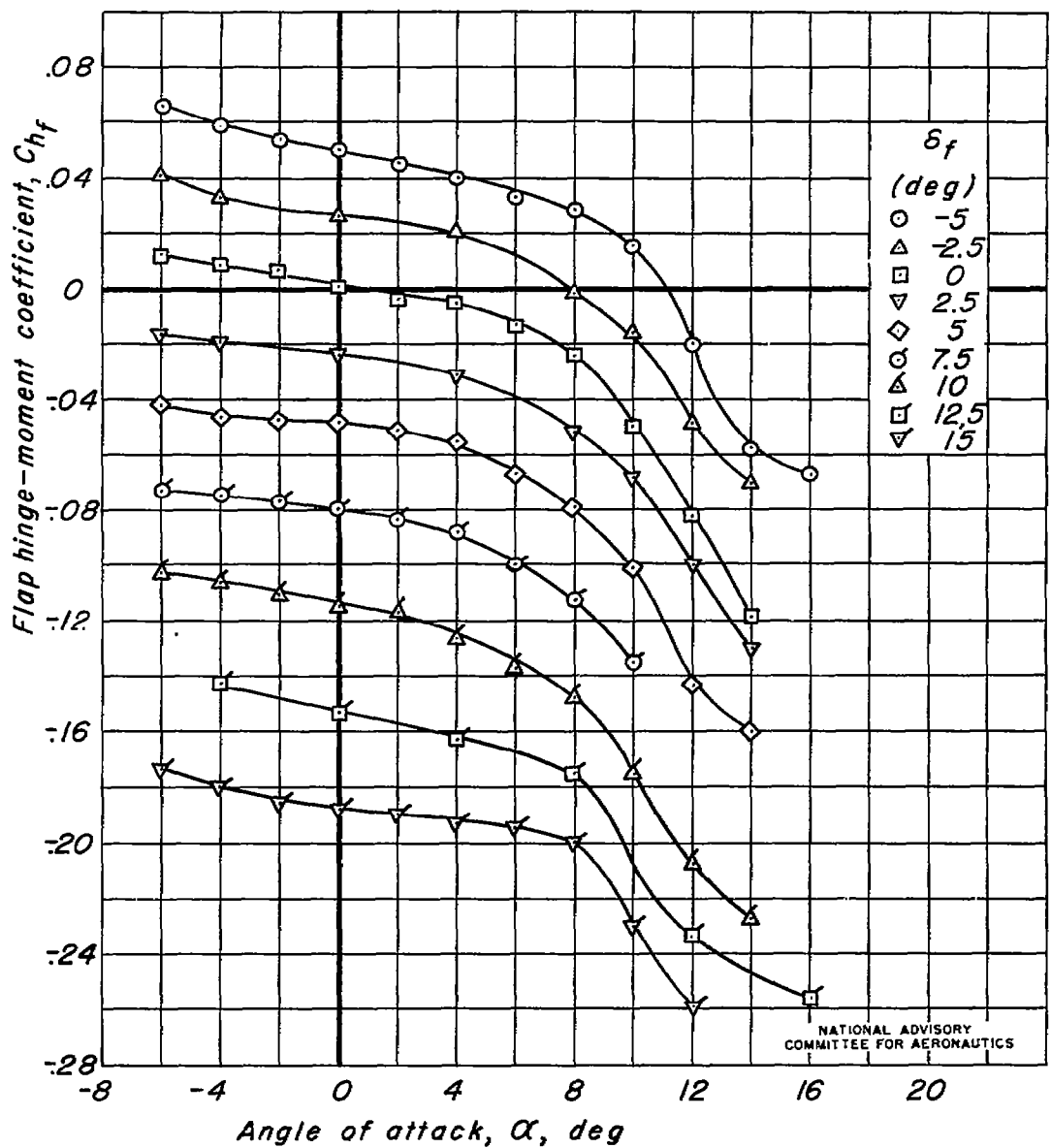
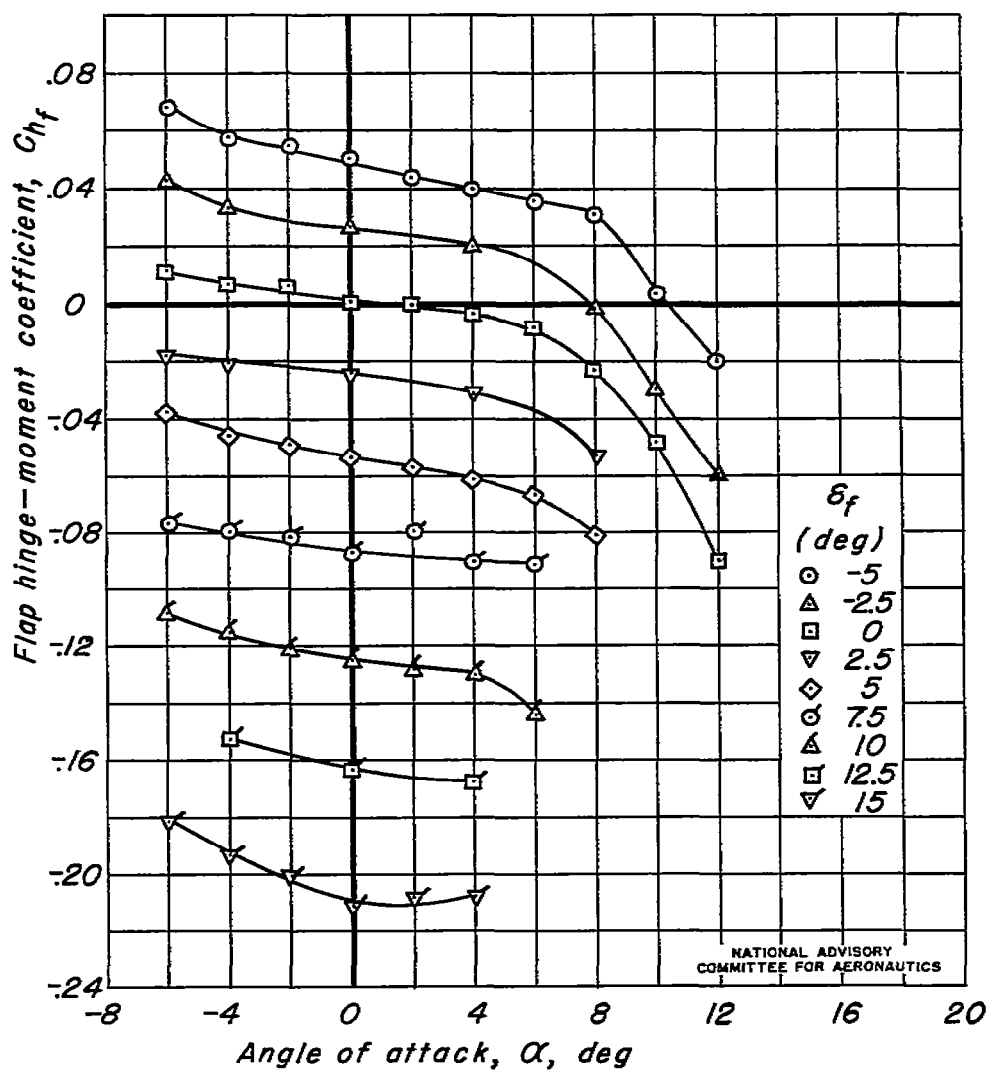
(b) $M, 0.60$

Figure 8.—Continued.

(c) $M, 0.70$ *Figure 8.-Continued.*

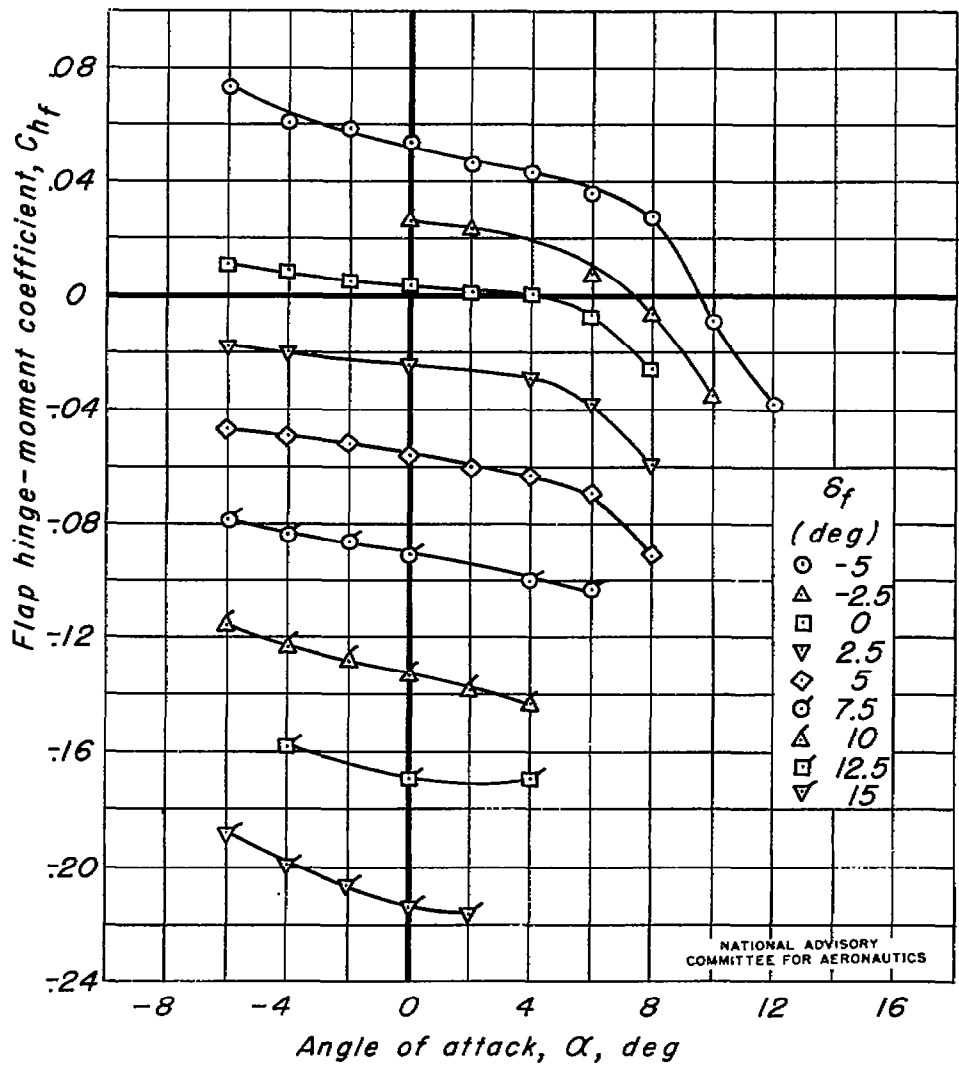
(d) $M, 0.75$

Figure 8.—Continued.

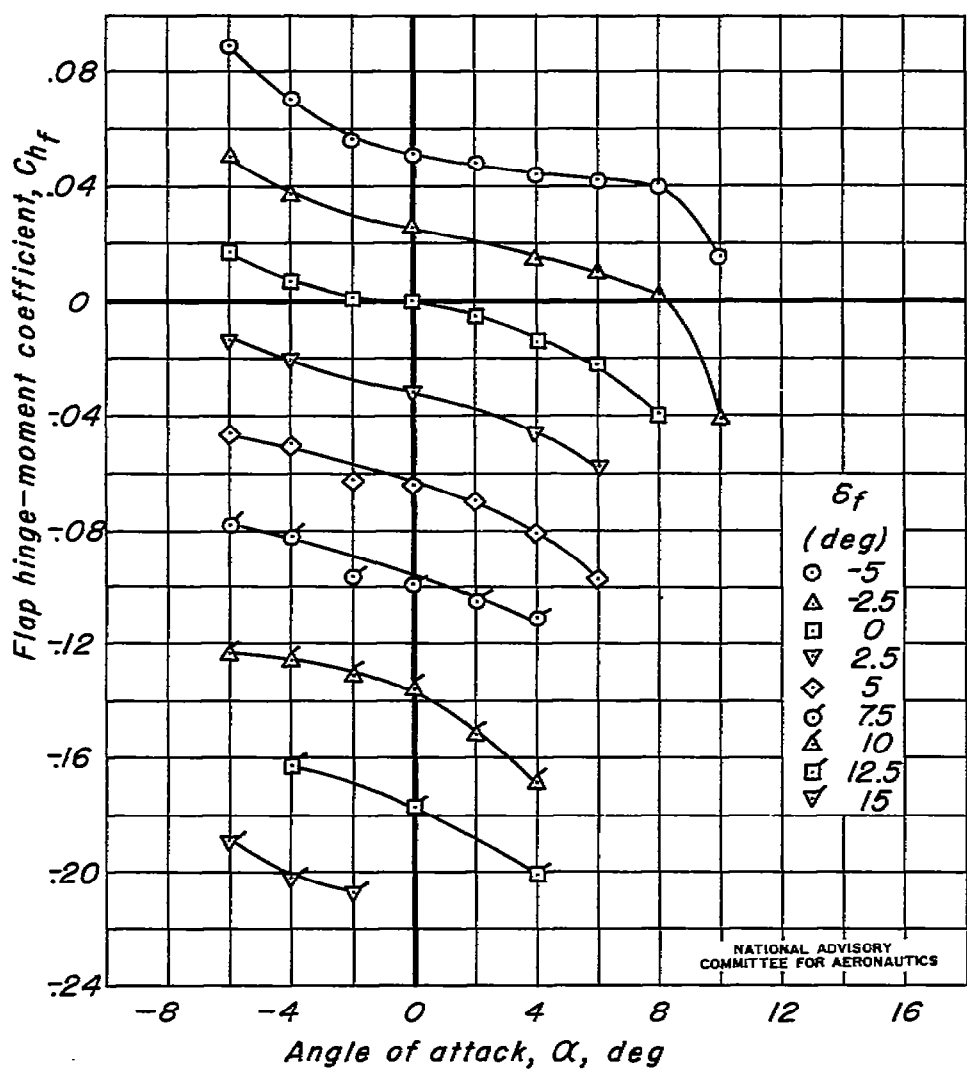
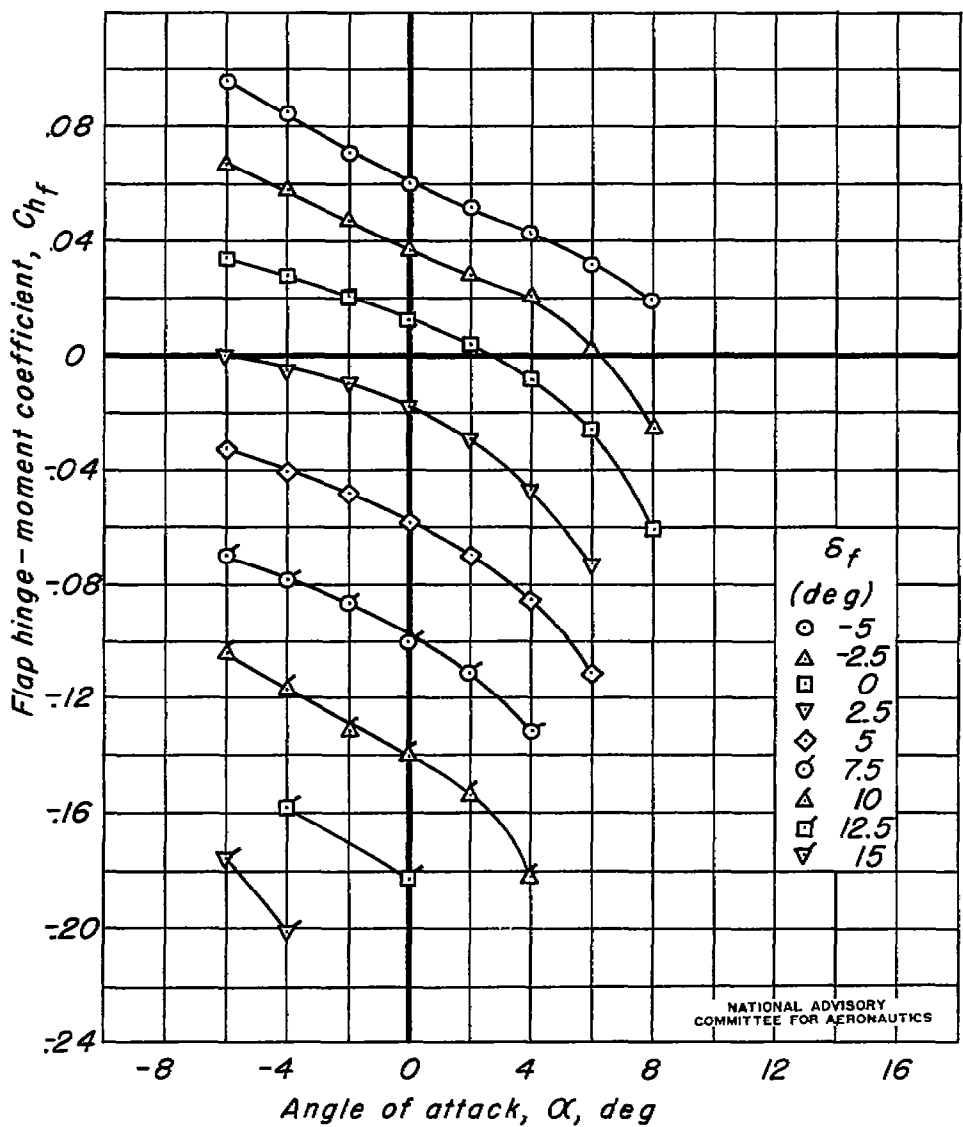
(e) $M, 0.80$

Figure 8.—Continued.

(f) $M, 0.825$ *Figure 8.—Continued.*

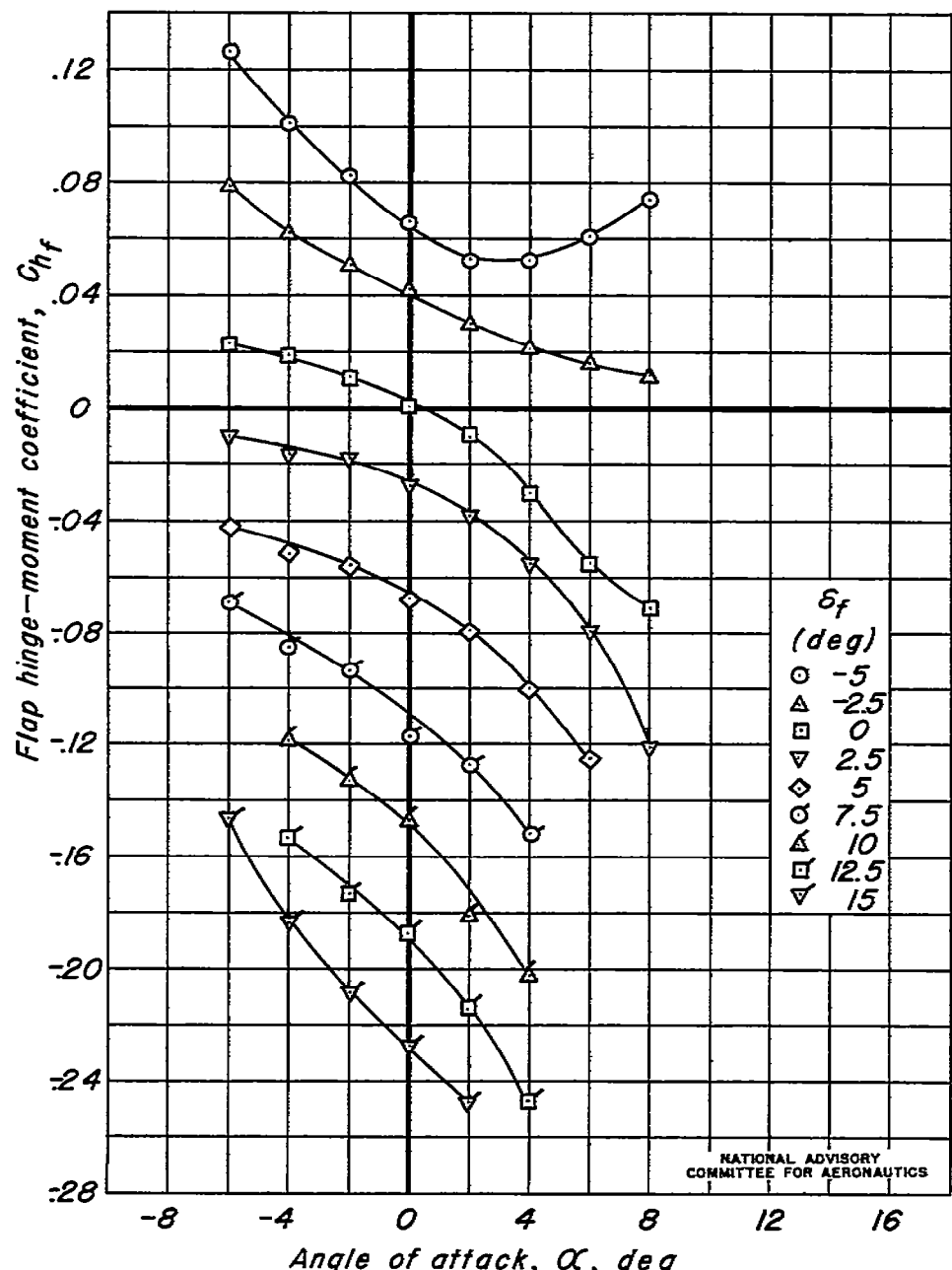
(g) $M, 0.85$

Figure 8.—Continued.

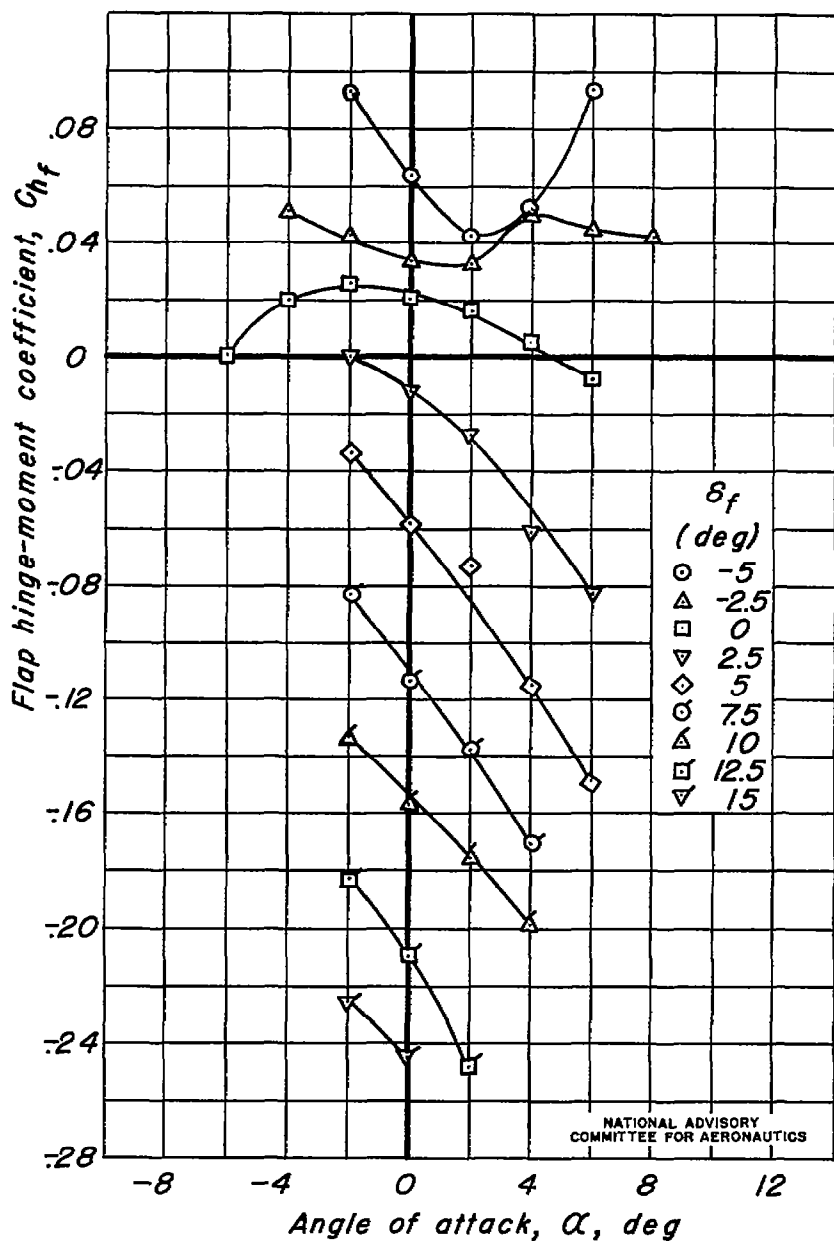
(b) $M, 0.875$

Figure 8.—Concluded.

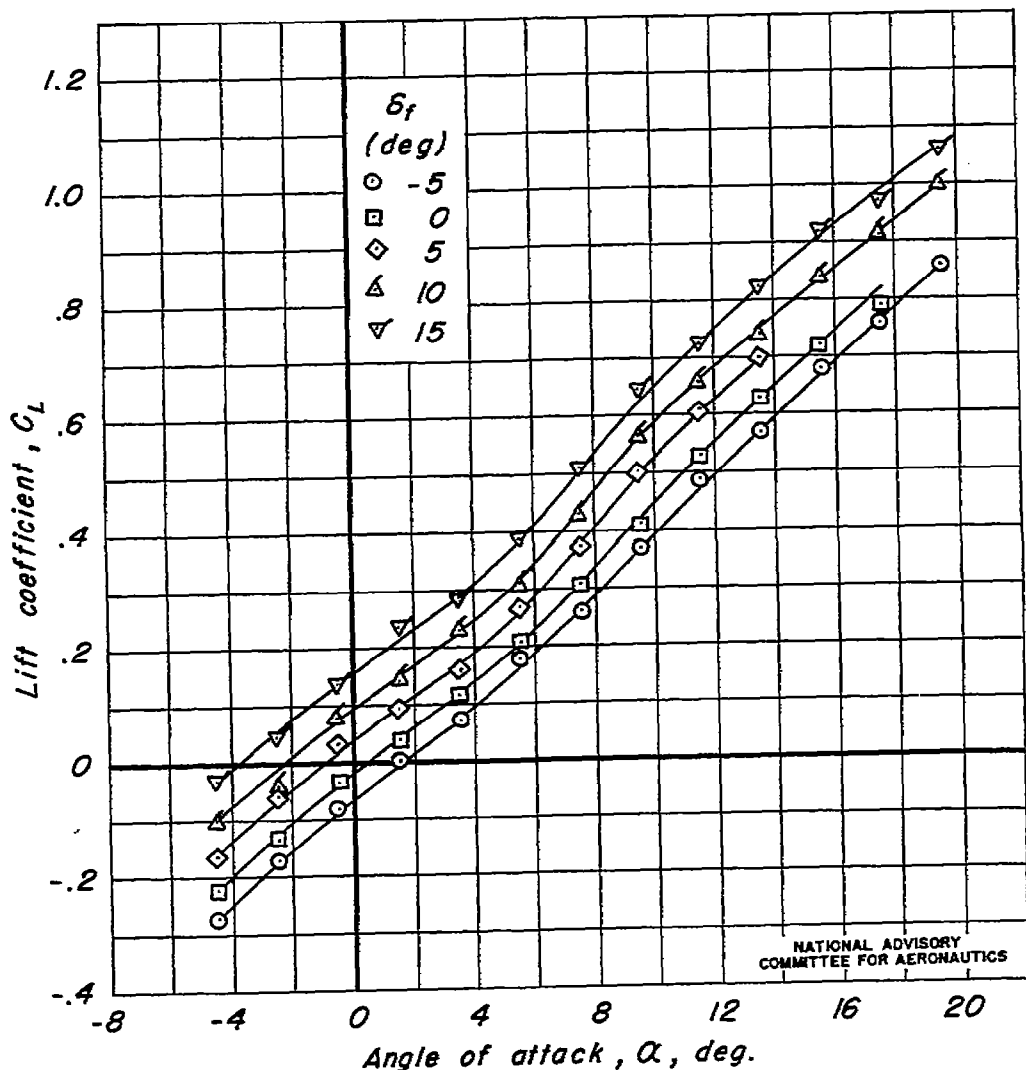
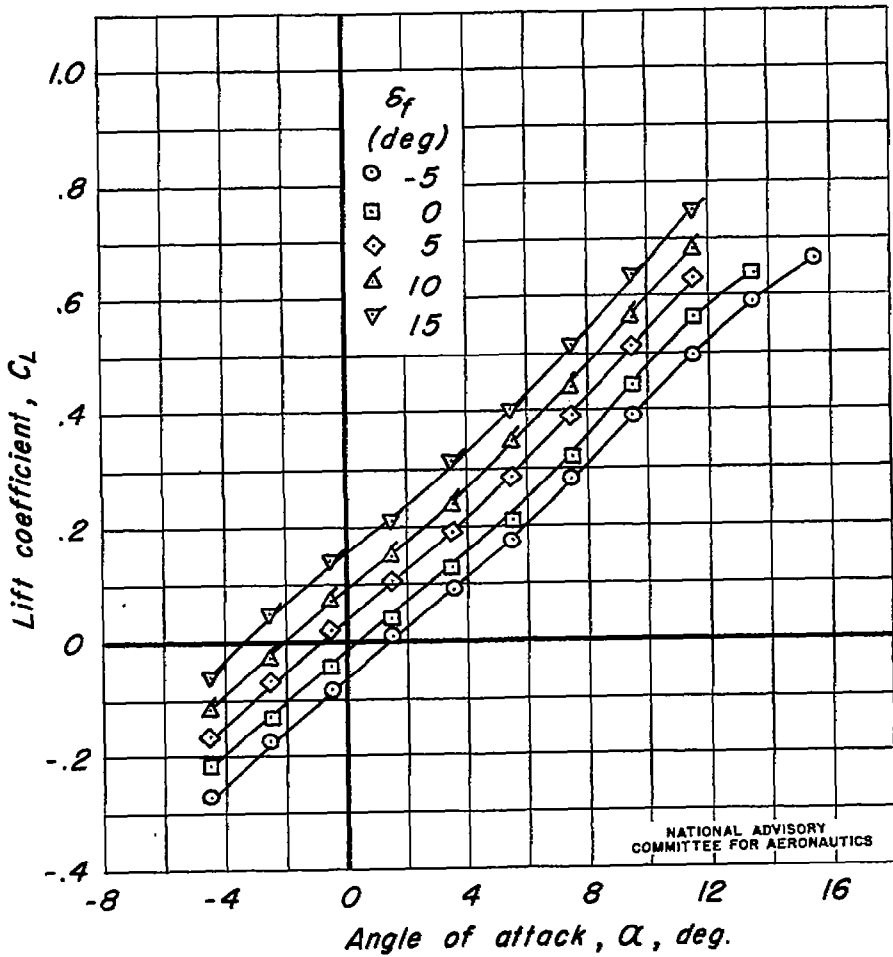
(a) $M, 0.40$

Figure 9.—Variation of lift coefficient with angle of attack.

Swept back 45°; δ_t , 0°

Fig. 9 b

NACA RM No. A7J22



(b) $M, 0.60$

Figure 9.—Continued.

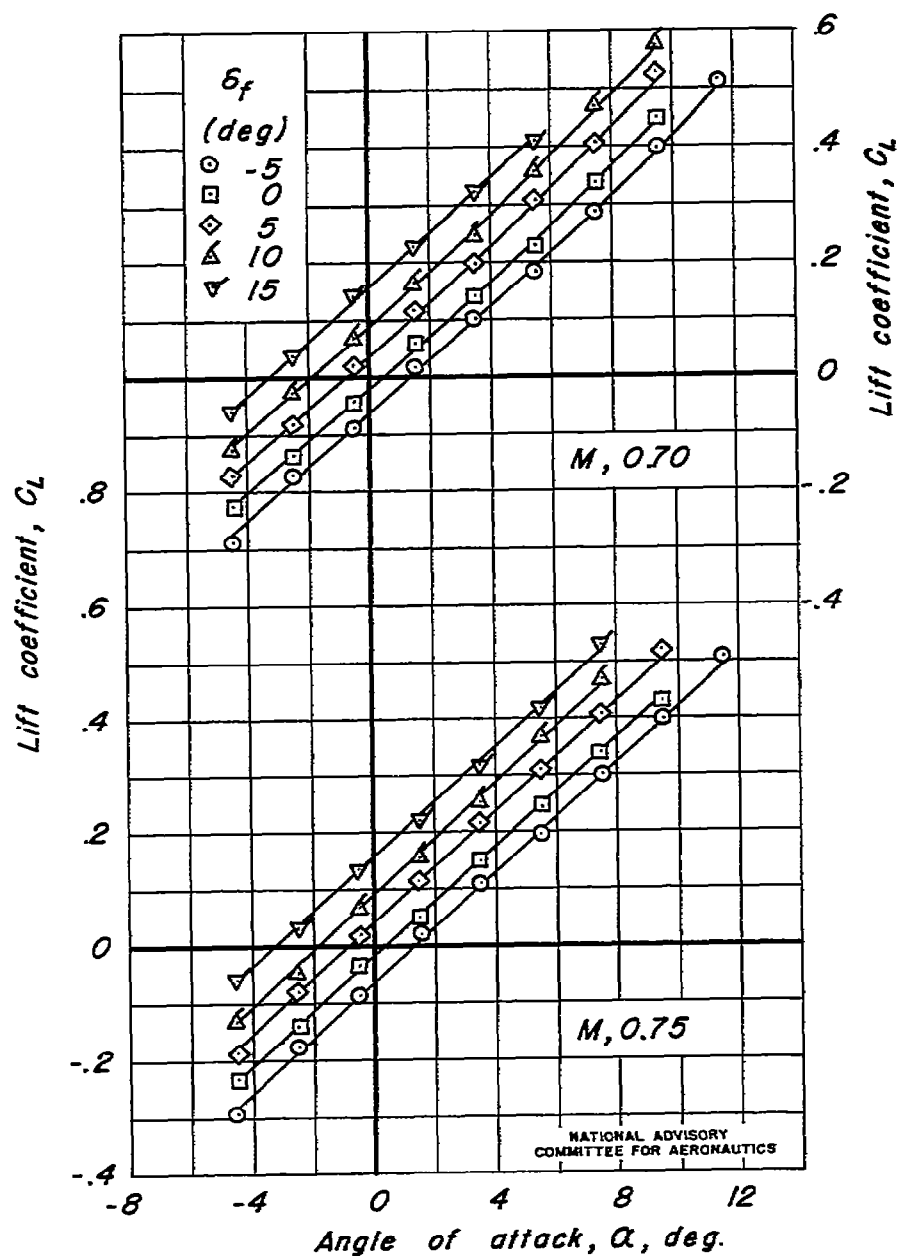
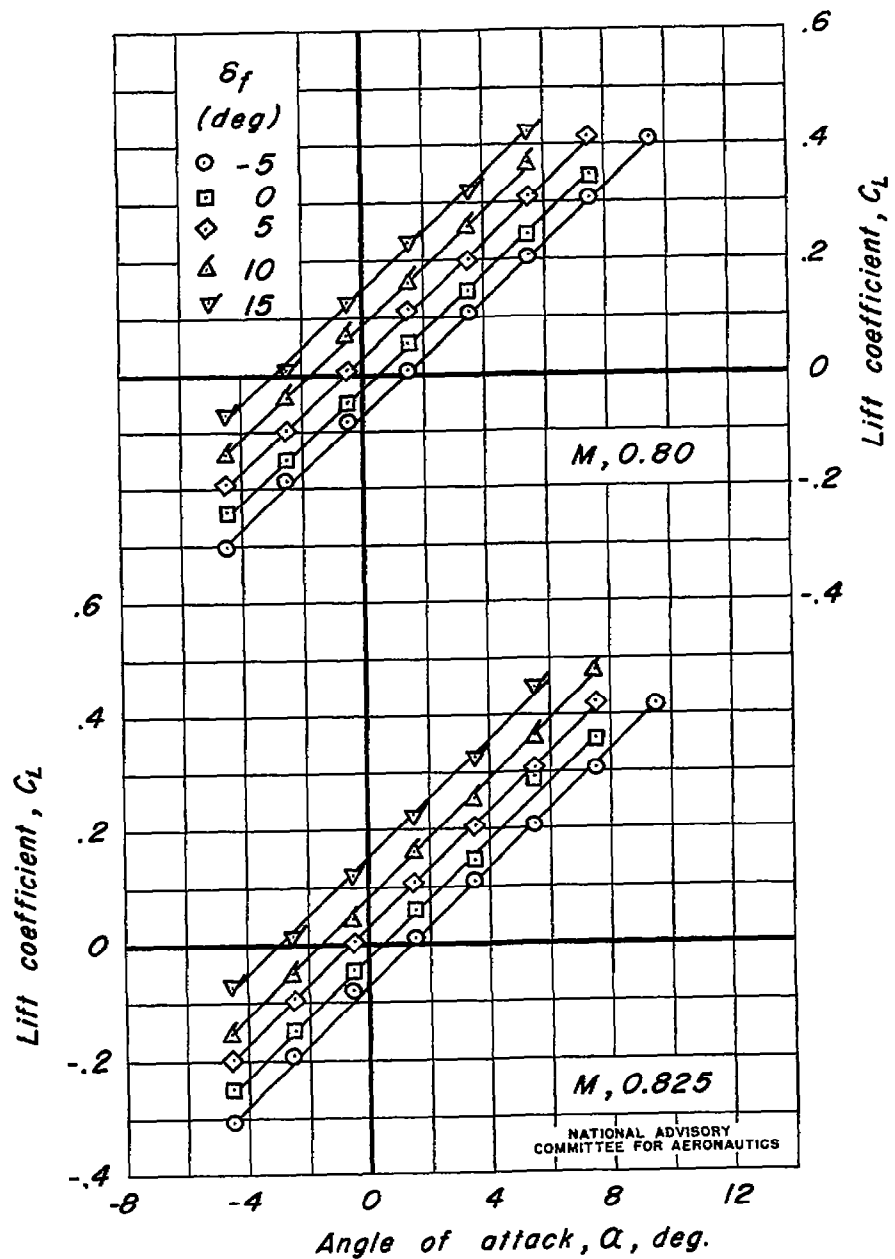
(c) $M = 0.70; 0.75$

Figure 9.-Continued.

Fig. 9 d

NACA RM No. A7J22



(d) $M, 0.80; 0.825$

Figure 9.-Continued.

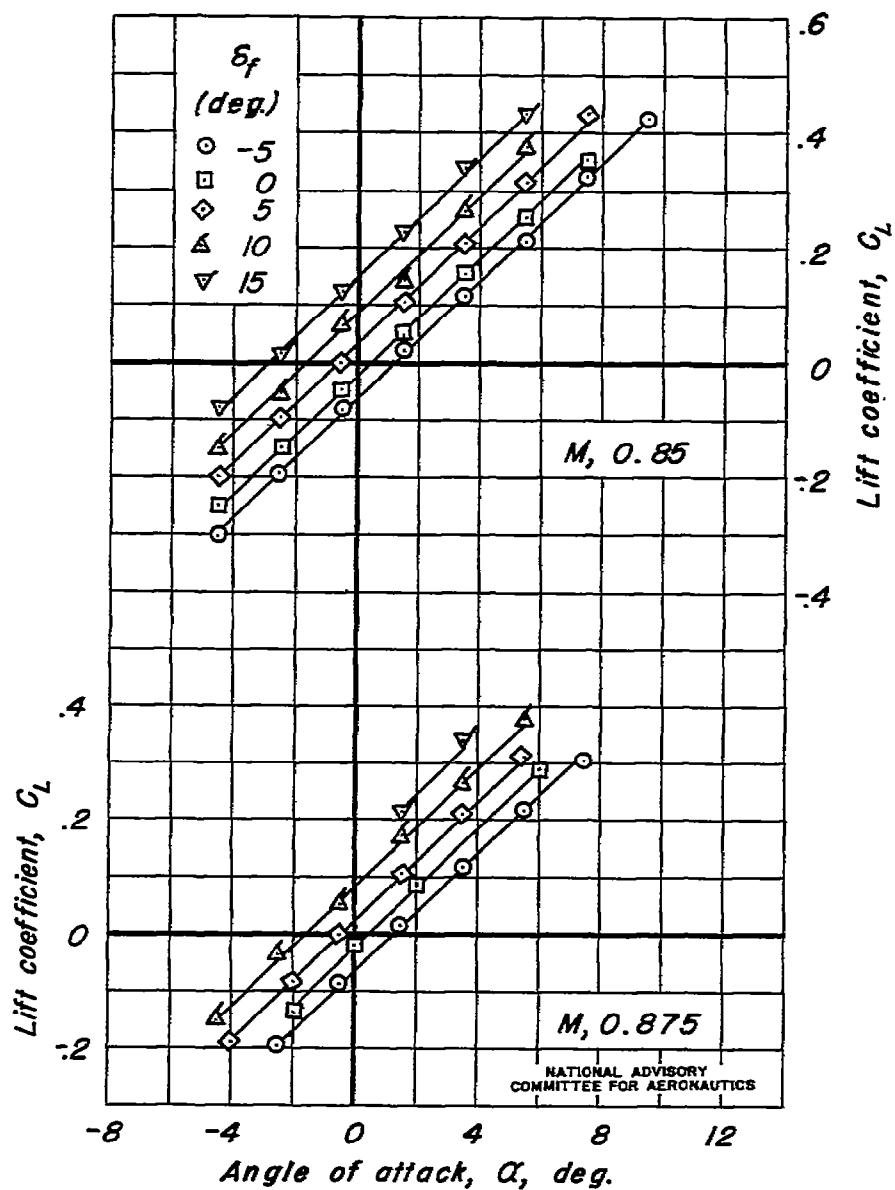
(e) $M = 0.85, 0.875$

Figure 9.—Concluded.

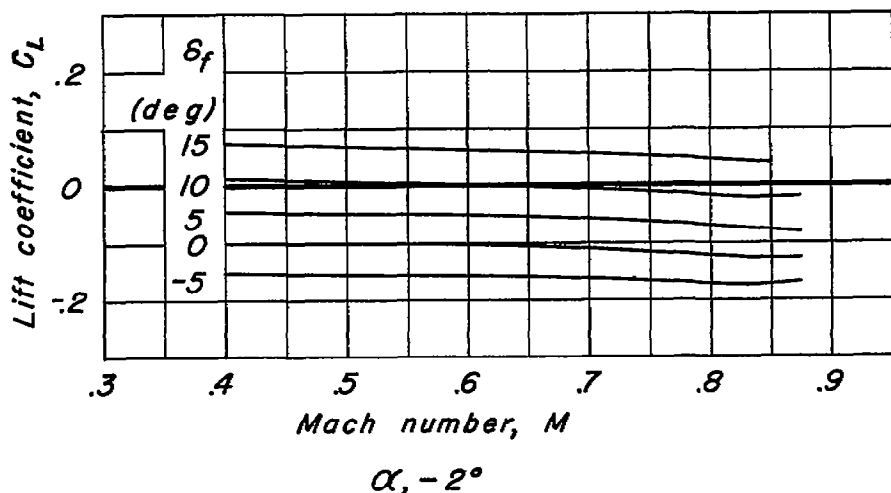
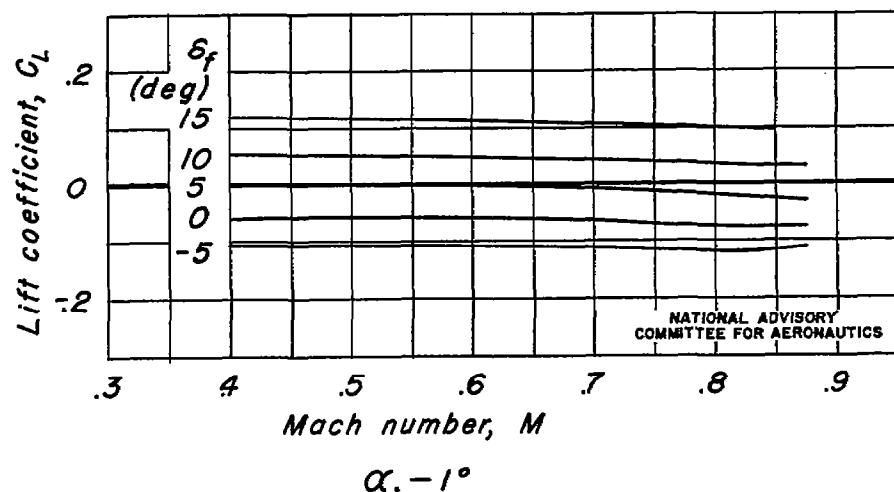
 $\alpha, -2^\circ$ NATIONAL ADVISORY
COMMITTEE FOR AERONAUTICS $\alpha, -1^\circ$ (a) $\alpha, -2^\circ; -1^\circ$

Figure 10.—Variation of lift coefficient with Mach number.

Swept back 45° ; δ_t , 0° .

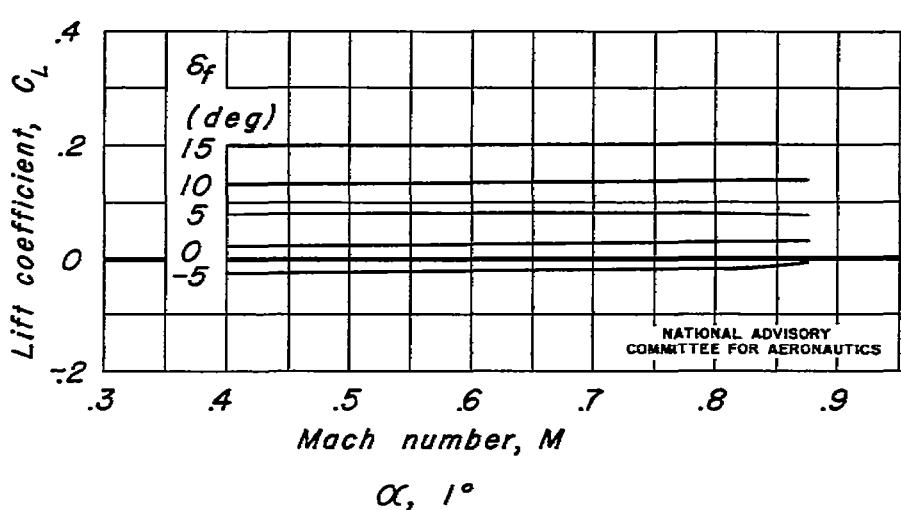
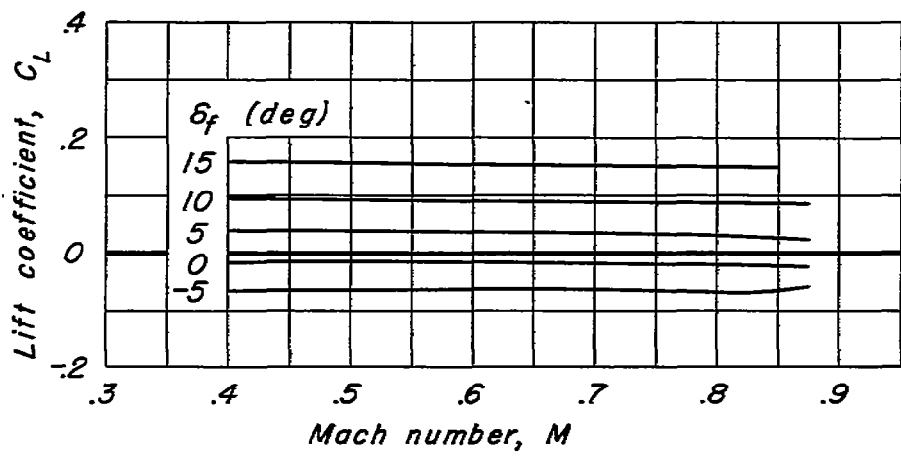
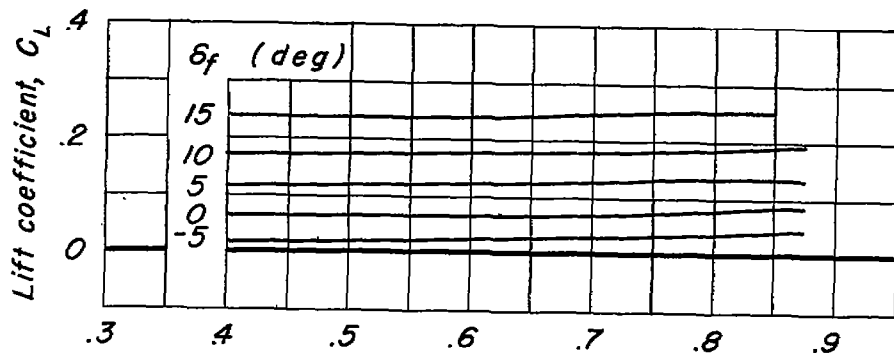
(b) $\alpha, 0^\circ, 1^\circ$

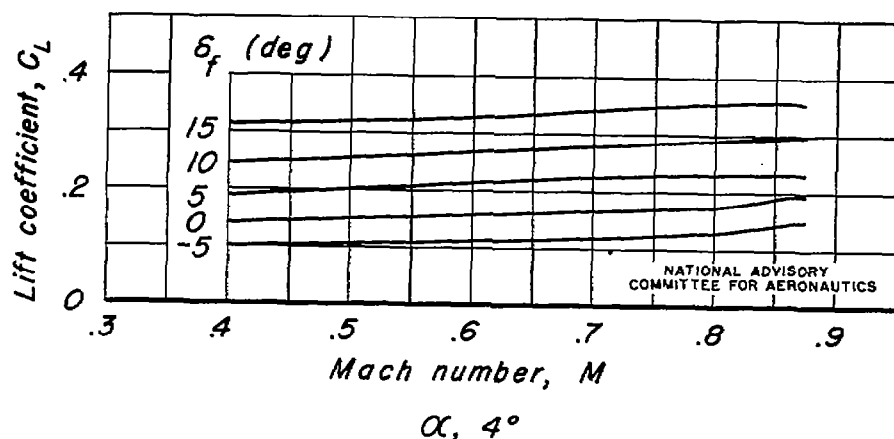
Figure 10.—Continued.

Fig. 10 c

NACA RM No. A7J22



$\alpha, 2^\circ$



$\alpha, 4^\circ$

(d) $\alpha, 2^\circ; 4^\circ$

Figure 10.—Continued.

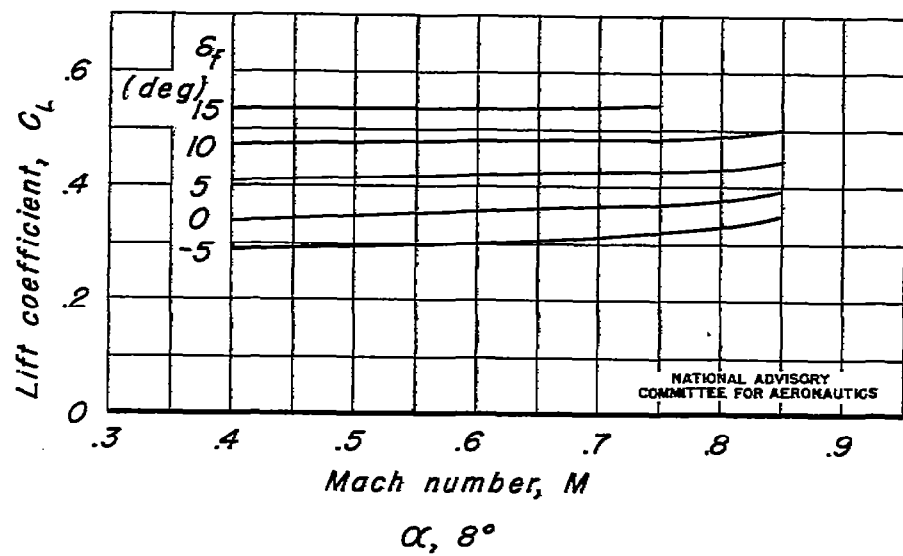
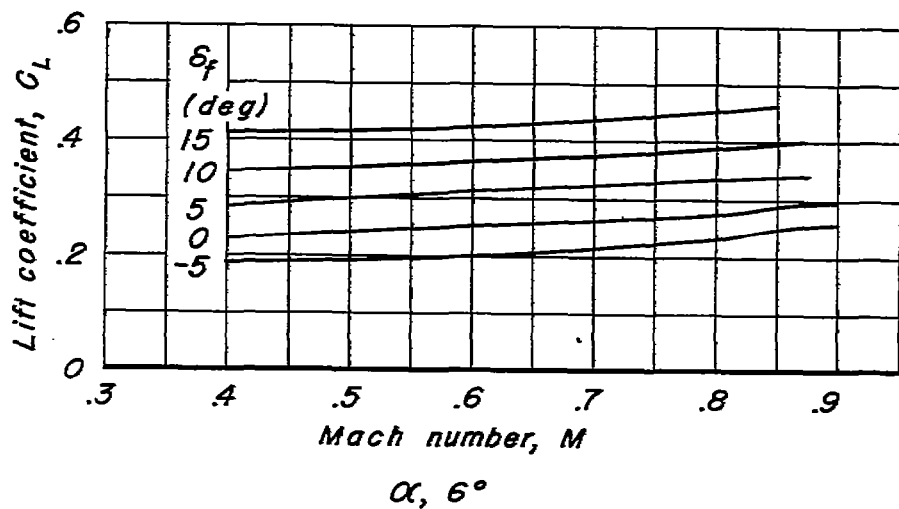
(d) $\alpha, 6^\circ; 8^\circ$

Figure 10.—Concluded.

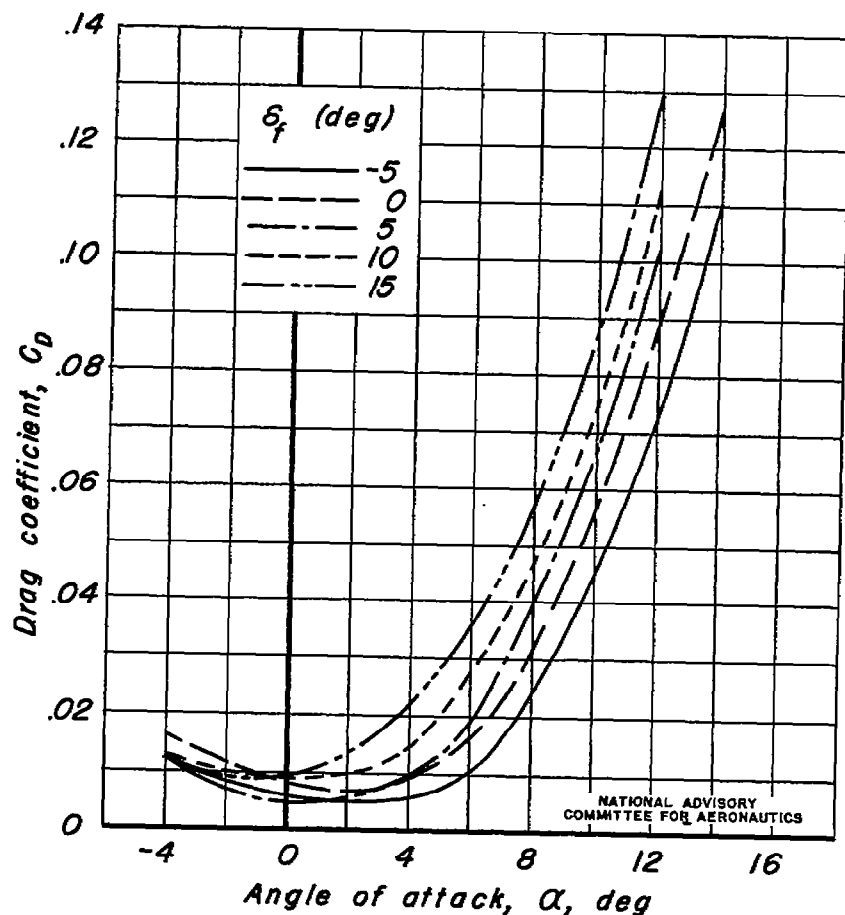
(a) $M, 0.40$

Figure 11.—Variation of drag coefficient with angle of attack. Swept back 45° ; $\delta_f, 0^\circ$.

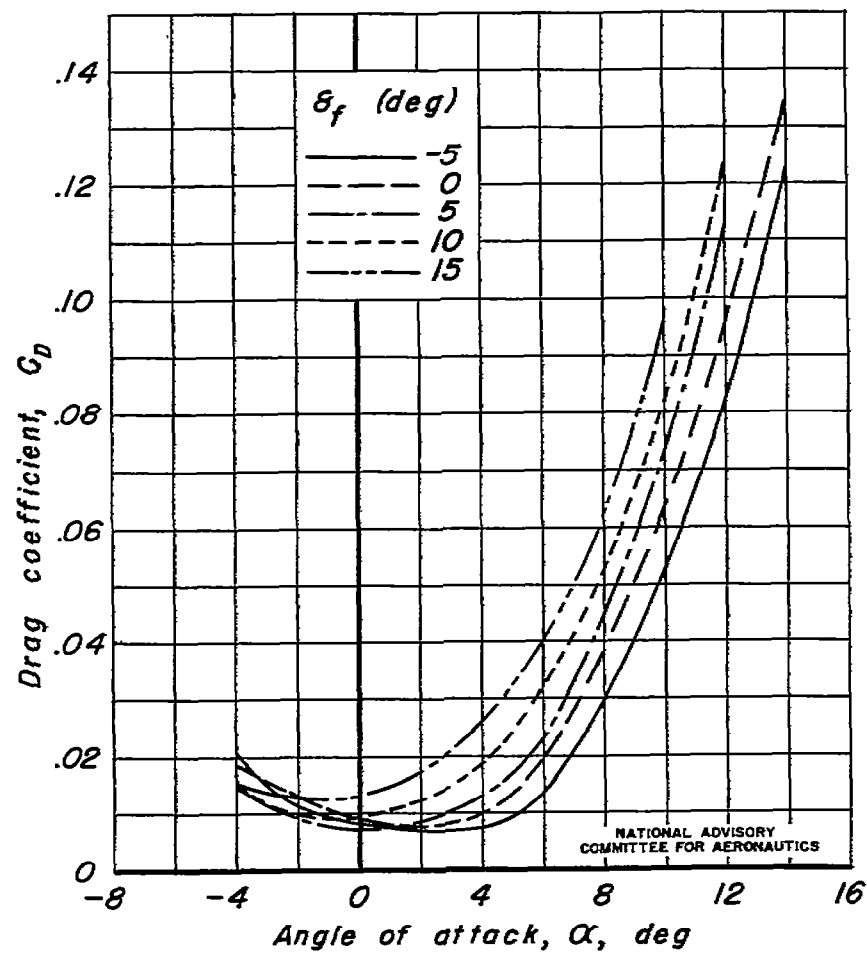
(b) $M, 0.60$

Figure 11.—Continued.

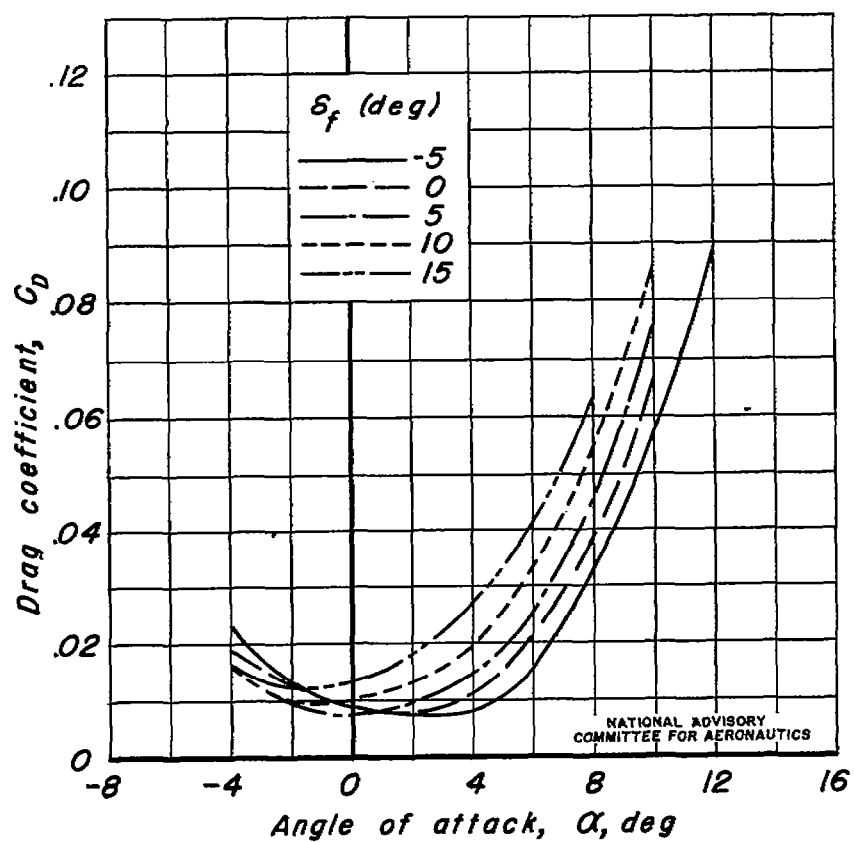
(c) $M, 0.70$

Figure 11.—Continued.

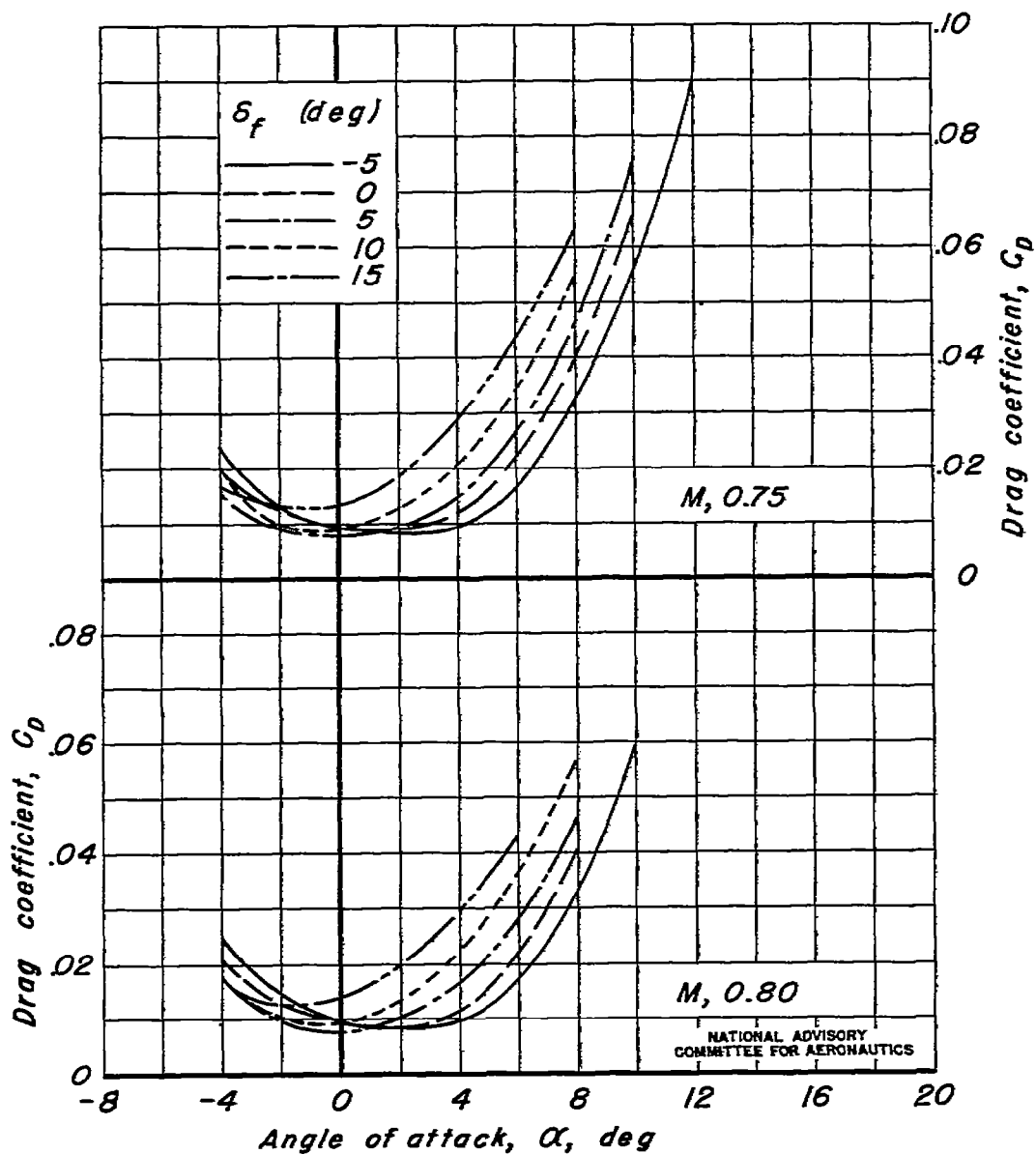
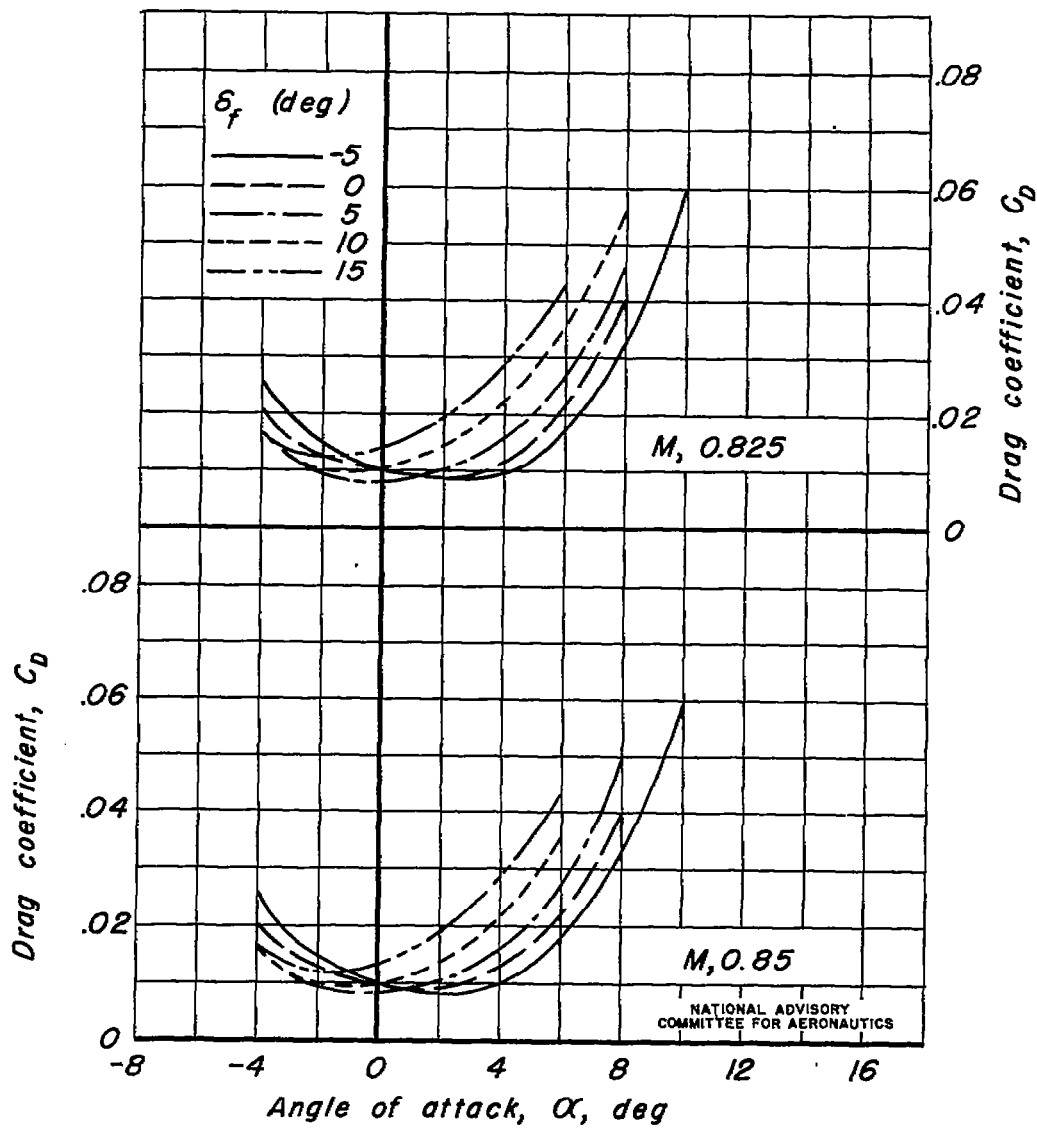
(d) $M, 0.75; 0.80$

Figure 11.—Continued.

Fig. 11 e

NACA RM No. A7J22



(e) $M, 0.825; 0.85$

Figure 11.—Continued.

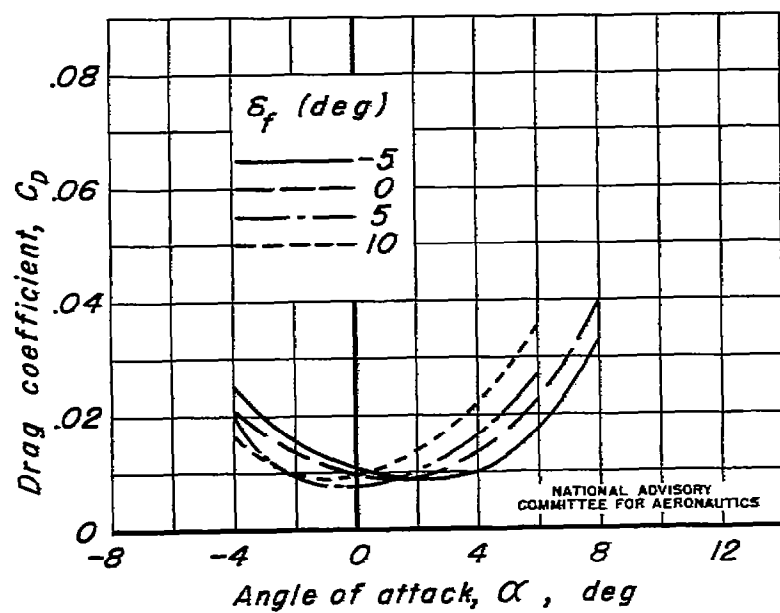
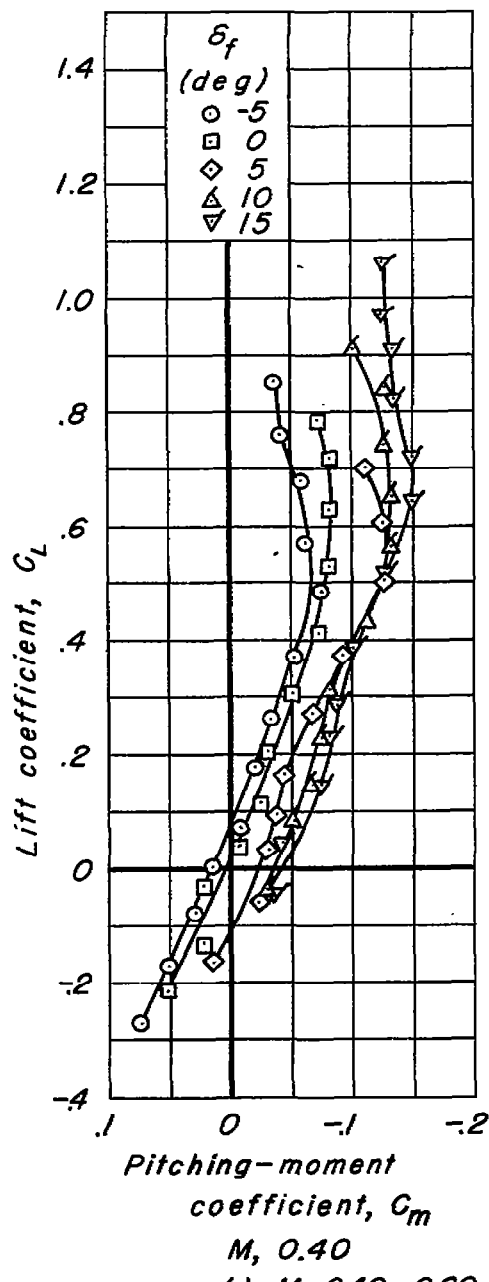
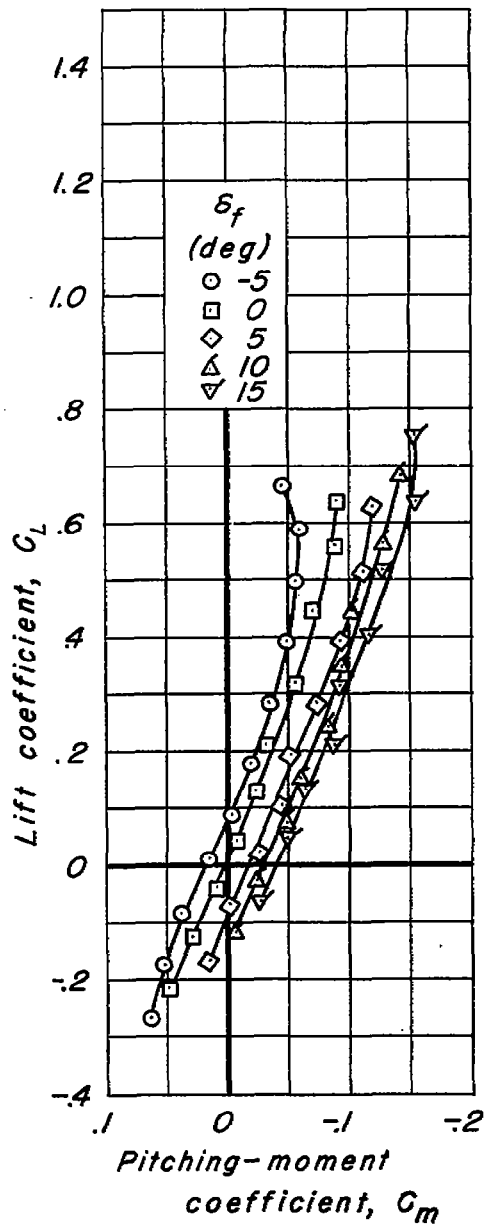
(f) $M, 0.875$

Figure II.-Concluded.



$M, 0.40$
(a) $M, 0.40; 0.60$



NATIONAL ADVISORY
COMMITTEE FOR AERONAUTICS

Figure 12.—Variation of pitching-moment coefficient with lift coefficient. Swept back 45° ; $\delta_t, 0^\circ$

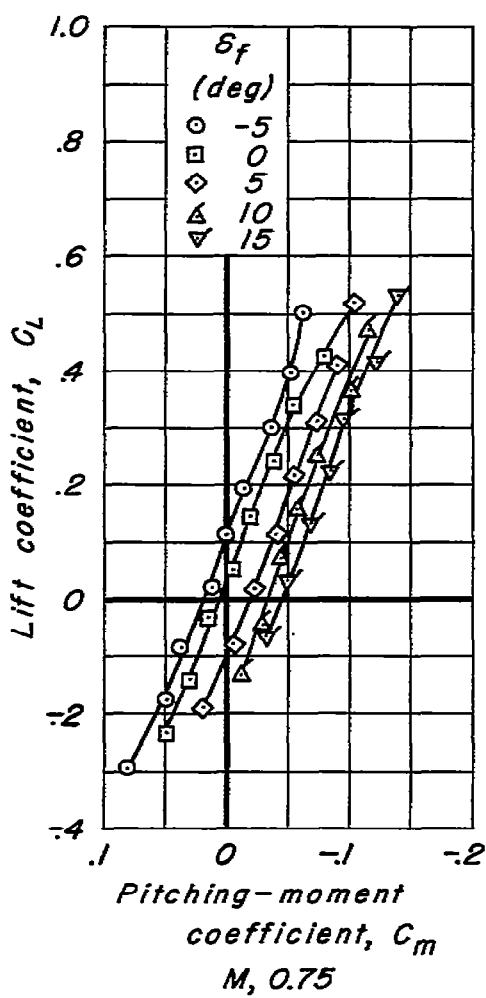
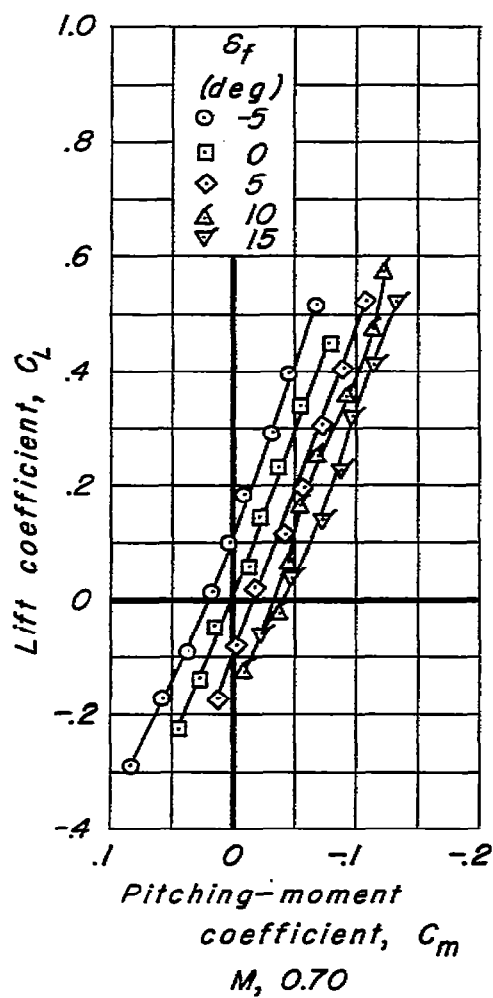
(b) $M, 0.70; 0.75$ NATIONAL ADVISORY
COMMITTEE FOR AERONAUTICS

Figure 12.—Continued.

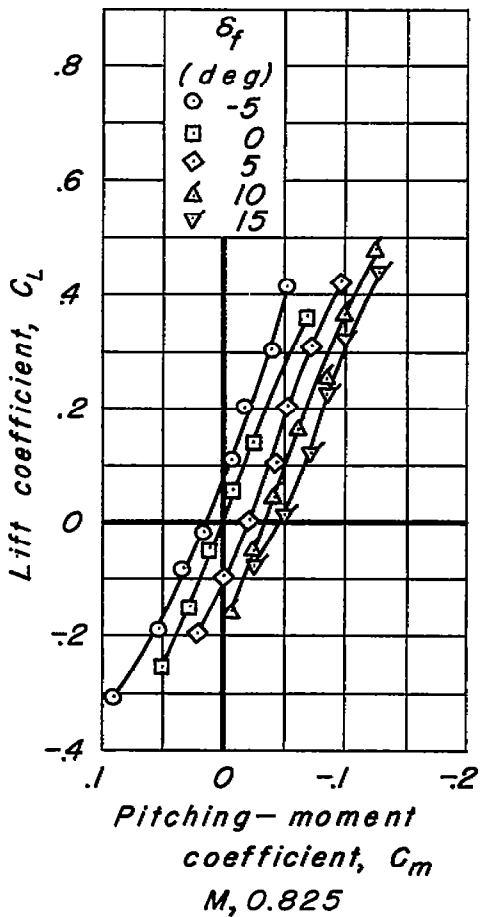
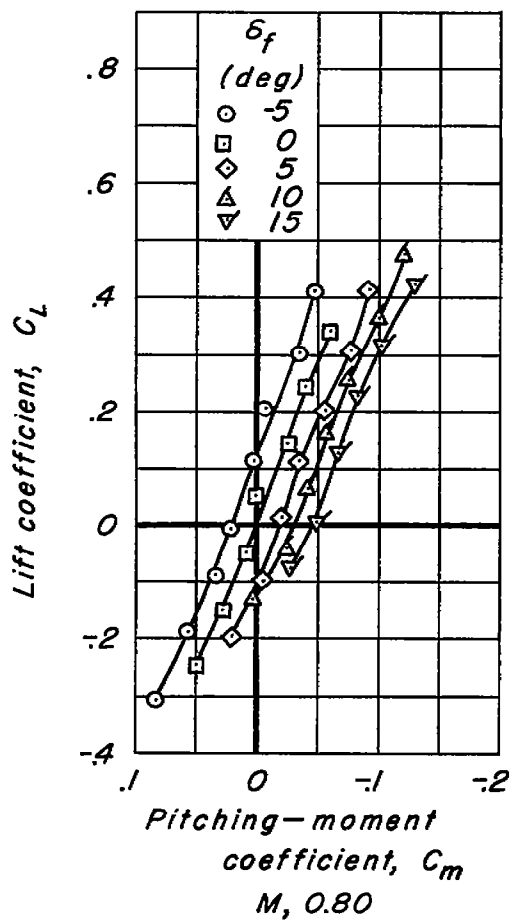
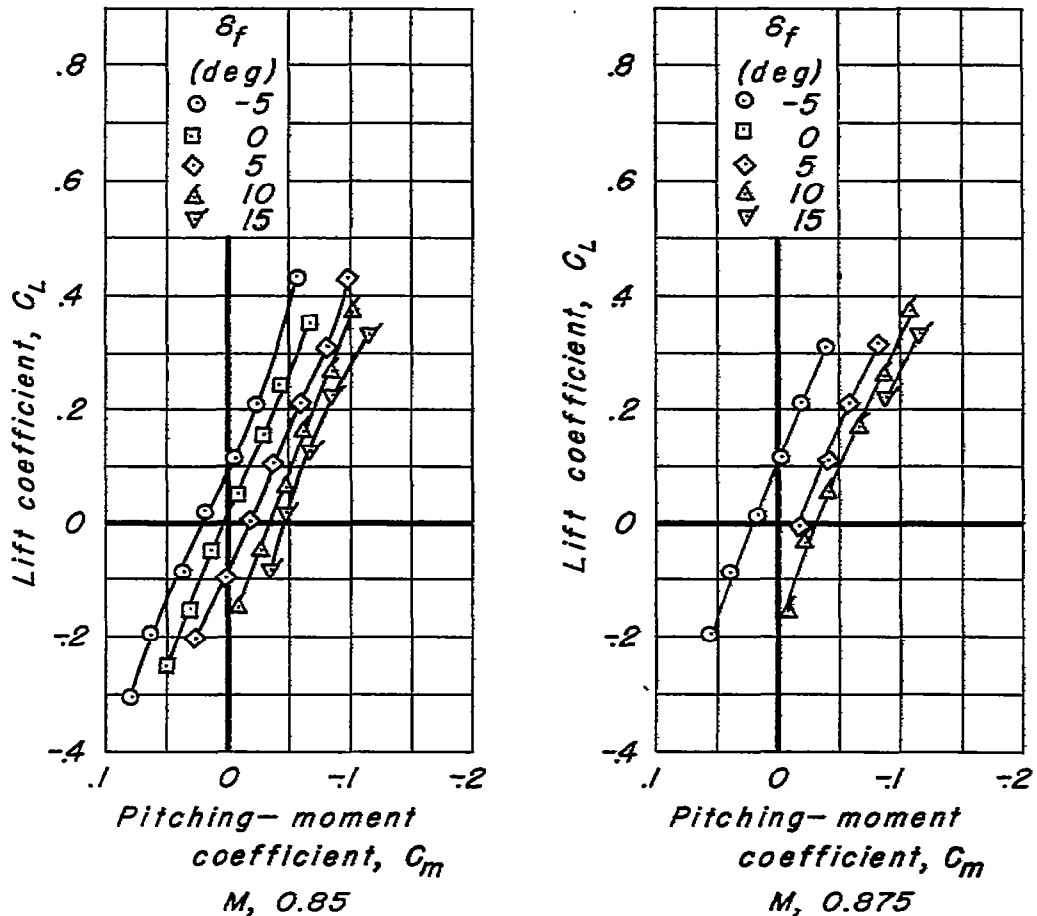
(c) $M, 0.80; 0.825$ NATIONAL ADVISORY
COMMITTEE FOR AERONAUTICS

Figure 12.—Continued.

NATIONAL ADVISORY
COMMITTEE FOR AERONAUTICS(d) $M, 0.85, 0.875$ *Figure 12.—Concluded.*

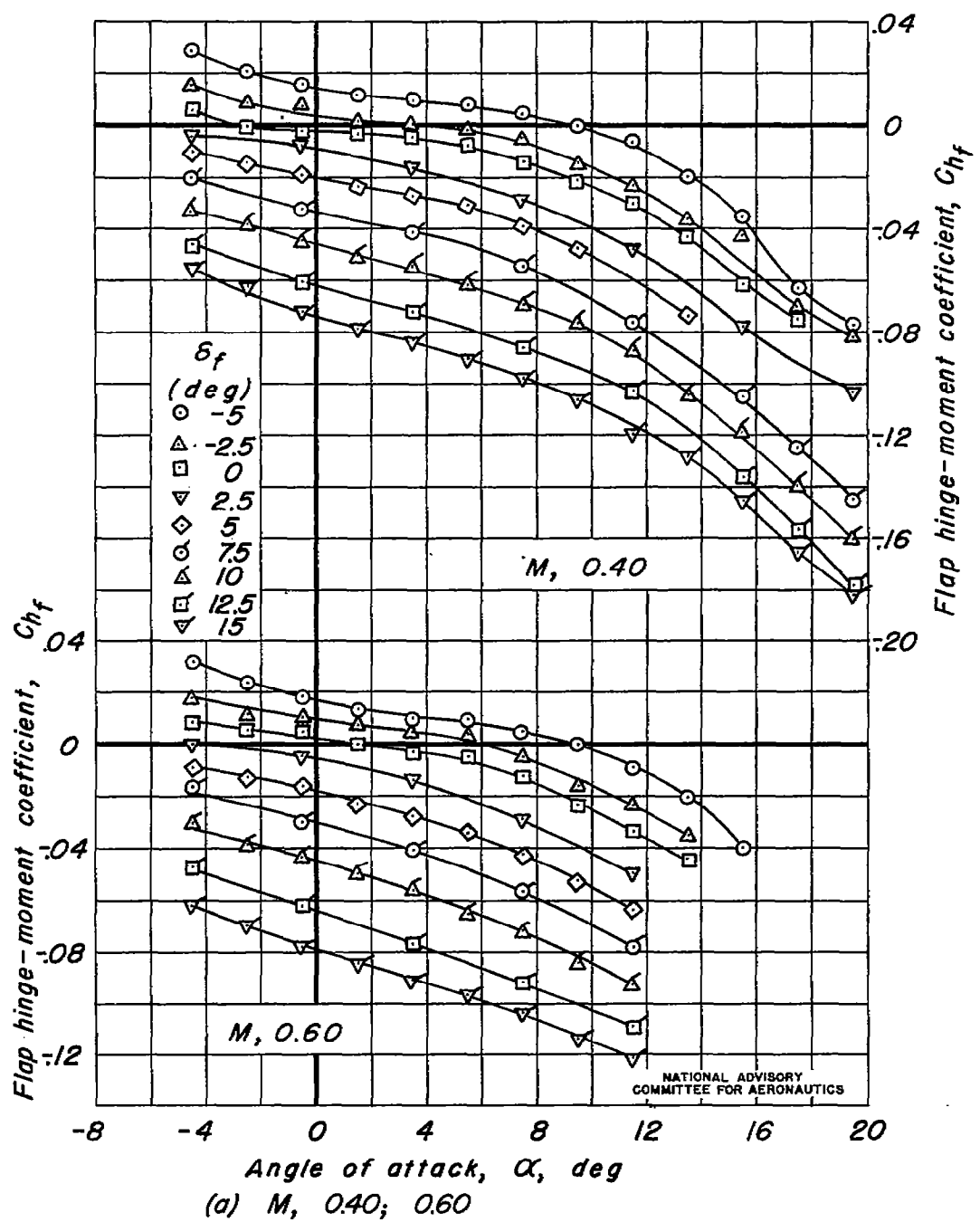


Figure 13.—Variation of flap hinge-moment coefficient with angle of attack. Swept back 45°; δ_t , 0°.

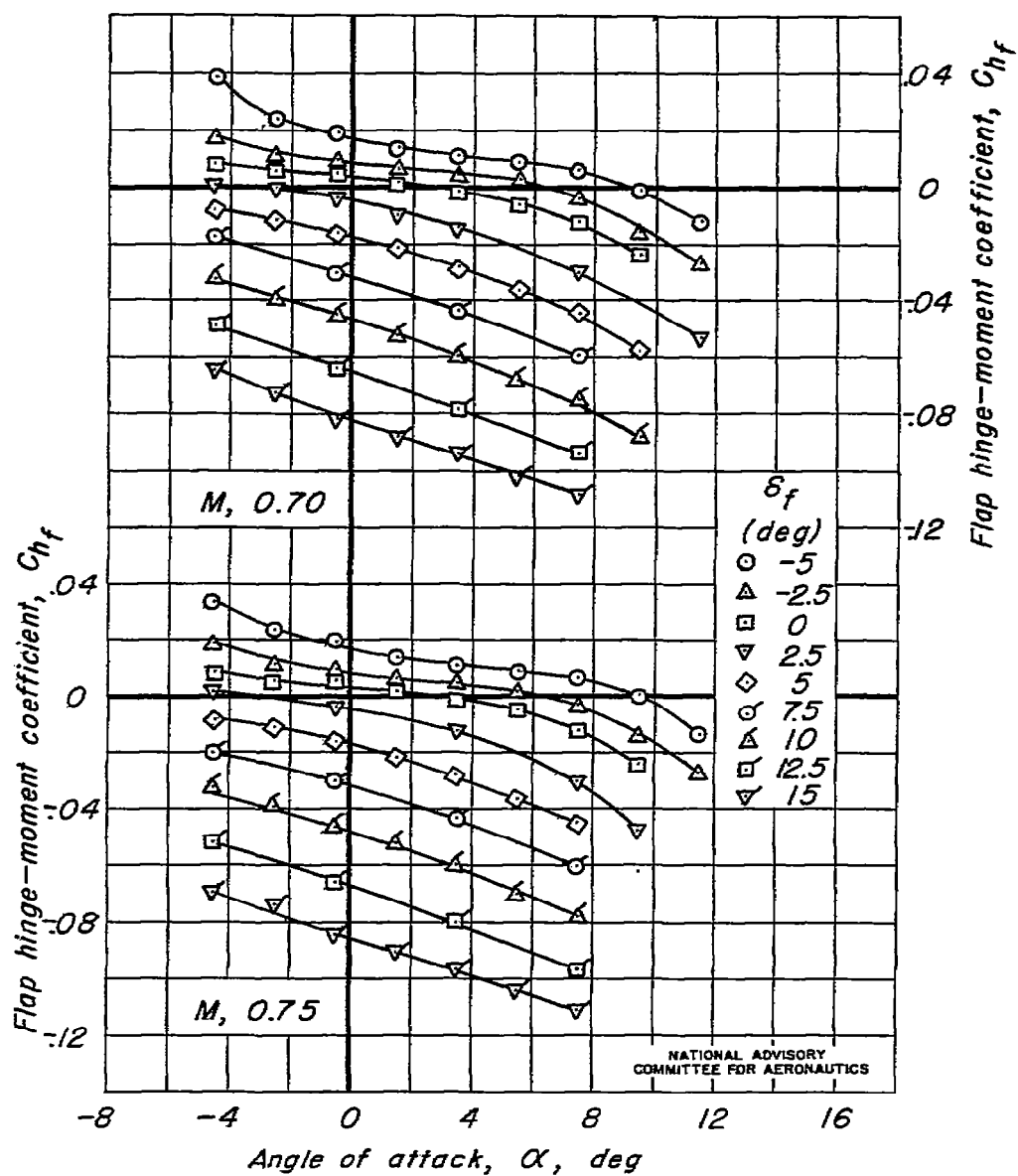
(b) $M, 0.70; 0.75$

Figure 13. — Continued.

Fig. 13 c

NACA RM No. A7J22

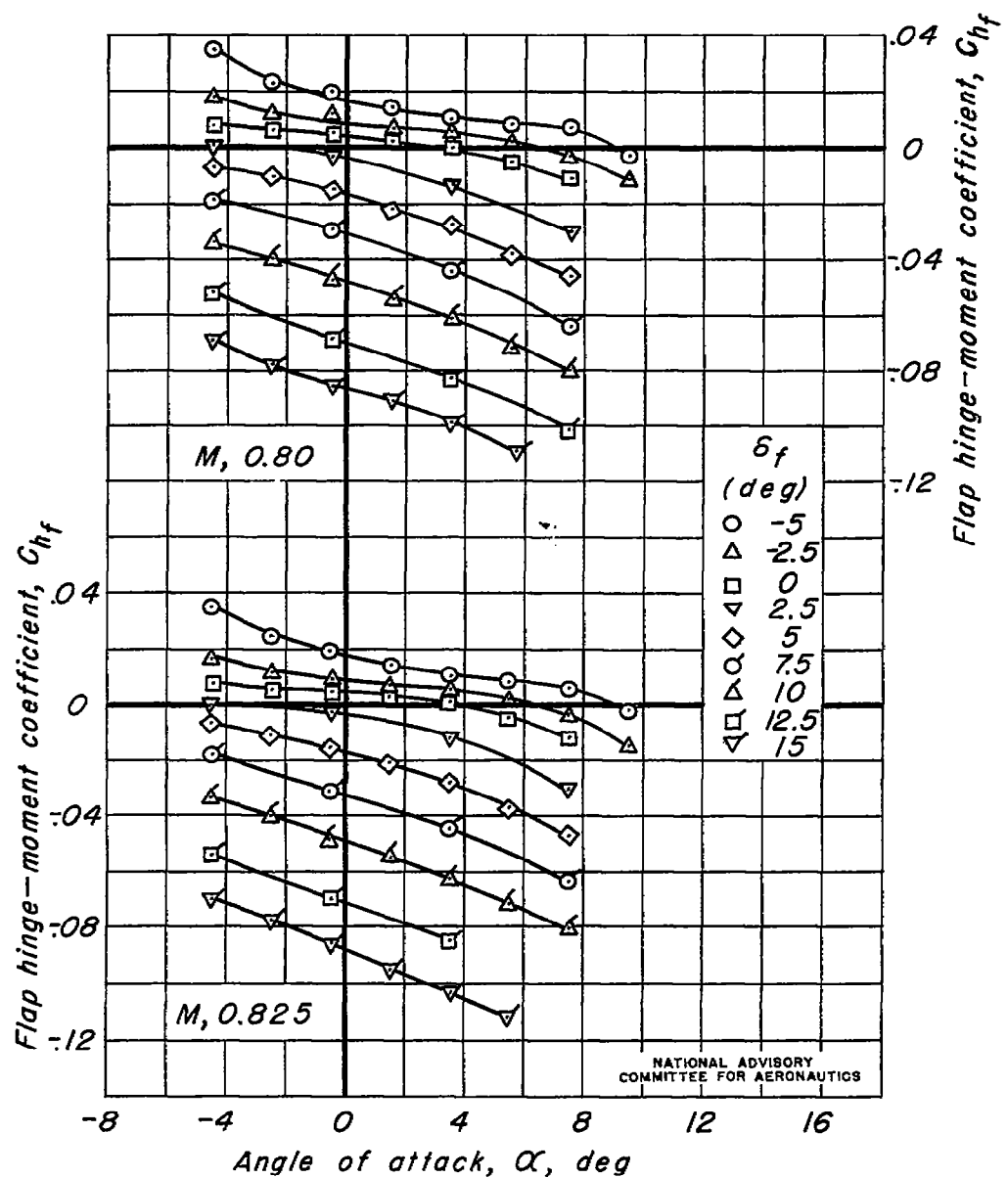
(c) $M, 0.80; 0.825$

Figure 13. — Continued.

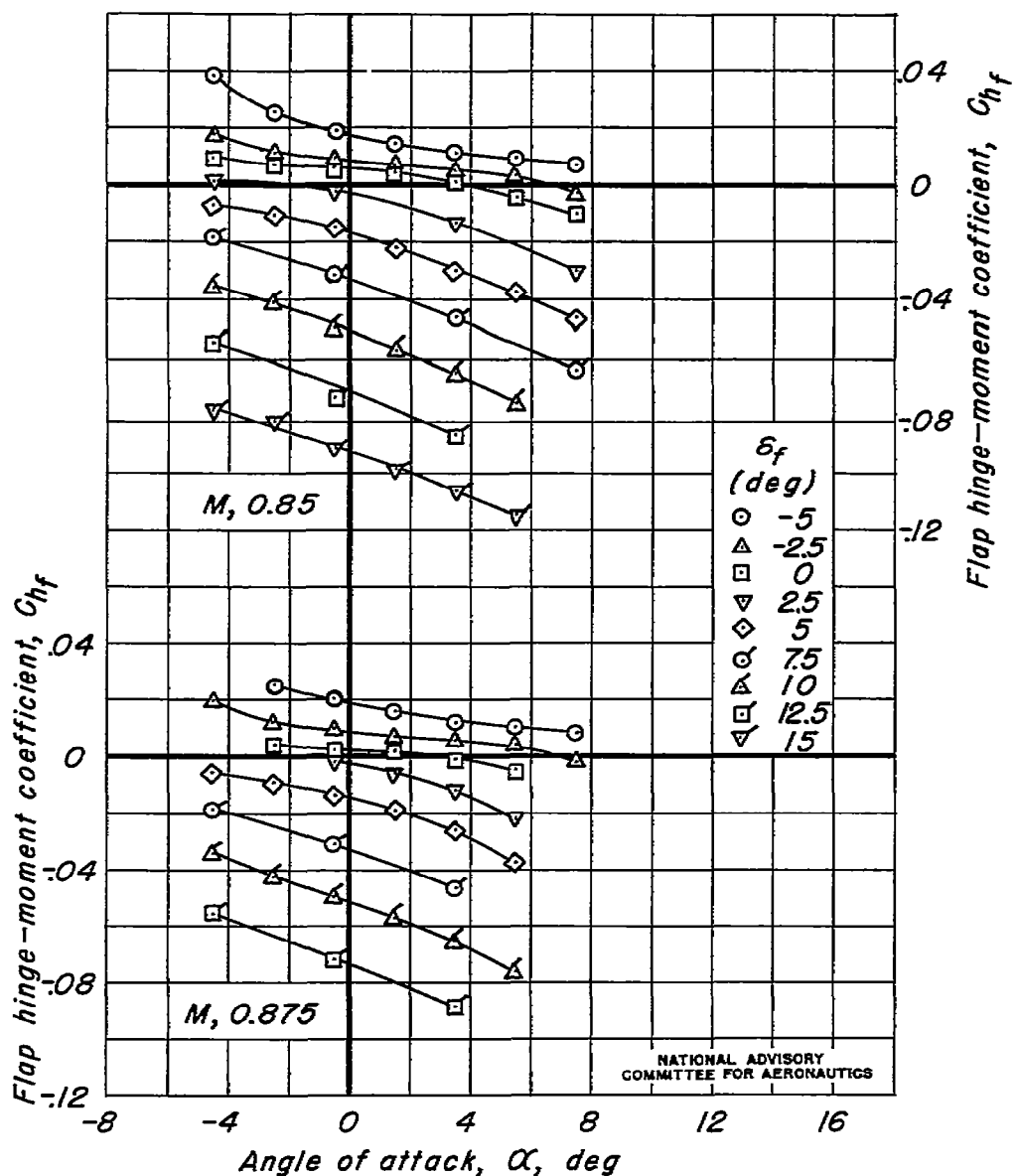
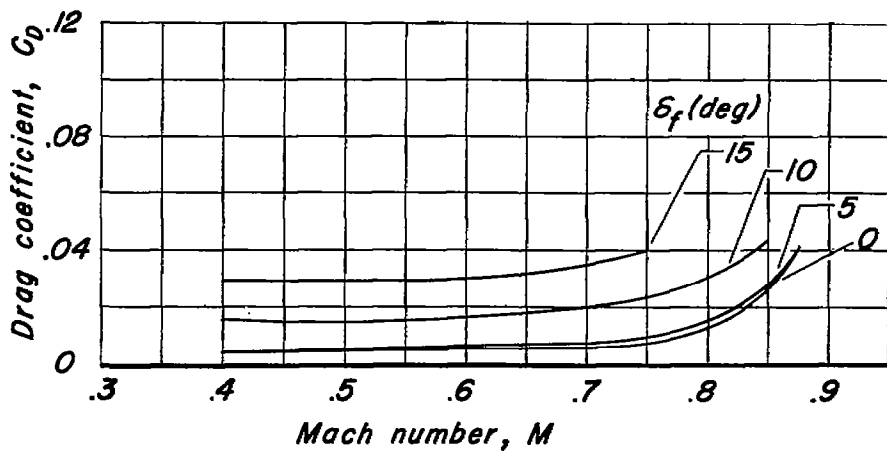
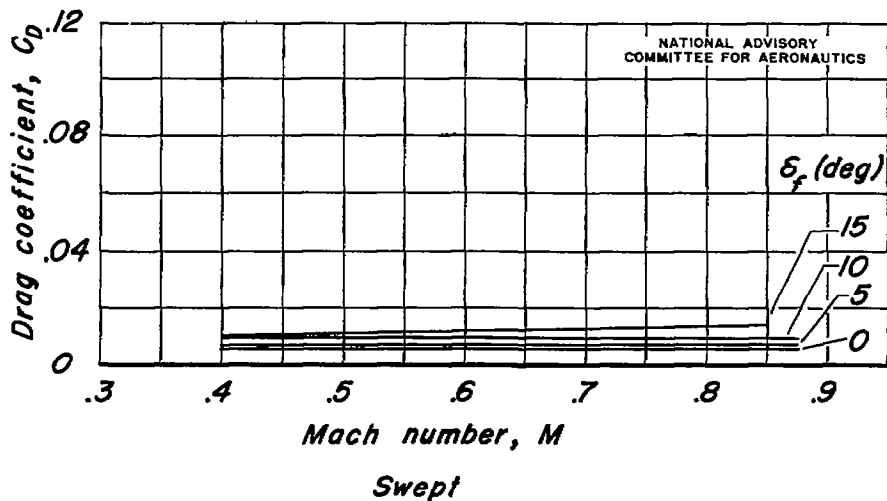
(d) $M, 0.85; 0.875$ *Figure 13.— Concluded.*

Fig. 14

NACA RM No A7J22



Unswept



Swept

Figure 14.—Variation of drag coefficient with Mach number.
Unswept and swept back 45°; angle of attack 0°.

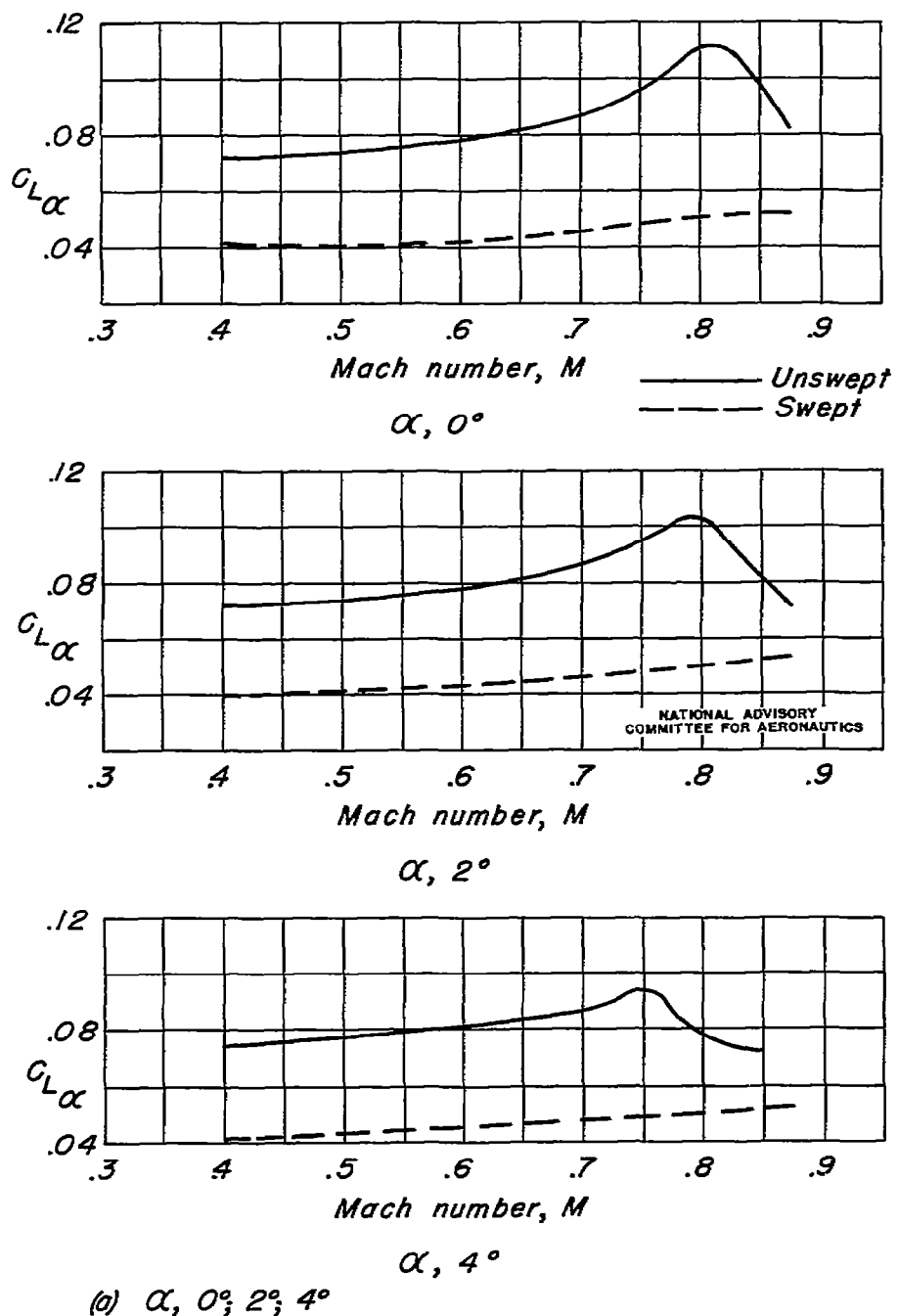


Figure 15.—Variation of lift parameter $C_{L\alpha}$ with Mach number. Unswept and swept back 45°; δ_f , 0°.

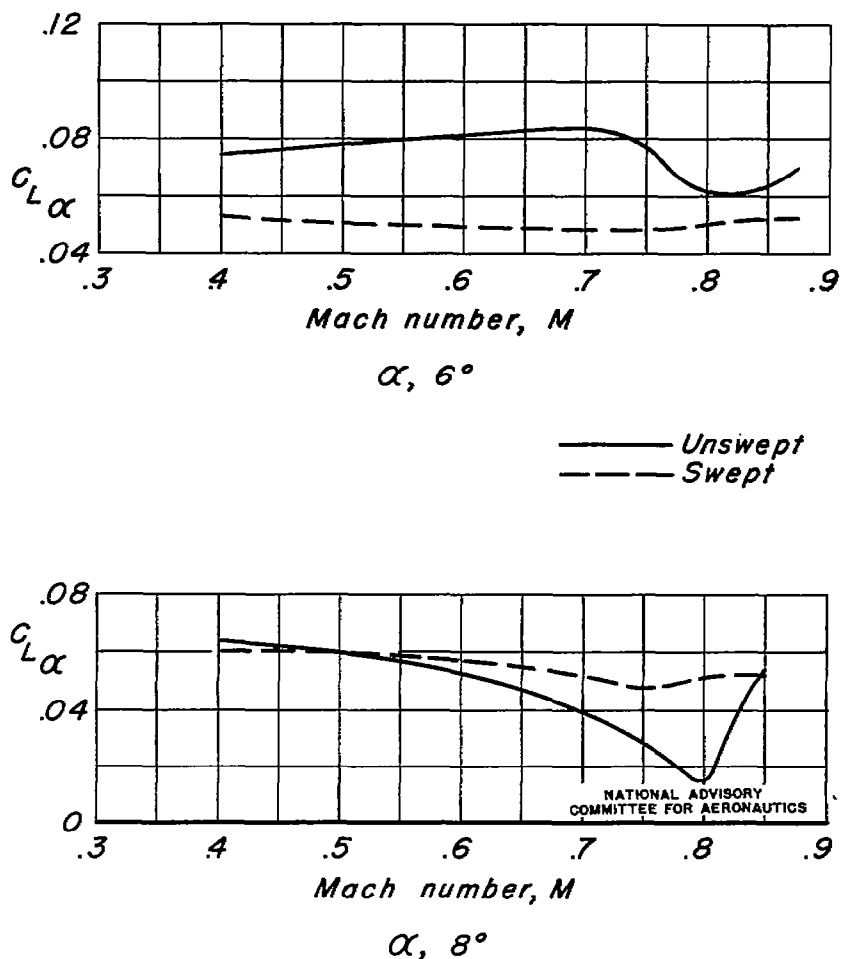
(b) $\alpha, 6^\circ; 8^\circ$

Figure 15.—Concluded.

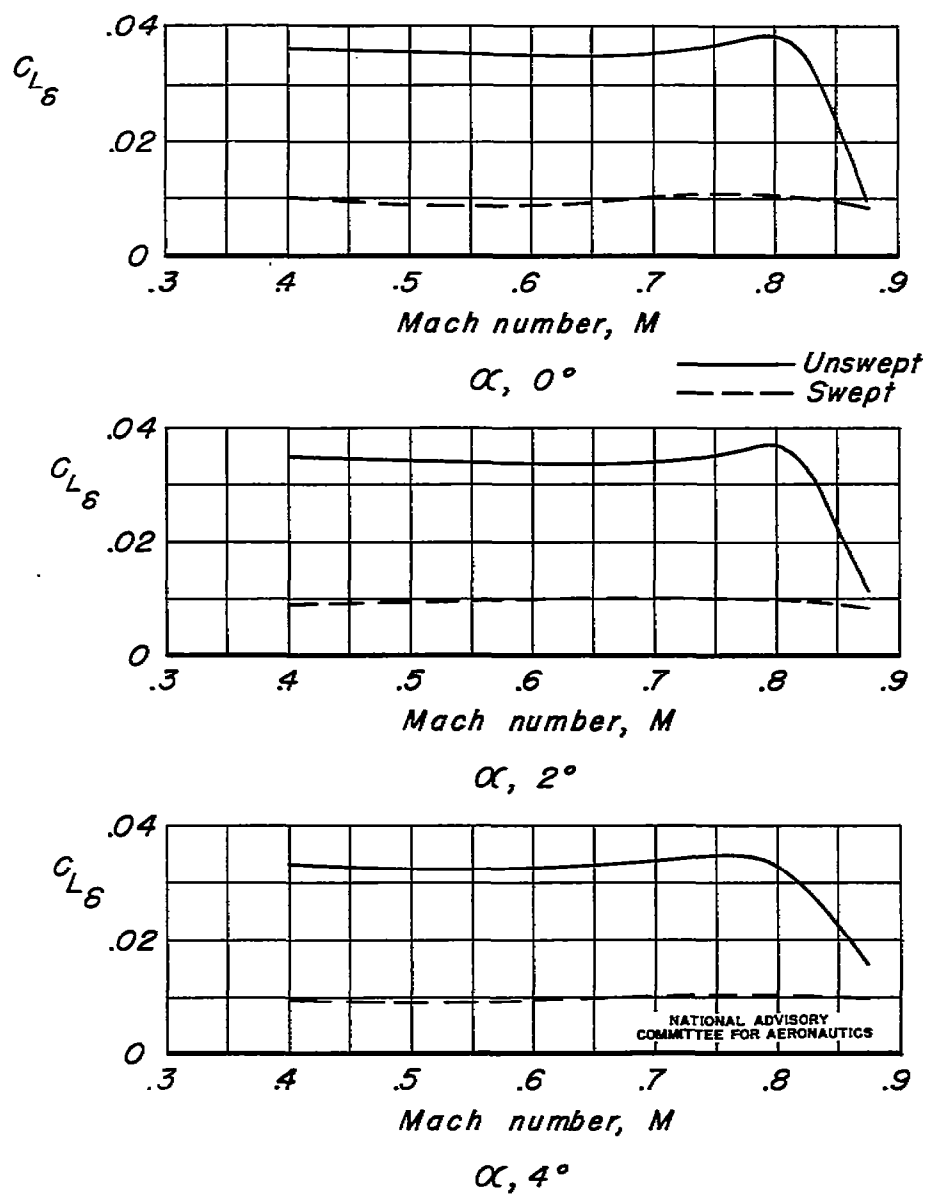
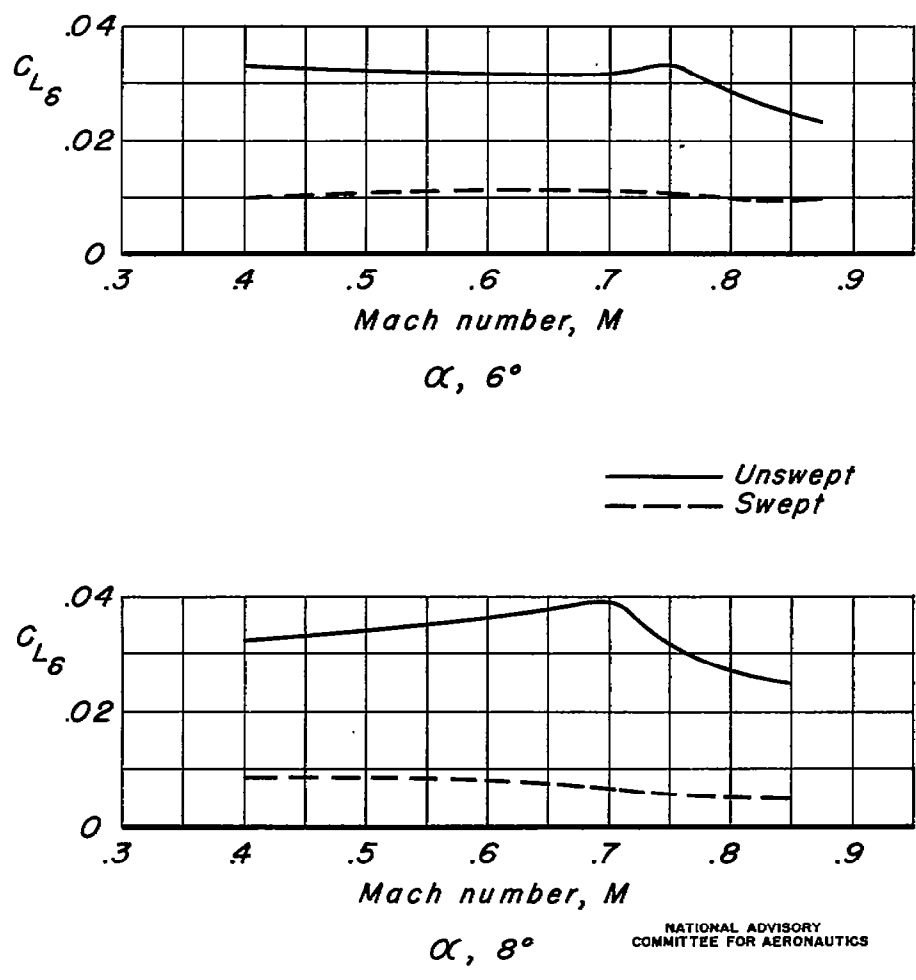
(a) $\alpha, 0^\circ; 2^\circ; 4^\circ$

Figure 16.—Variation of lift parameter C_{L_6} with Mach number. Unswept and swept back 45°, $\delta_f, 0^\circ$.

(b) $\alpha, 6^\circ; 8^\circ$ *Figure 16.—Concluded.*

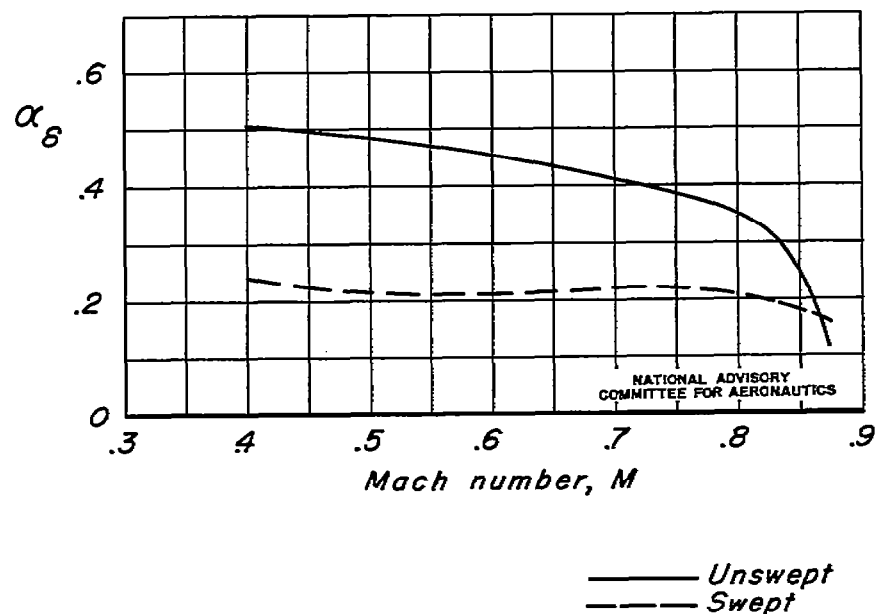


Figure 17.—Variation of lift effectiveness parameter α_s with Mach number. Unswept and swept back 45° ; angle of attack, 0° ; δ_f , 0°

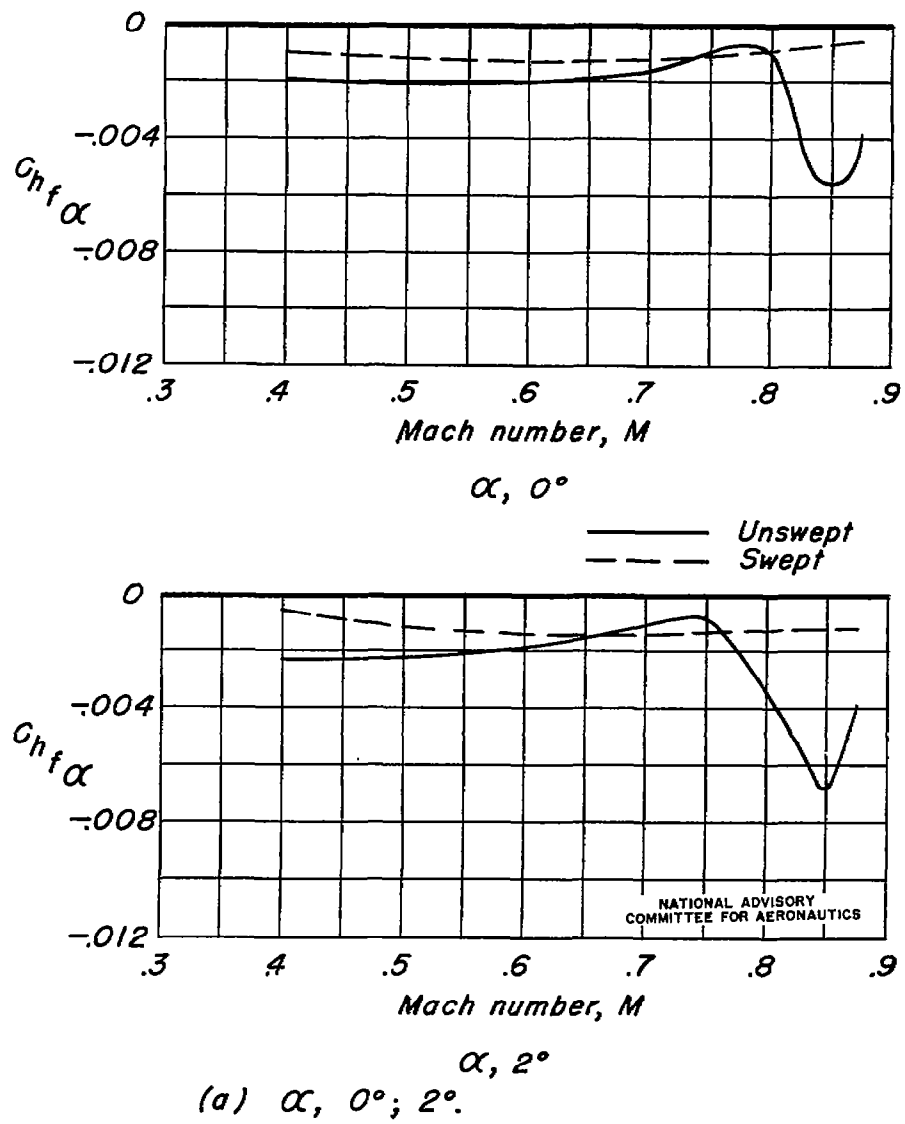
(a) $\alpha, 0^\circ; 2^\circ$.

Figure 18. — Variation of flap hinge-moment parameter

$C_{hf}\alpha$ with Mach number. Unswept and swept back 45°;
 $\delta_f, 0^\circ$.

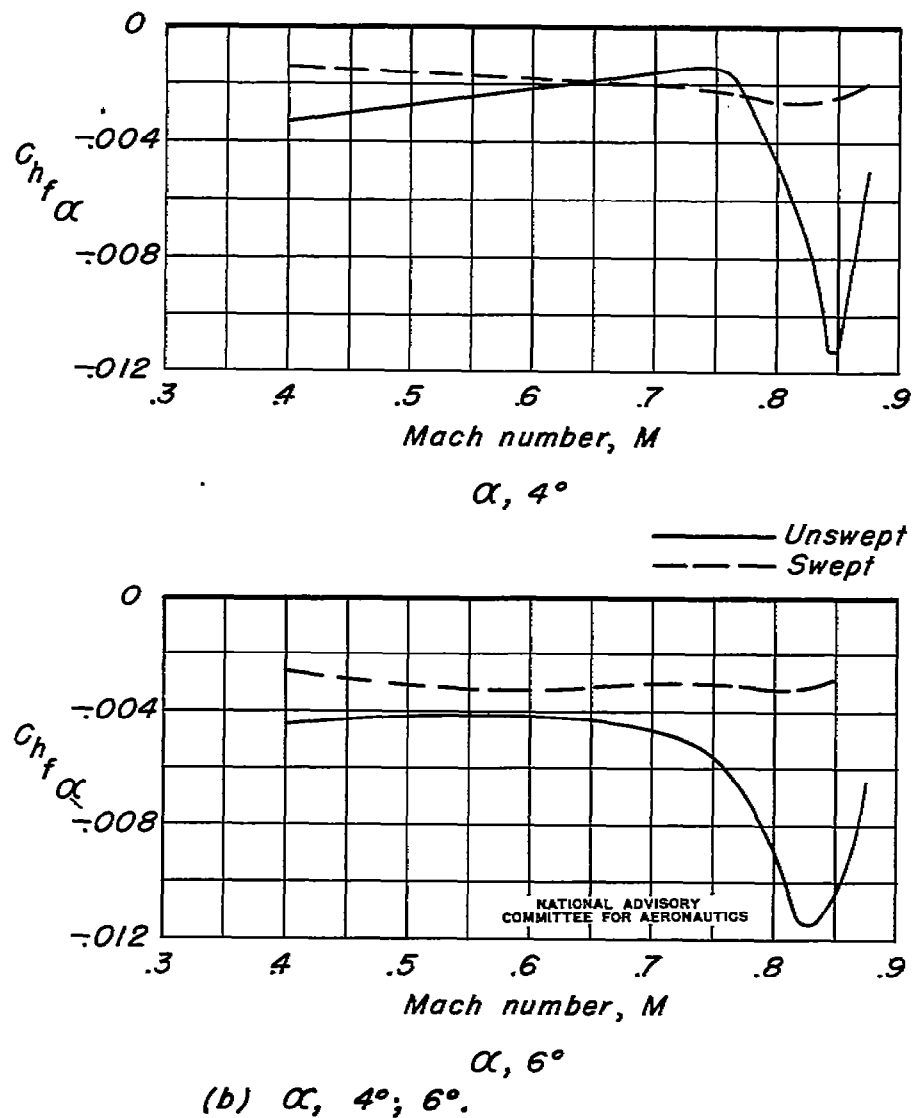
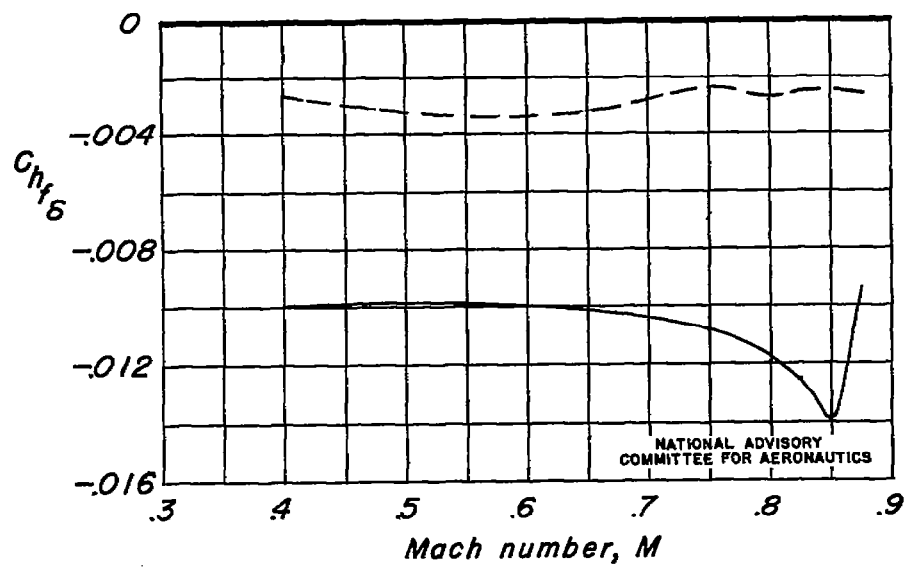
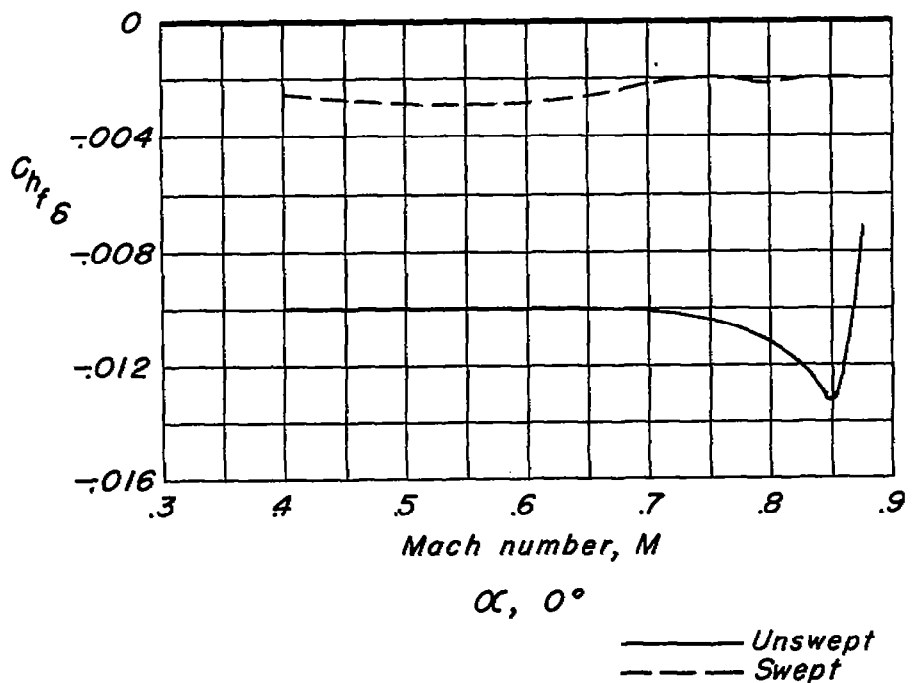
 $\alpha, 6^\circ$ (b) $\alpha, 4^\circ; 6^\circ$.

Figure 18. — Concluded.

Fig. 19 a

NACA RM No. A7J22



(a) $\alpha, 0^\circ, 2^\circ$

Figure 19.—Variation of flap hinge-moment parameter C_{hf_6} with Mach number. Unswept and swept back 45° ; $\delta_f, 0^\circ$.

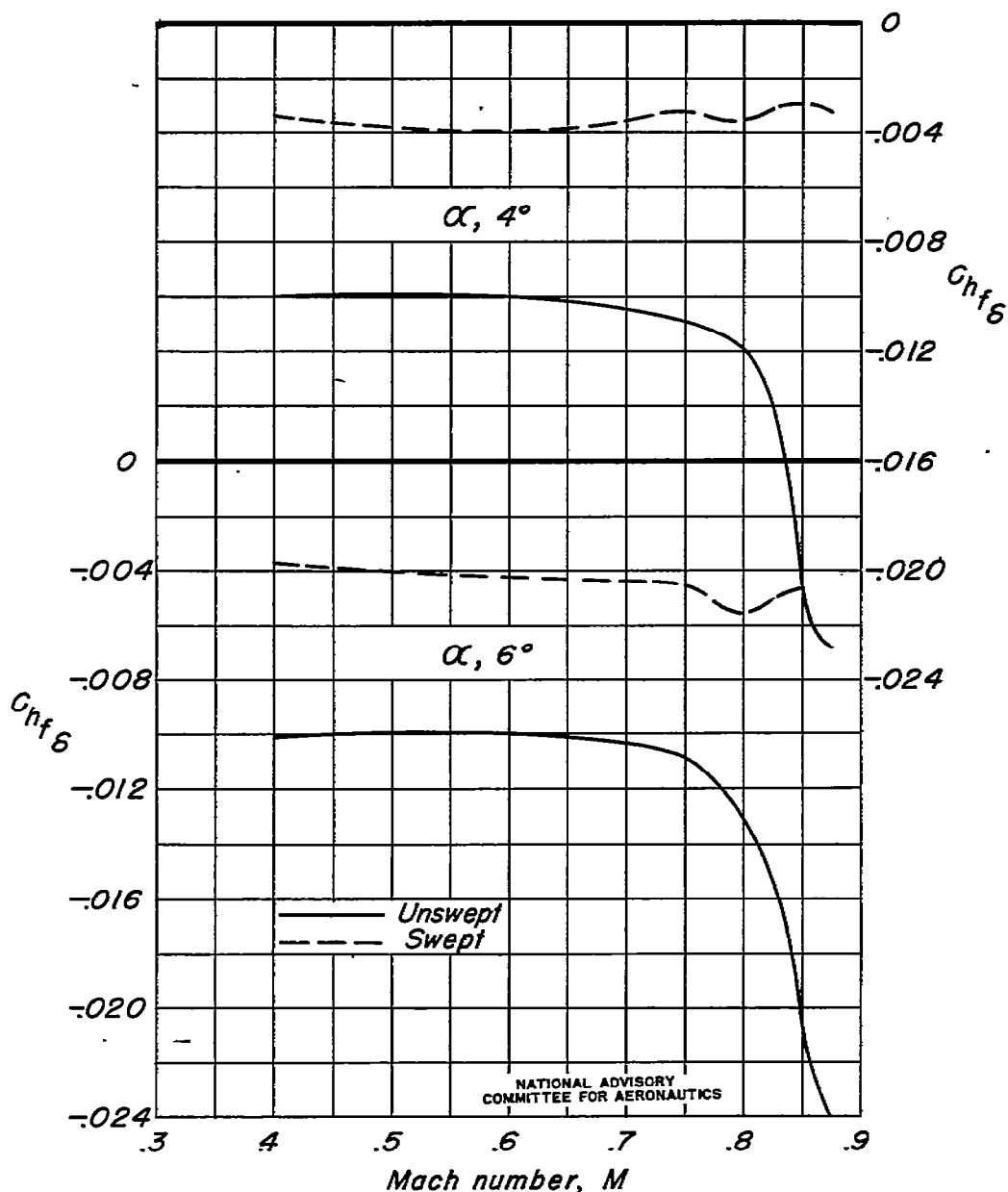
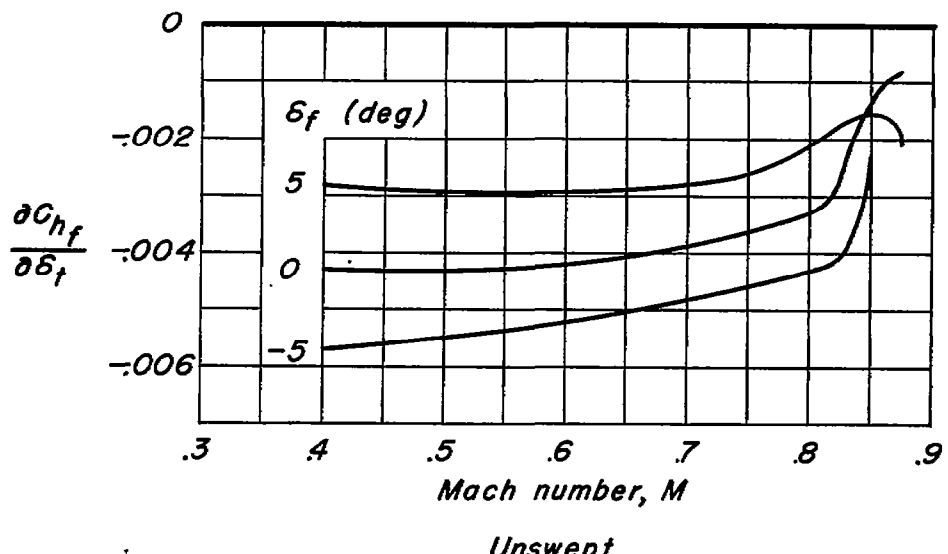
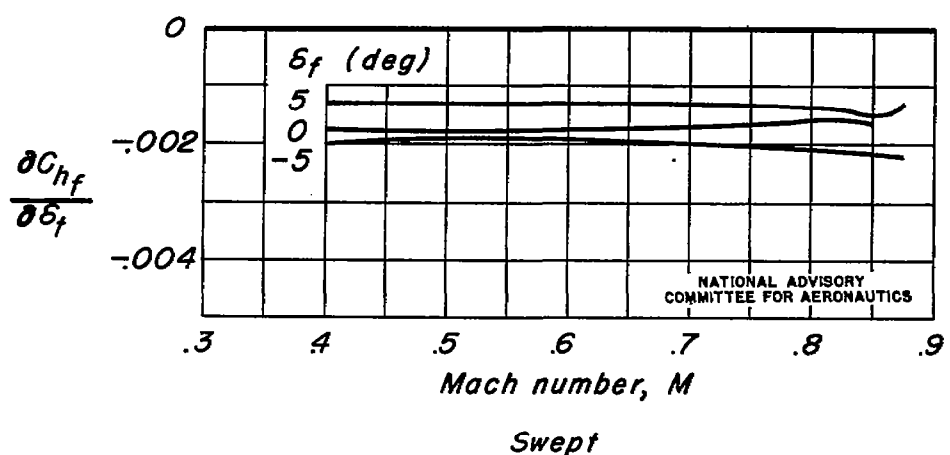
(b) $\alpha = 4^\circ; 6^\circ$.

Figure 19. — Concluded.



Unswept



Swept

Figure 20.—Variation of tab effectiveness with Mach number. Unswept and swept back 45° ; angle of attack, 0° ; δ_f , 0° ; tab angle approximately -5° .

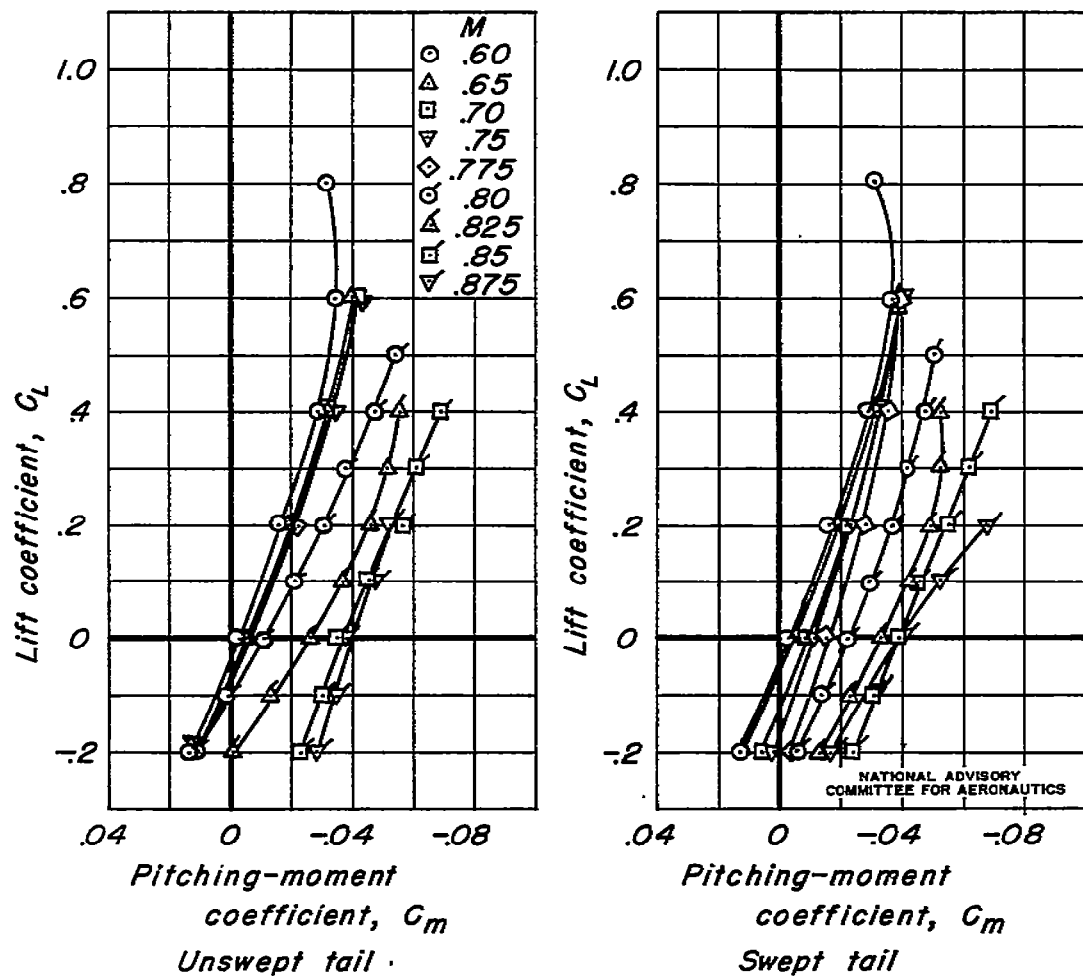


Figure 21.—Predicted variation of pitching-moment coefficient with lift coefficient for an airplane with the horizontal tail unswept or swept back 45°. Elevator, 0°.

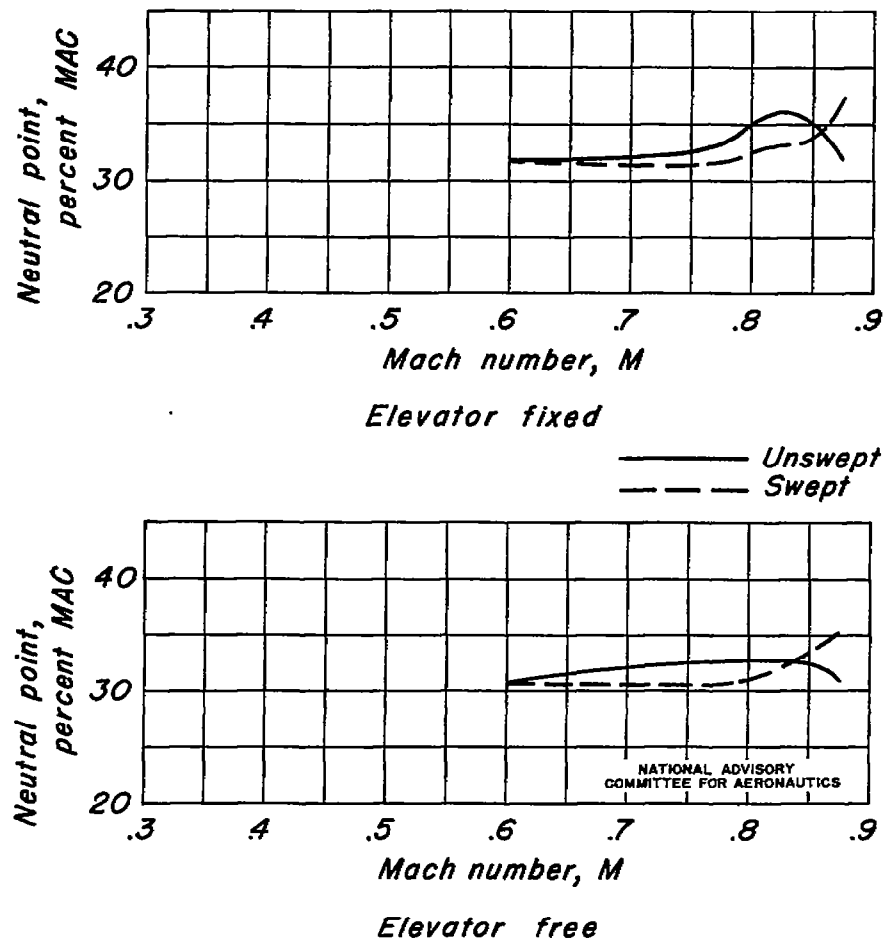


Figure 22.—Predicted variation with Mach number of neutral point for an airplane with the horizontal tail unswept or swept back 45°. Equal static longitudinal stability at Mach number of 0.60; wing loading, 50 pounds per square foot; sea level.

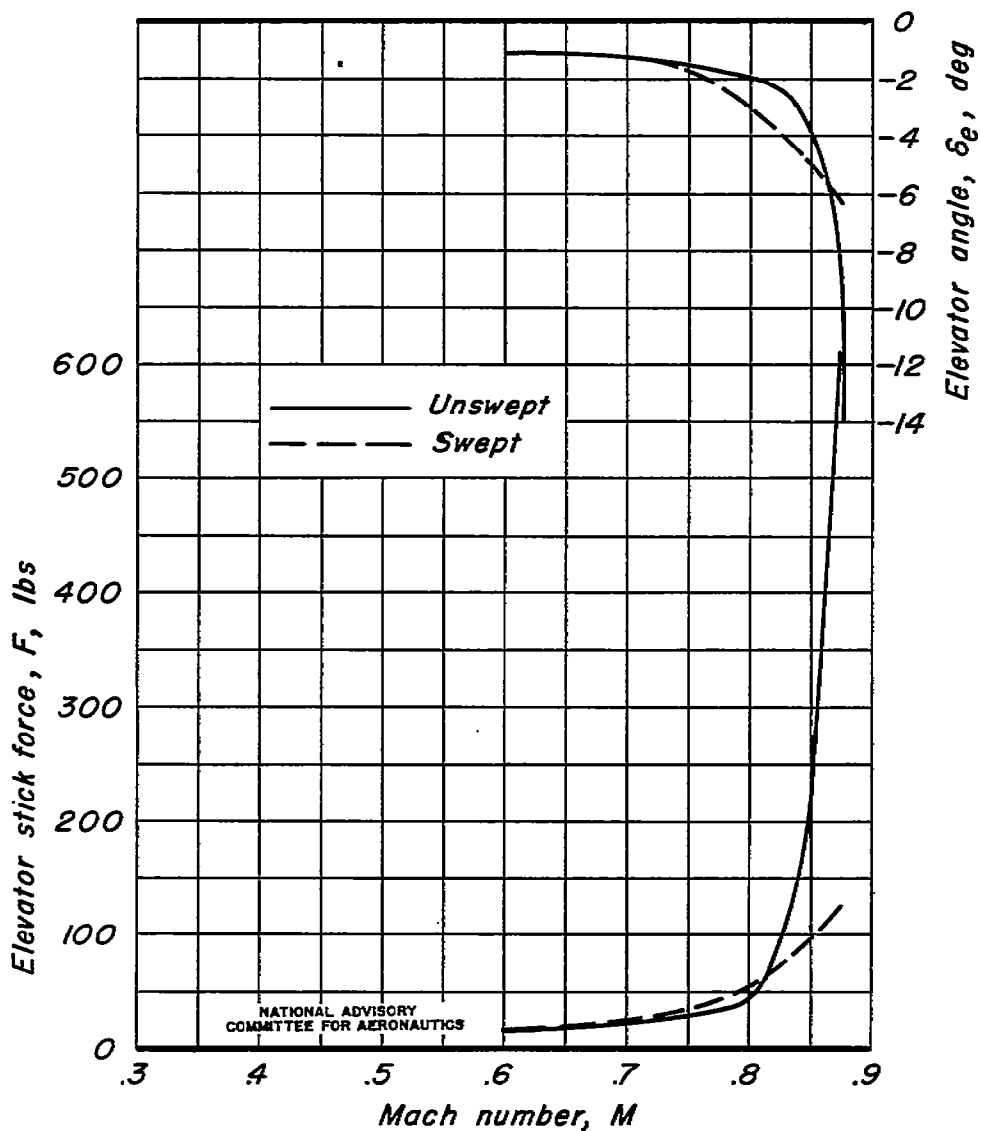


Figure 23.—Predicted variation with Mach number of elevator stick force and angle for an airplane with the horizontal tail unswept and swept back 45°. Equal static longitudinal stability at Mach number of 0.60; wing loading, 50 pounds per square foot; sea level.

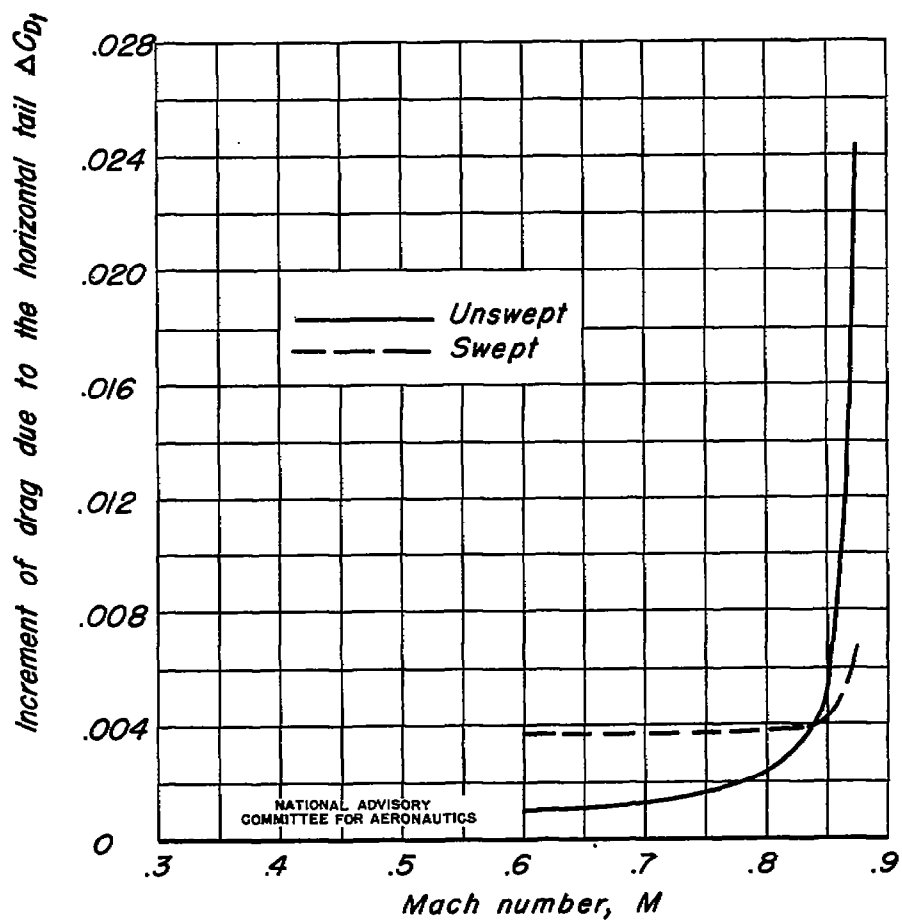


Figure 24.—Predicted variation with Mach number of the horizontal tail drag for an airplane with the horizontal tail unswept and swept back 45° ; wing loading, 50 pounds per square foot; sea level.